Bachelor's project

NTNU
Norwegian University of Science and Technology
Faculty of Engineering
Department of Energy and Process Engineering

Tinus Furnes Alsos
Haakon Halstensen
Simen Myrrusten

PV Systems on Refrigerated Warehouses

A study in two parts - Examining production-load correlation and exploring regional differences influencing production and finance in Norway

Supervisors: Federico Zenith and Mats Jønland
May 2021

Bachelor's project in Renewable Energy

NTNU
Kunnskap for en bedre verden

TrønderEnergi

Tinus Furnes Alsos
Haakon Halstensen
Simen Myrrusten

PV Systems on Refrigerated Warehouses

A study in two parts - Examining production-load correlation and exploring regional differences influencing production and finance in Norway

Supervisors: Federico Zenith and Mats Jønland
May 2021

Bachelor's project in Renewable Energy
May 2021

Norwegian University of Science and Technology
Faculty of Engineering
Department of Energy and Process Engineering

NTNU
Norwegian University of
Science and Technology

Preface

This bachelor thesis is submitted as the final project in the subject TFNE3001 – Bachelor Thesis Renewable Energy, which accounts for 20 credits. The bachelor thesis is the final assessment of the degree in Bachelor of Science in Renewable Energy Engineering, Faculty of Engineering, Department of Energy and Process Engineering at the Norwegian University of Science and Technology (NTNU). The thesis is written in collaboration between students Tinus Furnes Alsos, Haakon Halstensen and Simen Myrrusten.

The thesis is provided by TrønderEnergi, an energy company based in Trondheim with ambitions of creating values through environmentally friendly energy production and energy-related services that support the region. The original statement presented by TrønderEnergi was *Flexibility and power potential of PV systems at refrigerated warehouses.* Throughout the work period, the thesis evolved to:

Examine the correlation between PV production and load at refrigerated warehouses, as well as the impact of geographical and financial factors on PV systems at refrigerated warehouses across Norway.

Prior to the final selection of the thesis, several different themes in a wide range of possible areas were explored, as there are many subjects related to renewable energy that is both important and interesting. Common ground was found related to PV systems. Additionally, it was important for the group to select a thesis in which the members could combine their renewable engineering skills with programming and creative problem-solving. Therefore, a thesis subject that challenged us to create our own models was preferred.

Working with this bachelor thesis has been a rewarding experience. Throughout the work period, we have acquired knowledge about PV fundamentals, PV history, PV market status both worldwide and in Norway, PV economy, climatic factors for PV in Norway, as well as the power market in Norway. Additionally, we have improved our skills in Python programming, created unique models, gotten familiar with PVsyst simulation tool and done both financial and statistical analysis. Finally, and maybe most importantly, we have improved our soft skills such as communication, planning, decision making, problem-solving, self-reflection and teamwork.

We want to express our sincerest gratitude to our supervisors, Federico Zenith from NTNU/Sintef and Mats H.G. Jønland from TrønderEnergi for support, guidance and feedback throughout the process of writing this thesis. Their help and guidance have been of utmost importance.

Further gratitude is awarded ASKO Midt-Norge, ASKO Vestby, Login Eiendom and Trondheim Havn for not only answering questions and concerns regarding the thesis but also providing us with load profiles and energy production data from their respective refrigerated warehouses. Thor Christian Tuv from FUSen has also been helpful with information.

Trondheim, 20/05/2021

Tinus Furnes Alsos | Haakon Halstensen | Simen Myrrusten

Abstract

Despite recent years of rapid development, PV power constitutes for only 0.4 % of the total installed capacity of power production in Norway, making this an area with huge potential for expansion. Finding suitable areas for instalment is crucial for utilizing this potential. Refrigerated warehouses are a special case that fit in this category, as their consumption increases during summer months with higher ambient temperatures, coinciding with increased potential for production from solar power. This thesis will investigate this suggested correlation for five different locations in Norway over a period of 25 years, in addition to uncovering differences in these locations related to production and finance over the same period. The selected locations represent major cities in Norway from each of the five different bidding zones and are, from South to North, Kristiansand, Oslo, Bergen, Trondheim and Tromsø.

The background section of the reports is divided into three main chapters, covering the basis for answering the thesis. This includes a review of PV technology, covering PV history, PV fundamentals and influencing factors on the performance of PV panels. In addition, the meteorological conditions of Norway are explored, extracting relevant information and statistics on elements such as irradiance, temperature and precipitation. The final chapter covers the electricity market, providing information on how power is bought and sold, in addition to both current and historical price differences across regions for selected cities.

In order to answer our selected thesis, a load profile was needed, together with production values from PV systems in selected locations. A load profile was gathered by asking several relevant companies for data, and through a selection process, the load profile from ASKO Midt-Norge in Trondheim was selected. For producing production results, the computer software program PVsyst was used by designing a system and simulating production results in each city. The designed PV system has a capacity of 1181 kWp, covering 6000 m^2. The Pearson correlation between the selected load profile and PV productions was calculated using Python to examine the fit between refrigerated warehouses and PV system using a statistical measurement.

The financial analysis is also performed in Python by gathering grid tariffs and historical electricity price data for the different regions and importing the production values from PVsyst. Several considerations regarding the implementation of electricity prices, installation costs and maintenance cost have been made to produce a cash flow analysis. Financial results parameters are provided in the form of net present value (NPV) based on yearly cash flows and a discount rate of 4%, in addition to calculating the internal rate of return (IRR). The amount of overproduction was discovered and curtailed if it exceeded a certain amount.

Based on the analysis, it is found that there is a moderate correlation of 0.3552-0.4209 between simulated PV production and load at the refrigerated warehouse. PV production is highest in Kristiansand at 920 $MWh/year$, and decreases northwards to Tromsø at 575 $MWh/year$. This is due to higher irradiance south in Norway. Bergen is the exception and has the second-lowest production due to cloud coverage, despite being south of Trondheim.

At refrigerated warehouses, PV systems are a suitable measure to reduce energy demand and costs as a result of seasonal and intradaily similarities in production and load. PV systems can contribute to peak shaving at refrigerated warehouses, but the financial benefit of this is lost mainly due to curtailing. The load-production correlation would be better utilized without curtailing and the cost reductions would see a 20.8 - 45.2 % increase, depending on the city.

From an overall perspective, considering both regional PV production and financial differences, Kristiansand is the most suited for utilizing PV systems on refrigerated warehouses. Oslo and Trondheim share second place, not so far behind Kristiansand. Bergen is significantly worse suited, while Tromsø is by far the worst with the lowest production and a poorly suited electricity bill structure.

Contents

List of Figures

List of Tables

List of Abbreviations and Terms

Air Mass (AM)	Coefficient defining the direct optical path length through the Earth's atmosphere.
Angle of Incidence (AOI)	Angle between a horizontal plane and direct radiation.
Azimuth angle	Angle of deviation from true south in the northern hemisphere.
Bidding zone	A geographical area within which market participants are able to exchange energy without capacity allocation.
Capacity	Regarding energy producing, the maximum output of energy, measured in Watt
Curtailing	Regarding energy production, deliberate reduction in energy output
Diffuse irradiation	Radiation from the sun reflected and scattered aerosols in the atmosphere.
Direct irradiation	Energy from direct solar beams striking an area.
Discount rate	The rate used to discount the future cash flows.
Internal rate of return (IRR)	The discount rate to get a net present value of zero.
Inverter	An electric device converting direct current to alternating current
Irradiance	Output of energy from the sun registered at earths surface.
Irradiation	Irradiance integrated over time.
Latitude	Angular distance of a place north or south of the earth's equator.
LCOE	Levelized cost of electricity.
Linke turbidity	A factor used to approximate the atmospheric absorption and scattering of solar radiation
Load profile	An overview of power consumption over time.
Net present value (NPV)	The current value of future cash flows.
p-n junction	The boundary layer between two oppositely doped semiconducting materials.
Pearson correlation	A statistical measurement for how linearly connected two sets of data are.
Photovoltaic (PV)	Conversion of light to electric energy.
PV array	An assembly of PV modules or panels.
PV solar cell	Or solar cell, the basic device which converts light to electric energy.
PV panel	Or PV module, an assembly of PV cells mounted.
PV production	Energy production from a PV device or system.
PV system	A system which produces PV energy.
Prosumer	Power customer that both delivers and consumes electricity.
Reflected radiation	Solar radiation reflected from the earth's surface onto a surface.
Refrigerated warehouse	An industrial facility to store and handle chilled and frozen foods.
Semiconductor	A solid substance that has a conductivity between that of an insulator and that of most metals.
Soiling	Regarding PV systems, the accumulation of dirt, snow or other particles covering the PV panels.
String	A series of connected PV panels.
Tilt angle	Regarding PV systems, angle of which PV panels are mounted.
Watt peak (Wp)	The measured power with standard test conditions.
Without curtailing (w.c)	Energy or financial considerations with no curtailing.

List of Programs

PVsyst 7.1.8 is a computer software program used for the study, sizing and data analysis of complete PV systems. It provides the user with several system options, as the program deal with grid-connected, stand-alone, pumping and DC-grid PV systems. Included in the software is extensive meteorological and PV system components databases provided by Meteonorm, in addition to general solar energy tools. The system is designed to satisfy the needs of architects, engineers and researchers. It is also well suited for educational purposes. [1]

Python 3.9.1 is a interpreted, object-oriented and open-source programming language [2]. The language is used to create web applications, read and modify files, handle data and perform complex mathematics, with more [3]. In this thesis the open-source libraries Pandas, Numpy, Numpy_financial and Matplotlib are used. Pandas and Numpy are used to import, clean and manipulate data, Numpy_financial provides financial algorithms, while Matplotlib are a data visualising tool used to create visualizations of the data.

Introduction and Background

This section is divided into four chapters, Introduction, PV (photovoltaic) Fundamentals, Meteorological Conditions of Norway and the Electricity Market. The introduction explains the relevance, the thesis statement, the limitations made, as well as the thesis outline. PV technology will give a brief overview of the history of PV solar cells and explain how PV systems work. Meteorological conditions of Norway presents the difference in climatic conditions across different regions of Norway. The electricity market explains how the power market operates, as well as how the power and electricity prices are set.

1 Introduction

At the end of 2020, the normal annual production of electricity was 153.2 TWh, with hydro power accounting for about 90 % [4]. By 2030, the electricity consumption is expected to grow by 23 TWh through electrification measures alone [5]. Further installations in Norwegian hydro power production is limited, as 88 % of Norwegian production capacity is already reached [6], with only 5 TWh increased production expected towards 2040 [7]. To meet the increased demand of electricity, other sources of clean electricity production such as wind and solar is required.

Wind power production is already under rapid development. At the beginning of 2021, the total installed capacity of wind was 3 977 MW, where 1405 MW was installed during 2020. The total installed capacity of solar power at the beginning of 2021 was only 160 MW, with 40 MW installed during 2020 and 50 MW during 2019. Solar power only constitutes 0.4 % of the total installed capacity in Norway. [6]

Grid-connected PV systems account for most of new capacity installed, representing 90 % of the solar capacity [6]. Figure 1.1 illustrates recent installed capacity and separates between stand-alone systems and grid connected systems. Even though only 15 % of PV installations are over 15 kW, these installations account for over 85 % of the total installed capacity [6], where big installations on large rooftops constitute most of the installed capacity for the past five years [7]. The future of solar PV in Norway is uncertain, but a significant increase is excepted. By some estimates, the PV capacity will reach 1.75 GW by 2040 [8], compared to today's 160 MW. For this to happen, finding potential areas suited for large PV installations is necessary.

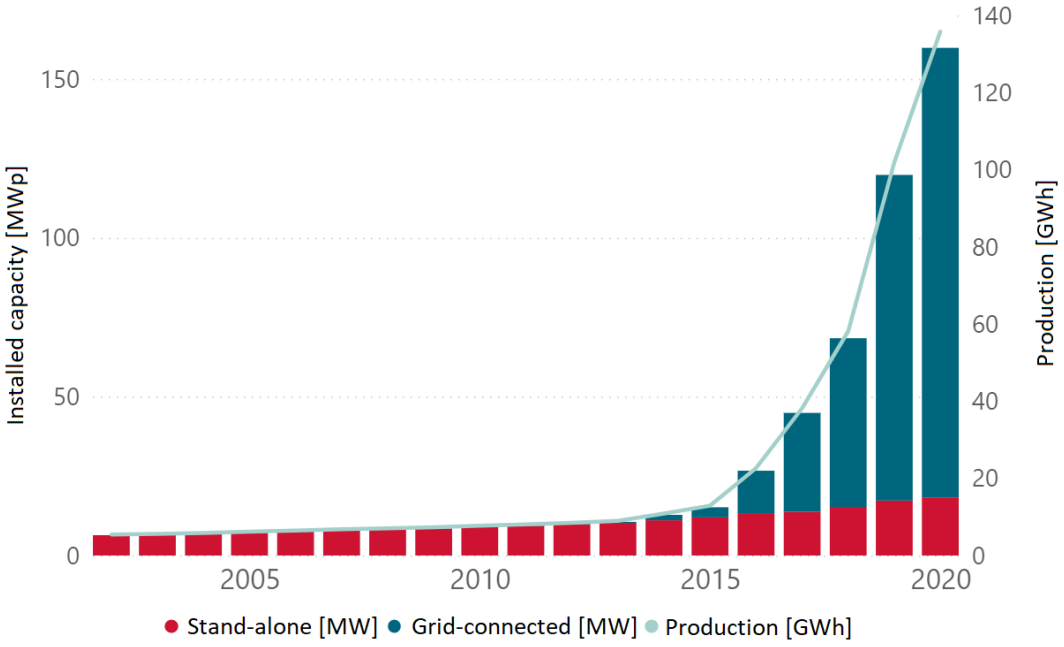

Figure 1.1: *Installed capacity and production from PV in Norway. Figure is edited from its original [9].*

Figure 1.2 illustrates the average monthly energy consumption in Norway from 2016 to 2020. The consumption in Norway is U-shaped with peak energy consumption during winter and low energy consumption during summer. This is caused by the cold temperatures during winter, leading to heating requirements. In addition, operations decrease during summer and the energy consumption sinks [10]. The consumption in February is lower than the consumption in March due to February being 3 days shorter.

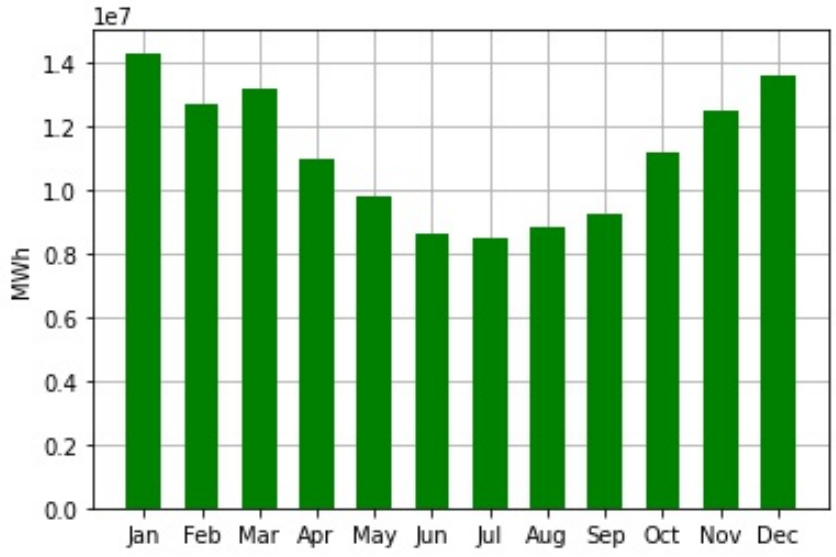

Figure 1.2: *The average monthly energy consumption in Norway from 2016 to 2020 [11].*

Figure 1.3 shows the production curve from a PV system installed at a school in Hedmark from 2014 and represents a typical production curve for Norwegian conditions. Production rises in spring, stays high during summer months, decreases in autumn and is nearly non-existent during winter.

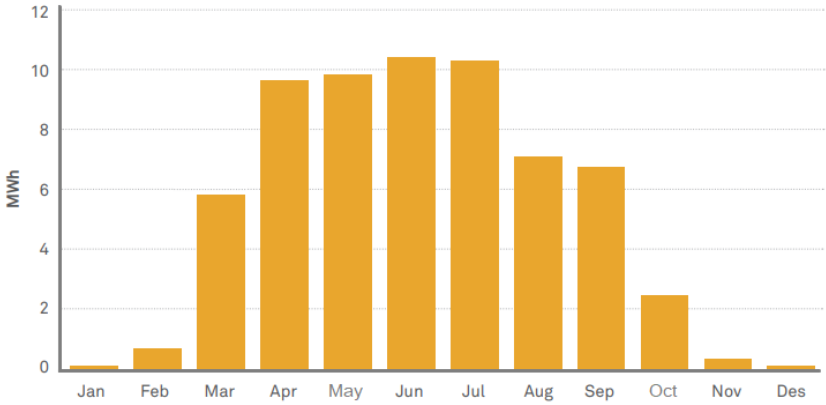

Figure 1.3: *Energy produced from a PV system in Hedmark, Norway in 2014. Figure is edited from its original [12].*

PV systems in Norway are most effectively used as a measure to reduce energy consumption from the grid. PV systems are directly connected to electricity consumers, such as warehouses, office buildings or private households. How well a PV system can contribute to energy cost reduction is dependent on the building's load profile. A good production-load relation is crucial with regards to energy and costs savings, and the potential profitability of the PV system. Figures 1.2 and 1.3 indicates that PV production and average energy consumption in is poorly correlated. Therefore, finding consumers that suit PV production might require looking at buildings with unique load profiles.

According to FUSen, a PV system provider in Norway, refrigerated warehouses are an excellent use case for PV systems. Refrigerated warehouses are industrial facilities with the purpose of storing and handling both chilled and frozen foods. Figure 1.4 illustrates the energy demand of a refrigerated warehouse in Norway from week 28 in 2018. During this week, temperatures rose up to 30° C, leading to large fluctuations in bought energy as the energy demand increases with temperature. [13]

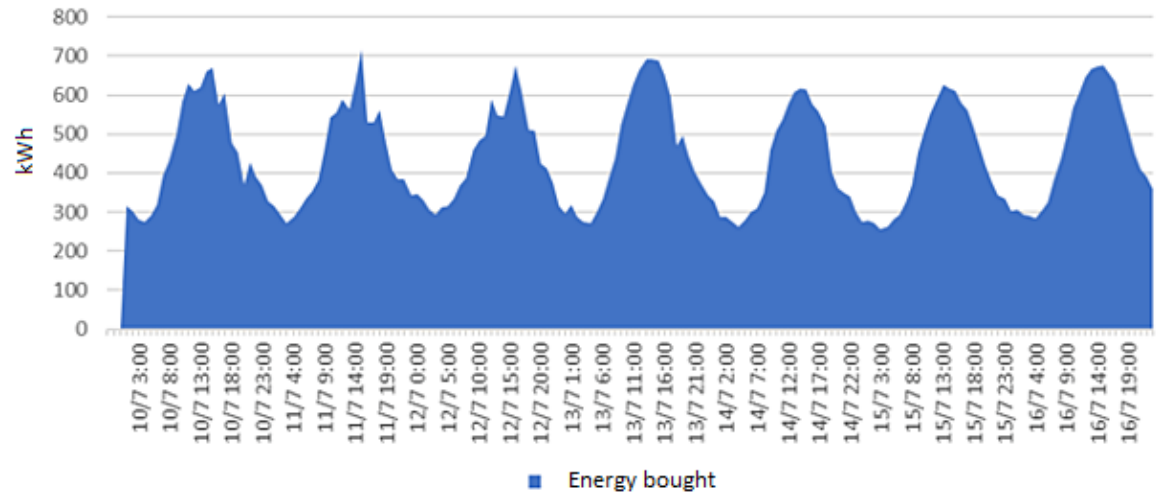

Figure 1.4: *Energy bought from a refrigerated warehouse in Norway during week 28, 2028 [13].*

Figure 1.5 illustrates how a PV system can be utilized to decrease the amount of energy bought from the grid for a refrigerated warehouse, by using the produced energy for shaving consumption peaks. This is observed with the orange field, covering consumption peaks. As can be seen from figures 1.4 and 1.5, refrigerated warehouses are presumably a good fit with PV systems on a daily time-frame. [13]

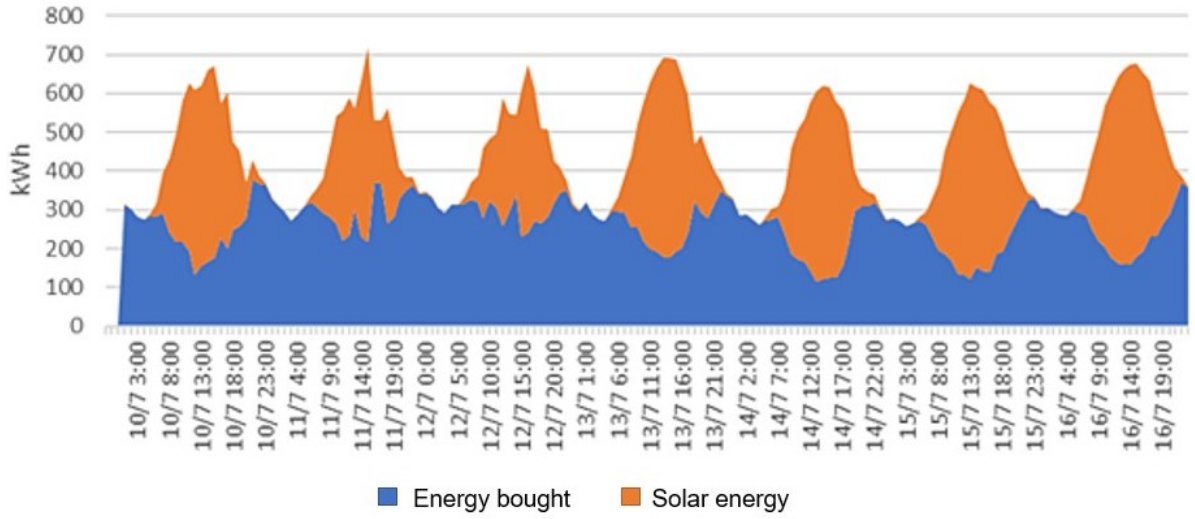

Figure 1.5: *Energy bought and energy produced from a PV system installed on a refrigerated warehouse during week 28, 2018 [13].*

In addition to reducing daily peak power consumption, there could be a seasonal fit between PV production and refrigerated warehouses' energy consumption. It is reasonable to assume that the energy consumption during summer increases at refrigerated warehouses as cooling demand increases with temperature. As figure 1.3 illustrates, PV production is also at its peak during the summer months, which could constitute a good fit between PV production and refrigerated warehouses' energy consumption. Therefore, the potential impact on cost reductions and energy consumption of installing PV systems on refrigerated warehouses could be better than other buildings or industries.

Several of the largest PV systems installed in Norway are on rooftops of refrigerated warehouses. According to a statistic from Multiconsult, in 2017 the 6 largest PV systems in Norway were located on refrigerated warehouses [14]. Recent years have seen further expansion in this field by different companies. One of these companies is ASKO, a major food-distributor in all regions of Norway, with a total of 100 000 m^2 of installed solar-panels allocated on 11 sub-companies [15]. Another major party is Login Eiendom, property owner for one of Norways largest food-distributors. Amongst several other installations, they made Norways largest single purchase of solar-panels with 13 000 m^2 of panels at their location in Vinterbro, just south of Oslo in 2019. The installation can be see in figure 1.6 [16].

Figure 1.6: *Login Vinterbro with PV system installed [17].*

Despite recent installments, there are still many refrigerated warehouses across Norway without PV systems. Therefore, there could potentially be a significant market for PV systems on refrigerated warehouses. Further examinations on how good correlation there is between refrigerated warehouses and PV production and how PV systems can be used to decrease energy costs is therefore interesting.

Norway extends across vast distances with varying climate, which has a significant impact on the production of a PV system. In addition, there are different energy cost structures in Norway depending on the region. Together, these differences in costs structure and production potential impacts the profitability of a PV system.

Because of the geographical differences in both climate and costs, it is to a certain extent unknown where PV systems are most optimally placed. Locating where in Norway PV systems are best suited might contribute to the further expansion of the PV market in Norway. Especially at refrigerated warehouses where the consumption is presumably at its peak when PV systems produce the most energy. Distinguishing the factors that have the most significant impact on the profitability of PV systems on refrigerated warehouses at different locations is therefore relevant.

1.1 Problem Definition

While PV energy is the largest growing energy source worldwide, Norway's use of PV energy has so far been limited. If PV is to be a significant part of the future energy mix of Norway, finding suitable applications for PV energy is important. One such application might be to reduce energy demand of refrigerated warehouses, as they have a high energy need to cool wares during summer, when PV production is at its highest. Additionally, since Norway extends from latitudes 58.0° to 71.2°, with varying climate across the country, PV production is different from region to region. Therefore, a two-part thesis statement, focusing on both PV systems on refrigerated warehouses and regional differences in PV production, is presented:

1. *What is the correlation between load at a refrigerated warehouse and power output from a PV system? If such correlation exists, how suitable are PV systems as a measure to reduce energy demand and costs at refrigerated warehouses?*
2. *What is the relative difference in installing PV systems on a refrigerated warehouse in five geographically different cities across Norway considering climatic and financial factors?*

1.2 Limitations

Due to limited time and with the objective of producing an end result where considered factors were explored to their fullest, simplifications in both scope and execution were made in several stages of the thesis. This section will put a spotlight on these limitations and evaluate their impact.

The basis of the assignment stems from ASKO Midt-Norge's load profile from 2020, a factor that might have an influence on results. Selecting a load profile from just a single year could include deceptive data due to abnormal consumption needs, irregular climatic conditions or errors in measurement. The same factors are relevant concerning the decision of using just the one location. The potential impact on this factor was a acknowledged at an early stage, and attempted avoided by comparing the available data and selecting a load profile deemed representative. Available complete data sets for multiple years from several locations were though scarce, as we were reliant on external contributions, thus leaving the impact unknown to an extent.

Simulations and final system design and in PVsyst is another limiting factor. The meteorological basis for Norwegian latitudes in PVsyst, provided by Meteonorm, is not ideally sufficient, and may influence production results. The insufficiency is caused by a lack of actual measured weather data in selected locations, resulting in reliance of satellite data, with increasing relevance for locations further North. Although tests performed at different locations to determine the accuracy of generated data were deemed uplifting, the potential impact of inaccurate meteorological data is considerable. Optimization of system settings, individual adjustments for each location and implementation of every available detailed loss factor in PVsyst was considered too time consuming and beside the scope of the thesis in order to be performed. Adjustments were thus limited to the most basic and influencing details, which might influence results.

The significance related to energy overproduction implications revealed itself during the execution of the thesis, and provided the opportunity of exploring an array of solutions. Although highly relevant and interesting, these were left unexplored and only partially mentioned in some sections. Designing an optimal facility is a thesis at its own, and were not the scope for this thesis. The selected size of the designed PV system was selected to keep the overproduction relatively low, while still being at a considerable size compared to real system in place at ASKO Midt-Norge.

Other aspects left out include an environmental approach to the thesis, investigating the impact on emissions through an extensive life cycle analysis (LCA). This has no impact on the results, and can only be considered supplementary if included. Evaluation of current regulations on energy production and PV-installment are disregarded, in addition to an assessment of politics regarding available or potential subsidies. In a developing market, coming years are likely to introduce changes that might influence results.

Gathering a precise financial estimates were not prioritised. Both the electricity prices and grid tariff might be a bit low, because neither inflation nor price increase were considered. However, the purpose of the economic analyses was to compare the five cities against each other. Whether the implementation of electricity prices are underestimated does not impact how the locations are compared. There are used financial parameters as IRR and NPV to measure the profitability of the case studies. These measurement must not be observed as an indication of the profitability of PV systems on refrigerated warehouses, but are used to compare the case studies against each other.

1.3 Thesis Outline

Chapter 2 covers information related to photovoltaics, hereinafter history, functionality, influencing factors and current status.

Chapter 3 gives insight on differences in meteorological conditions in five different cities in Norway that has an impact on PV systems.

Chapter 4 provides information regarding infrastructure, market regulations and pricing related to energy costs.

Chapter 5 provides information on the process of selecting a load profile for the thesis.

Chapter 6 explains how PVsyst is used to design a PV system and simulate production results, including insight on decisions made.

Chapter 7 explains how the parameters included in the financial analysis were gathered and implemented.

Chapter 8 explains how the Pearson correlation between PV production and the selected refrigerated warehouse was calculated.

Chapter 9 presents results related to correlation between the load profile from a refrigerated and production from PV systems.

Chapter 10 presents results in regional differences with regards to both production and financial aspects.

Chapter 11 extracts correlation results and discusses relevant segments.

Chapter 12 examines differentiating factors across regions in regards to production and financial results.

Chapter 13 provides a final conclusion for the thesis.

Chapter 14 suggests certain aspects of the thesis that would be improved by further research, in addition to relevant aspects left uncovered.

2 PV Technology

PV technologies utilize the most abundant energy source there is, the sun, to produce electricity [18]. This chapter will begin by giving a brief overview of the history of PV technology. Afterwards, the fundamentals of how PV systems work, from single a cell to large PV systems is presented. Lastly, an overview of influencing factors on the performance of PV is given.

2.1 History of PV technology

PV energy is the fastest growing energy source worldwide [19], but it has not always been this way. For long, PV energy has been far too expensive to have a meaningful contribution to the worlds energy needs. This section will provide a short overview of the history of PV technology, from how the photovoltaic effect was discovered to PV energy becoming the fastest growing source of clean energy.

2.1.1 The Discovery and Early Development of the Solar Cell

The history of the solar cell began in 1839, as the French physicist Edmond Becquerel discovered what is now known as the photovoltaic (PV) effect — the generation of voltage and electric current by illuminating a material with light. At age 19, experimenting in his father's basement, he discovered that a cell constituting of metal electrodes immersed in an electrolyte solution produced a current. The phenomena of converting sunlight into electrical energy were discovered, but the required technology to utilize the phenomena for any practical purposes was still far away. [20]

Several decades later, in the 1870s, Willoughby Smith, William Grylls Adams and Richard Evens Day discovered the photovoltaic effect in selenium. The discovery was utilized by the American inventor Charles Fritts, who constructed what is considered the first true solar cell in 1883. The solar cell was made from junctions of the semiconductor selenium covered by extremely thin layers of gold. The inventor claimed that the selenium cell produced a current "that is continuous, constant, and of considerable force – with exposure to sunlight." His claims were met with considerable scepticism – how can sunlight be converted into electric energy? Although his claims were confirmed by leading experts in electricity from Werner Siemens in Germany, the total efficiency of the cell was less than one percent, so low that the technology was largely unused until later in the 20th century. [20, 21]

The next several advancements in solar cell technology emerged from the Bell Labs. A semiconductor researcher, Russell Shoemaker Ohl, was experimenting with silicone samples during the 1940s, when one of his samples were accidentally cracked. Rather than dismissing the sample, he analysed it and discovered that current flowed through the sample when exposed to light. It seemed like the crack, which worked as a boundary level between silicone of slightly different impurities, caused an electrical field between the two sides, one which had become positively charged while the other was negatively charged. The cracked silicone sample led to the inadvertent discovery of a p-n junction, a fundamental part of modern solar cell technology. Although the discovery was profound, the solar cell which Ohl developed and patented was merely one percent efficient and was shortly outperformed by a new silicone single-crystal solar cell developed by Owls colleagues. [21]

Building on Ohl's discovery, D. M. Chapin, C. S. Fuller and G. L. Pearson from Bell Labs utilised the p-n junction to make significant improvements to solar cell technology [22]. They managed to describe to workings of p-n junctions, which facilitated further exploration of theoretical efficiency limits of solar cells. They discovered several limiting factors for energy conversion efficiency, such as recombination of electron-hole pairs, reflection, ohmic losses and the severe impacts of low- and high wavelength light in generating electron-hole pairs. In 1954, they presented a new silicone p-n junction solar cell with an efficiency of six percent. [21, 22]

Despite increasing efficiency, solar cells had little commercial use. Solar cells were too costly and ineffective to compete with other power sources in the energy sector, and were only really an alternative where other sources were unavailable – in remote locations and in space. In 1958, NASA launched its second satellite, the Vanguard 1, which is the oldest man-made object in earths orbit. Vanguard 1 was the first partly solar powered satellite, utilising six solar cells delivering a total of about 1 Watt of power with an efficiency of 10 percent. The solar powered radio remained operational for almost six years [23]. In comparison, Sputnik 1, the first artificial satellite successfully places in orbit, launched in 1957 by the Soviet Union, only managed to transmit data for three weeks before the battery-system on board failed [24].

2.1.2 Political and Environmental Incentives for PV Improvements

The solar cell market remained small and niche until the Arab oil embargo in 1973. With the jump in gas prices, the US government championed US energy independence, causing an increased focus on solar energy. Consequently, solar cell technology saw major improvements in efficiency and cost through materialistic and fabrication improvements [20]. Solar cells slowly but surely found wider terrestrial use, largely due to the US' enthusiastic support of PV technology — in 1977, The Solar Energy Research Institute was founded, president Jimmy Carter installed solar panels on the White House and the world production from PV cells exceeded 500 kW. [25]

The US focus on solar energy abruptly diminished during the 1980s due to a shift in the political climate. Rather than championing energy independence through increasing domestic energy production from alternative sources, the US, led by president Ronald Reagan, invested heavily into military control of the middle-east in order to protect their oil supply. As seen in figure 2.1, the US spent by far the most money on funding PV before Reagan's presidency. Throughout the next three decades, other countries played a more significant role in PV technology discoveries. There were still continuous improvements and discoveries in PV technology between 1980 and 2000. While the US reduced their funding of PV technology, other counties marked themselves in the global PV market. In the 1990s, Germany initiated the 1000 roof program, aiming to install 1000 PV roof systems, followed by a 100,000 roof program in 1999. Japan also initiated large PV support programs in the 1990s through subsidies. [25, 26]

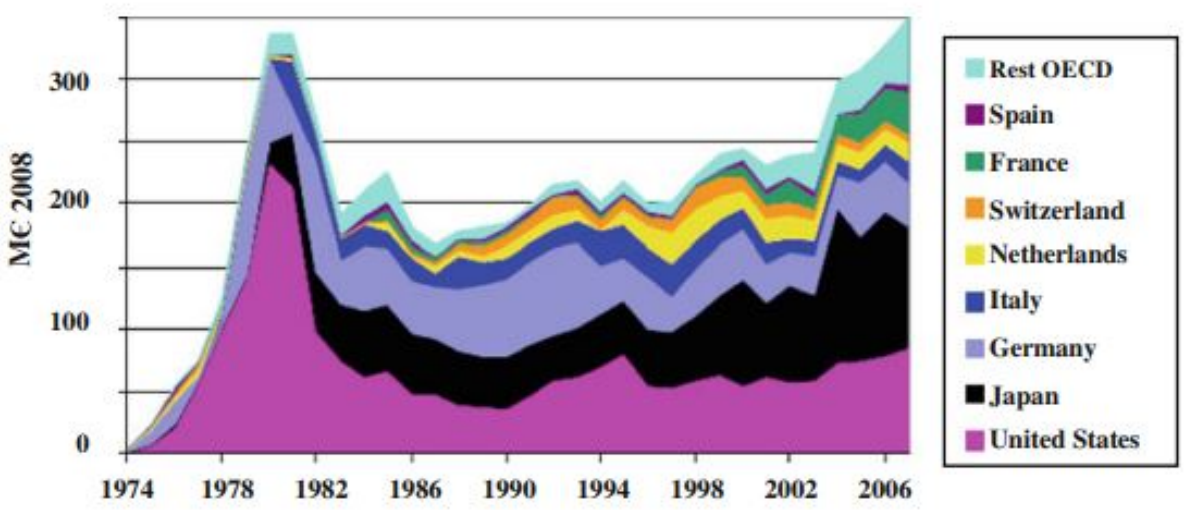

Figure 2.1: *Annual funding of PV by OECD countries between 1974 and 2008. US funding fell considerably in 1980. The total funding did not surpass 1980-levels until 2003. [25]*

With increasing awareness of the effect of global warming and the increased focus on harvesting energy from renewable energy sources, solar PV has become one of the most prominent solutions to the climate issue. PV technology is no longer limited to off-grid locations and spacecrafts – it is the fastest growing energy source, utilized all across the globe.

The prices for PV power has been dramatically reduced in the past decades. As shown in figure 2.2, the module price has dropped rapidly alongside the cumulative production growth. For each doubling in cumulative production, the price of PV modules went down by 25 % on average between 1980 and 2019 [27]. There are two main factors to the cost reduction of PV, technological improvements and large scale manufacturing.

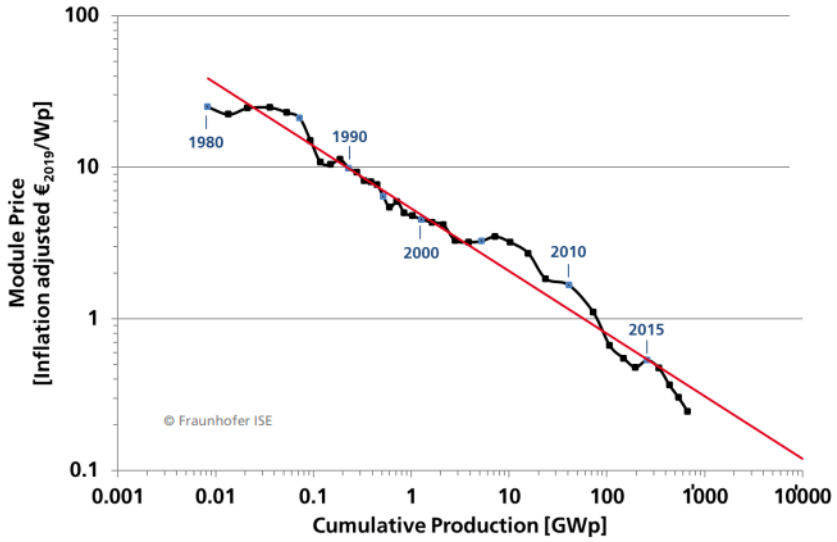

Figure 2.2: *Learning curve of all commercially available PV technologies, 1980-2019. [27]*

As shown in figure 2.3, the annual installed PV capacity is steadily growing. The total installed capacity increased from 23 GW to 627 GW in ten years from 2009, becoming the fastest growing energy source with regards to new capacity installed [19, 27]. China's focus on PV has had a massive impact on the world PV market. Through large scale PV power plants and increased efficiency throughout the entire value chain of PV systems, the cost of PV solar energy is lower then ever, being competitive with other renewables and non-renewables alike. In 2017 and 2018, China accounted for 54 % and 45 % of new PV capacity worldwide, respectively [28]. In 2019, China accounted for 26 % of new PV capacity. Despite China's decrease, the total global capacity additions of PV grew by 12 % to 115 GW in 2019, as PV demand increases worldwide, especially in Europe, rest of Asia and in the United States. [19]

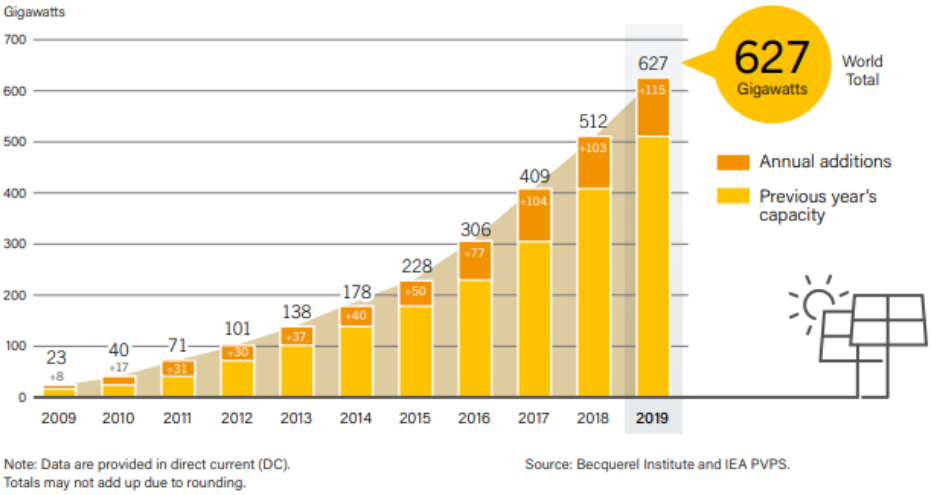

Figure 2.3: *Solar PV global capacity and annual Additions, 2009-2019. [19]*

Figure 2.4 shows the change in recorded solar cell efficiencies in laboratories between 1993-2019. The increase in efficiencies are noticeable, but small. The development in record solar cell efficiencies shows potential of future commercial PV systems. The efficiency of silicone based PV technology, which dominates the commercial marked (over 95 %), has increased from about 24 % to 26.7 % and 17 to 22.3 % for mono and multi crystalline modules respectively. The actual module efficiencies of commercial silicone PV modules are significantly lower, about 18 % for mono crystalline silicone and 16.7 % for mutli crystalline silicone. [27]

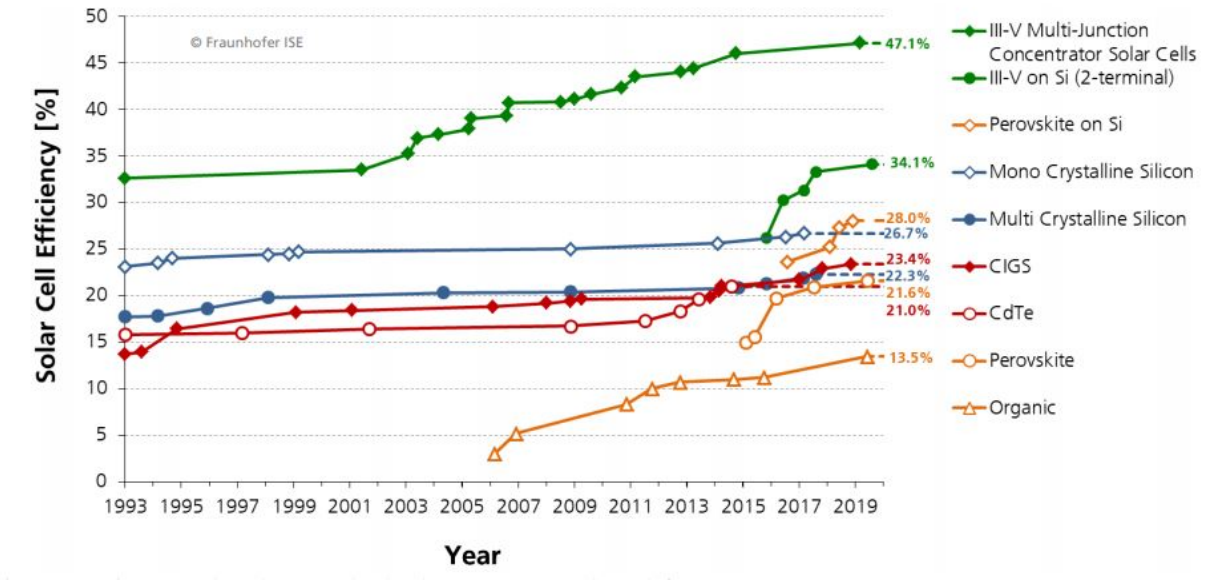

Figure 2.4: *Solar cell efficiencies in laboratories, 1993-2019. [27]*

As figure 2.5 shows, recent years have seen a change in market domination. After decades of having the majority marked share, si multi-crystalline has been overtaken by si mono-crystalline as the new standard. A rapidly changing market with new technologies emerging and present improving; price, efficiency and distribution is expected to change, but mono-crystalline and multi-crystalline is still expected to remain the regularly used technology in coming years. [27, 29]

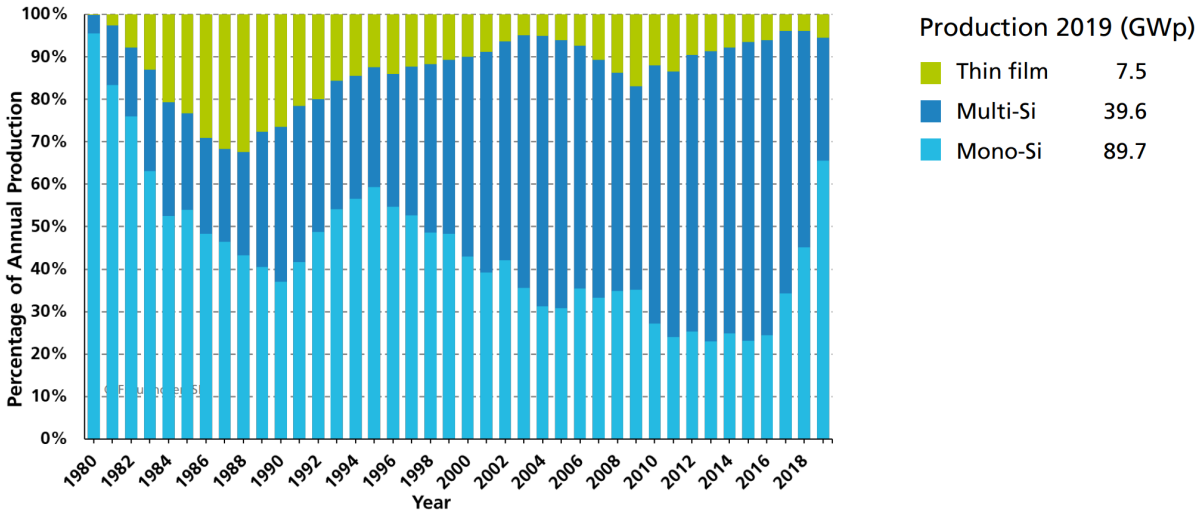

Figure 2.5: *PV Production by Technology, 1980-2019. [27]*

While single junction solar cells are fundamentally limited by its materiel's bandgap [30], multi junction cells can achieve significantly higher efficiencies through multi-junctions of III-V semiconductors with varying bandgaps, allowing for energy absorption of a wider range of the light spectrum. In 2020, Scientists at the National Renewable Energy Laboratory (NREL) managed to create a six-junction III-V solar cell with 47.1 % energy efficiency under 143 suns concentration, setting a new world record for the highest efficiency of a solar cell. A variation of the same cell recorded 39.2 % at one suns concentration, way beyond record solar cell efficiencies of single junction cells. Multi-junction cells are far too costly to be commercially viable, but might prove useful for future high technological equipment. [31]

2.1.3 PV Specifics in Norway

Relevant technologies in Norway follow the international development explored in figure 2.5 with mono-crystalline emerging as the most regular option. This has also been re-affirmed through e-mail correspondence with Thor Christian Tuv, solar energy expert from FUSen [29]. The standard orientation of rooftop-instalment in Norway is east/west mounted with an inclination of 10° which can be seen in figure 1.6. There are several reasons for this. An east-west solution will provide the user with a flatter production curve throughout the day compared to panels mounted directly to the south, with more production at morning and evening. South-oriented panels will deliver higher production during shorter intervals mid-day, requiring up-scaled inverters, leading to increasing costs. In addition, an east-west orientation prevents the issue of self-shading of panels. [32]

The total investment of PV systems includes modules, inverters, other equipment and installation cost. Added up, the sum varies greatly between reports and suppliers, but generally the price in NOK/Wp decreases with size. A report from Solenergiklyngen estimated around 10 NOK/Wp for larger grid-connected systems in 2018 [33]. Solenergiklyngen defines 100 kWp to 1 MWp as large grid-connected systems. Another report from WWF estimated 12 NOK/Wp for grid-connected system on commercial buildings with larger than 10 kWp. This report also predicts the price will decrease further to 10.1 NOK/Wp in 2025 and 8.6 NOK/Wp in 2030. These estimates, including the estimate for 2020, originated from 2015, when the report was published. [34]

2.2 PV Fundamentals

PV systems are typically complex systems, with several different technologies utilized to create a useful, electricity-generating device. The most fundamental part of a PV system is the solar cell. To create any type of functional solar cell, you need a few things: Semiconductors assembled to create a p-n junction and a front and rear contact to allow current flow through an external circuit. Additionally, all competitive solar cells today have several additional layers to improve efficiency. The phenomena which allow solar cells to convert solar energy into electrical energy is the photovoltaic effect. To understand this effect, some basic information about the behaviour of electrons and semiconducting materials is needed. [18]

2.2.1 Semiconductors and Energy Bands

From quantum mechanics, it is known that electrons surrounding the nucleus of an atom can only exist in discrete energy levels. The outermost layer is called the valence band, and the electrons in the valence band are less attached to the nucleus compared to the innermost bands where the electrons have the minimum energy (maximal negative energy). Consequently, due to the loose connection of the valence electrons, their electrons are the only ones that interact with other atoms. If a valence electron absorbs packages of energy called photons, the electron can jump into a higher energy level called the conduction band. At the conduction band, the electron is free from the previous nucleus and can move around to other atoms, making them negatively charged and leaving the original atom as a positively charged ion. [18]

The characteristic of a semiconductor is that it can work both as an insulator and a conductor. What differentiates semiconductors from insulators and conductors is the width of the forbidden zone, represented by the band gap between the valence band and the conduction band. As can be seen in figure 2.6, the band gap of insulators is wide, narrower for semiconductors, and for conductors, the conduction band and valence band are overlapping. [18]

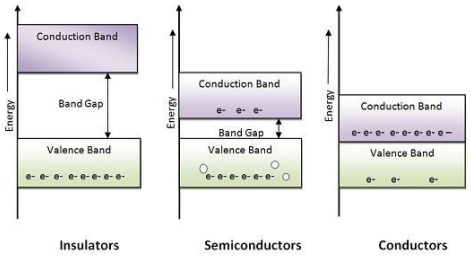

Figure 2.6: *Energy bands of insulators, semiconductors and conductors respectively, left to right [35]. Figure is edited from its original.*

The band gap is the required energy an electron must absorb to be able to jump levels from the valence band to the conduction band. The gap between the conduction band and valence band is the forbidden zone where electrons cannot exist. If an electron absorbs energy less than the energy required to jump to the conduction band, the excess energy is converted into kinetic energy in the electrons, releasing heat, and the electron stays in its current band. [18]

If an electron absorbs the right amount of energy and successfully jumps to the conduction band, it can move throughout the material. However, the electron will most likely recombine, falling back into the valence bond of an atom. This is where the p-n junction enters. With the presence of an electric field created by the p-n junction, the electron will if sufficiently close to the field, follow through the path of the field rather than recombining. If an electron absorbs energy less than the energy required to jump to the conduction band, the excess energy is converted into kinetic energy in the electrons, releasing heat, and the electron stays in its current band. [18]

2.2.2 p-n Junction

A p-n junction is the boundary layer between two oppositely doped semiconducting materials. A doped semiconductor (extrinsic semiconductor) is an originally pure semiconductor (intrinsic semiconductor) that has been introduced to small amounts of impurities. In a p-n junction, one layer is positively doped, whereas the other layer is negatively doped, and are consequently referred to as the p-side and n-side respectively. Doping causes the n-side to be electronically neutral but have excess electrons. Similarly, the p-side is also electronically neutral but has excess positive holes in its structure. If the p-side positive holes where to be filled by electrons, the new structure would be more uniform and the atoms would be slightly negatively charged. If an electron absorbs energy less than the energy required to jump to the conduction band, the excess energy is converted into kinetic energy in the electrons, releasing heat, and the electron stays in its current band. [18]

Crystalline silicon (c-Si) is the most common used material in PV-technology, and solar cells [27]. Silicone is a group IV atom, meaning it has four valence electrons, allowing crystalline structure as shown in figure 2.7. The black circles represent silicon atoms, with the curved lines connecting the atoms represent electron pairs in covalent bonds being shared by the atoms. Each atom in the structure has eight valence electrons, filling the valence band and making a uniform structure. [37]

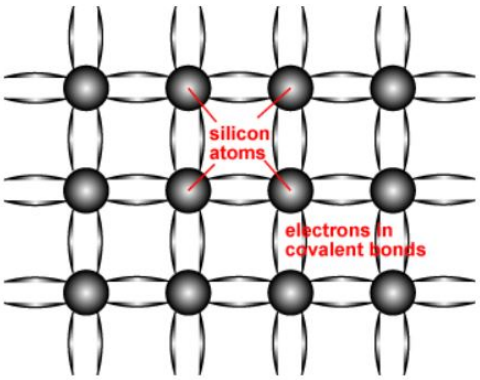

Figure 2.7: *Crystalline structure of silicone. [36]*

The n-layer is commonly created by doping a group IV material, such as silicone, with small amounts of a group V atoms, such as phosphorous (P). The concentration of phosphorous may vary from one part per thousands of silicone to one part per billions of silicone. In other words, there is a small amount of doping material required. Phosphorous, being a group V element, has one more valence electron than silicon. Consequently, the n-layer has additional electrons available for conduction.

Figure 2.8a shows n-doped silicone with one extra electron, which is not a part of the crystalline structure. Figure 2.8a shows p-doped silicone with one extra positive hole, which is not a part of the crystalline structure. In the n-layer, electrons are majority carriers since they are in excess, whereas holes are minority carriers. [37]

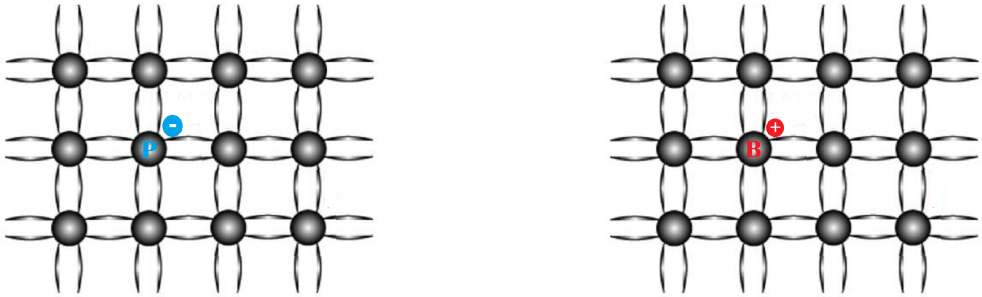

(a) *N-doped silicone by adding phosphorous. The blue circle represents an excess electron.*

(b) *P-doped silicone by adding boron. The red circle represents a positive hole.*

Figure 2.8: *n-doped and p-doped silicone [36]. The figure is edited from its original.*

The p-layer is doped with group III atoms, such as boron (B). While group V atoms have one more electron than silicone, group III atoms have one less. This causes the structure to have positive holes, as shown in figure 2.8b. Positive holes are not actual charges, but rather represents a lack of electrons, causing the hole to be relatively positive. The electrons around the hole shift around due to an imbalanced charge, causing the hole to be displaced. Subsequently, positive holes can be seen as moving around similarly to electrons. In the p-layer, holes are in excess and are subsequently majority carriers, whereas electrons are minority carriers. [37]

When a p-layer and n-layer are connected, a p-n junction forms. The positive holes of the p-layer attract the excess electrons of the n-layer while the electrons of the n-layer attract the holes from the p-layer. When excess electrons from the n-layer diffuse over to the p-layer and combine with the positive holes, they leave behind positive ion cores. When holes from the p-layer layer diffuse to the n-layer, they leave behind negatively charged ion cores. On the boundary between the p-layer and n-layer, an electric field form between the oppositely charged ion cores. The area covered by the electric field is called the depletion region, since the region is depleted of free carriers due to the electric field. Figure 2.10 shows the p- and n-layer before joining and figure 2.10 shows a p-n junction after assembly. Some holes from the p-side combine with the free-electrons of n-side, creating an electric field directed towards the p-side. [37]

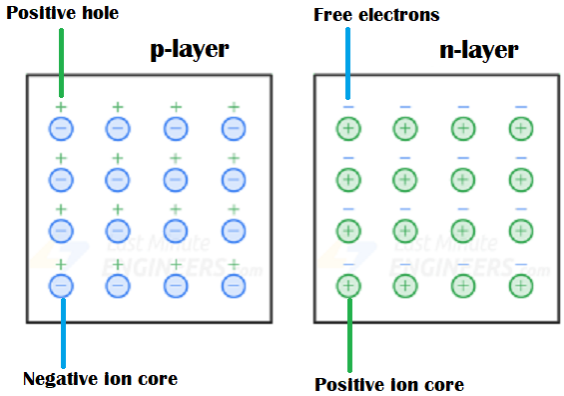

Figure 2.9: *p-doped and n-doped material before assembling. The ion cores are stationary whereas the positive holes and electrons move around. Figure is edited. [38]*

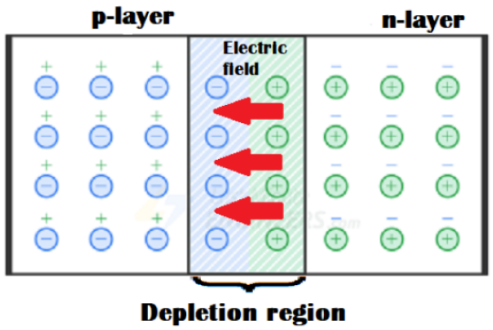

Figure 2.10: *p-n Junction created after assembly. The electric field that occurs is marked in red. Figure is edited. [38]*

When a p-n junction assembly is illuminated, electrons jump to the conduction band and leave behind positive holes. Pairs of electrons and positive holes generated by light absorption are called electron-hole pairs, and their behaviour is utilized to create current. Ideally, if an electron-pair is generated on the n-side, as shown in figure 2.11, the minority carrier (hole) will cross the boundary level of the p-n junction. The electron cannot cross the electric field due to the direction of the fields. By applying an external circuit as shown in figure 2.12, the electron will flow through the external circuit creating current, and combine with an excess hole in the p-layer. [37]

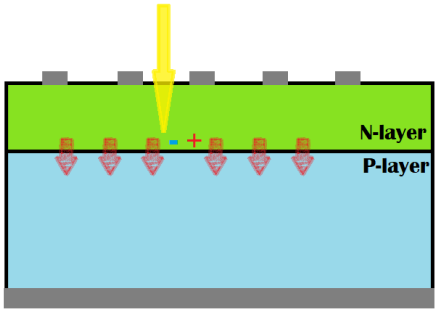

Figure 2.11: *Light is absorbed in the n-layer and an electron-hole pair is generated. - is an electron while + is a hole.*

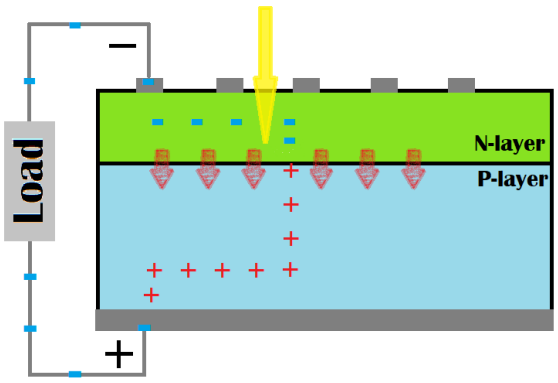

Figure 2.12: *The minority carrier (hole) crosses the depletion layer whereas the majority carrier (electron) is drawn to the p-layer, but cannot cross the barrier and must go through the external circuit.*

The likelihood of an electron-hole pair recombining is largely dependant on where in the solar cell the electron-hole pair was generated. The electron will always recombine unless the minor carrier is collected by the electric field of the p-n junction. Thus the probability that a carrier is collected (the collection probability) is largely dependant on the distance between the photon absorption area and the depletion area. The collection probability is largest in the depletion area, as the electric field quickly pushes the electrons to the n-layer and holes to the p-layer. If an electron-hole pair is generated deep inside the p-layer or at the top of the n-layer, the collection probability is substantially reduced. [37]

Several design considerations can be made to increase the collection probability. First and foremost, the layer thickness of the n-layer and p-layer is adjusted such that as many photons as possible with a large enough wavelength to knock loose electrons are absorbed close to the depletion layer. In the case of Si-cells, the n-layer has better absorbent qualities and is placed closer to the surface. Since most of the light is absorbed close to the surface, the n-layer is made very thin such that the generated electron-hole pairs occur close to the depletion layer. The thickness of a Si-cell n-doped semiconductor ranges between 0.1 to 2 μm. The thickness of the p-layer is way wider, between 150 to 300 μm, as making it thin does not improve efficiency, but the production cost of thinner wafers are higher. [20, 37]

2.2.3 PV Cell Structure

A primitive solar cell consisting only of a p-n junction connected to an external source would have very low efficiency due to different loss factors. To combat energy loss, PV cells consist of several layers as shown in figure 2.13. In addition to the emitter (n-layer), base (p-layer), the p-n junction created at the boundary between the two (not visualized in figure 2.13) and the front and rare contact conducting current through an outer circuit, solar cells have an anti-reflective top cover and a back cover [39].

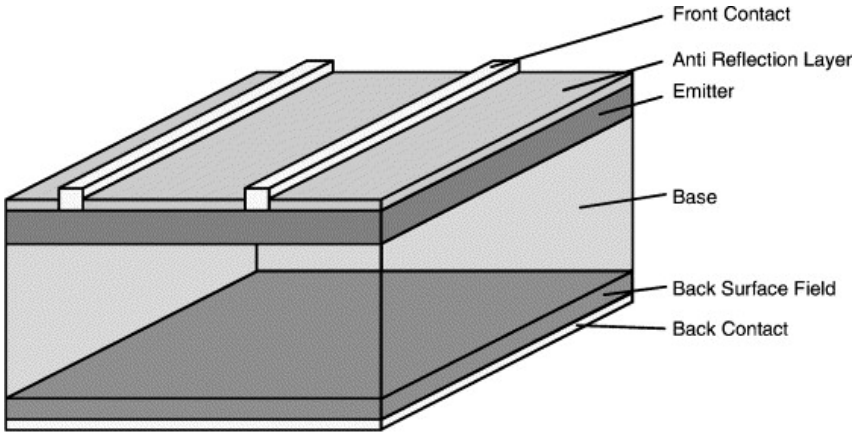

Figure 2.13: *Basic structure of a typical solar cell [39]. Dimensions does not reflect reality.*

The top layer of a solar cell (visualized as the anti-reflection layer in figure 2.13) most importantly needs to transmit most of the light with wavelengths corresponding to the absorption wavelength of the p-n junction assembly. In the case of silicone solar cells, photons need energy of at least 1.12 eV in order to create electron-hole pairs [20], and the top layer consequently needs to transmit most light with wavelengths no longer than 1.2 μm [37] in order to increase the absorption rate.

Although reflection can be significantly reduced by adding anti-reflective (AR) coating with an optimized refractive index to the top layer, there are other considerations such as structural strength, light scattering, thermal resistance, UV exposure and vulnerability to water vapour that also need to be considered [37, 40]. Most solar cells use a single layered AR coating of silicon nitride or titanium oxide [41], whereas special high-efficiency solar cells use more expensive multi layered coatings [40]. The AR coating causes the characteristic blue colour of the most common solar cell type – polycrystalline silicone, which otherwise would have had the grey colour of silicone [41].

Another way to reduce reflection is by using textured surfaces of silicone in reverse pyramid formation, as shown in figure 2.14 to trap light within the cell. In addition to reducing reflection, the light that otherwise would have been reflected will be more horizontally aligned when passing through the cell due to the oblique walls of the reverse pyramid structure, which increases the probability of absorption in the n-layer and ultimately increases collection probability [40]. Textured surfaces have some disadvantages, such as unwanted light trapping of non-absorbable wavelengths, which causes unfortunate high temperatures, reduced self-cleaning capabilities as dust and soil gets more easily stuck, and increased cost [42]. Consequently, most commercial solar cells do not utilize this technology [37].

The top/front cover of the solar cell has more roles than reflection. It needs to be impervious to water, as water or water vapour can cause corrosion of the metal contacts, subsequently reducing the power output and lifetime of the PV cell. In addition, the top layer should increase cell robustness and rigidness. It should also be stable under UV exposure and have low thermal resistivity to reduce the chance of overheating, causing efficiency loss [37]. Low iron content glass is most commonly used, due to its properties and low cost through mass manufacturing [26, 37]. The glass is usually between 3-4 mm thick but can be reduced to 0.85 mm for light-weight applications. An alternative for special applications where low weight is required or that does not need to consider extreme conditions, is several different types of transparent polymers [26].

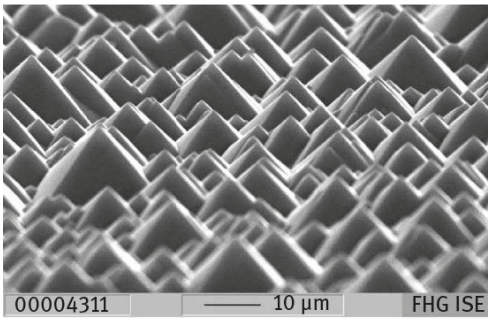

Figure 2.14: *Scanning electron microscope photograph of a random pyramid textured silicon surface [26].*

Between the front and rear cover, covering the p-n junction, polymer encapsulants are usually used to mechanically bind the different components of the complete PV assembly. The encapsulant has strong adhesive qualities, as well as being impervious to both water and oxygen to avoid corrosion. Like the top cover, the encapsulant needs to transmit as much of the light of relevant wavelengths on its top side, losing no more than 1-2% of energy, and withstand high doses of UV radiation and fluctuations in temperature as well as cumulation of humidity [26]. Since the 1970s, ethyl vinyl acetate (EVA) has been the prevailing encapsulant material. EVA is produced in thin sheets and is heated to 150 $^{\circ}C$ at assembly to a viscous liquid state, ensuring that the encapsulant completely covers the cell matrix. [26, 37]

The rear cover needs to address many of the same concerns as the front cover, such as temperature fluctuations and ingress of water and water vapour [37]. More importantly, the back cover needs to provide electric isolation between the cell assembly and the ambient environment. Cell voltages may reach upwards of 1500 V versus ground and the rear cover therefore needs to provide electric safety [26].

There is a wide variety of back covers available today. Most manufacturers of c-Si modules use polymer sheets laminated with polyurethane interlayers. Although most back covers consist of a mixture of polymers, glass-glass modules with rear- and top cover made of glass is becoming more common as thinner glass is available. Back covers mainly improve durability, safety and combat hazards related to electricity and weather conditions, but they can also contribute to module efficiency. One way to achieve this is by using white backsheets, which recycle light that hits around the cells back into the solar cells. Additionally, white back covers absorb less light than darker ones, reducing cell temperatures, which improves PV performance. [26, 43]

Figure 2.15 shows the cross-section of part of a solar cell within a module. The glass, including AR coating which gives the blue colour, is 3.2 mm thick. The encapsulant layers, (2) and (4), has a thickness of 0.4-0.5mm [37]. The cell-matrix is between 0.1-0.5 mm [37], while the backsheet (5) is some hundreds of microns thick. The interconnection ribbons (6) are equally spaced across a single cell. In this case, there are five ribbons spaced with 26.0mm, resulting in a 156mm wide cell ($6 \cdot 26.0\text{mm} = 156\text{mm}$). The spacing between each cell is usually 2-3mm. [26]

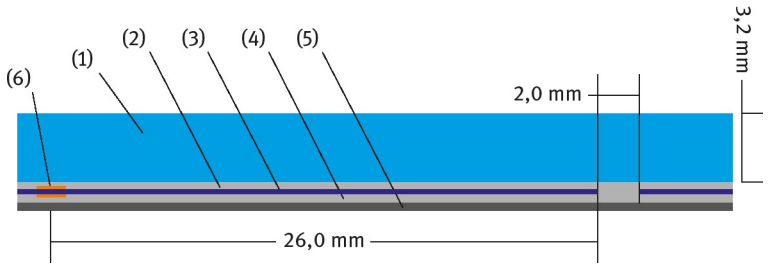

Figure 2.15: *Cross section of a single cell from a module, with front glass (1), front encapsulant (2), cell matrix (3), rear encapsulant (4), backsheet (5) and interconnection ribbon (6) [26].*

2.2.4 PV System

Most solar cells are square-shaped with 156 mm long edges. A single solar cell only delivers a maximum output voltage of about 0.5 V. To achieve a more favourable output, solar cells are series connected into modules. Most modules (also referred to as panels) consist of a total of 60 cells, with 6 strings containing 10 cells each [26]. Modules usually weigh between 15 and 23 kg, depending on manufacturer [44]. An example from Munchen Solar can be seen in figure 2.16 below. The cells within a module are integrated with bypass diodes, preventing complete power loss in the case of a malfunctioning cell within the string [40].

Figure 2.16: *10 x 6 multicrystalline solar panel from Munchen Solar [45].*

The dimensions of a single module of 60 polycrystalline silicon solar cells are usually about: 1000 mm width, 1860 mm length and height between 30-50 *mm* mostly dependant on the frame used [26, 46]. Some manufacturers use 72 cell modules, with 6 strings containing 12 cells each, with slightly different dimensions. These modules sometimes use shorter solar cells of about 125mm [26]. Although these two module constructions are the most common, there is no limit to the dimensions of solar cells, and a wide variety of types of both cells and modules are available.

The solar cells are interconnected using copper wires called ribbons. The ribbons conduct current from a single cell to common module wires. At the back of modules, junction boxes are placed for convenient wiring to other modules or electrical equipment [18]. Wires usually cover about 3 % of the cell area and cause a loss in light absorption. Additionally, electric losses occur in the wires, amounting to about 3-4 % energy loss [26].

Solar cells are constructed as previously described in chapter 2.2.3. The cells are put together into modules and covered by an outer aluminium frame [26]. Figure 2.17 shows the assembly from a solar cell to PV-system. PV panels include one or more interconnected modules. Panels are further interconnected in series or parallel into large PV arrays, tailored to meet system output requirements.

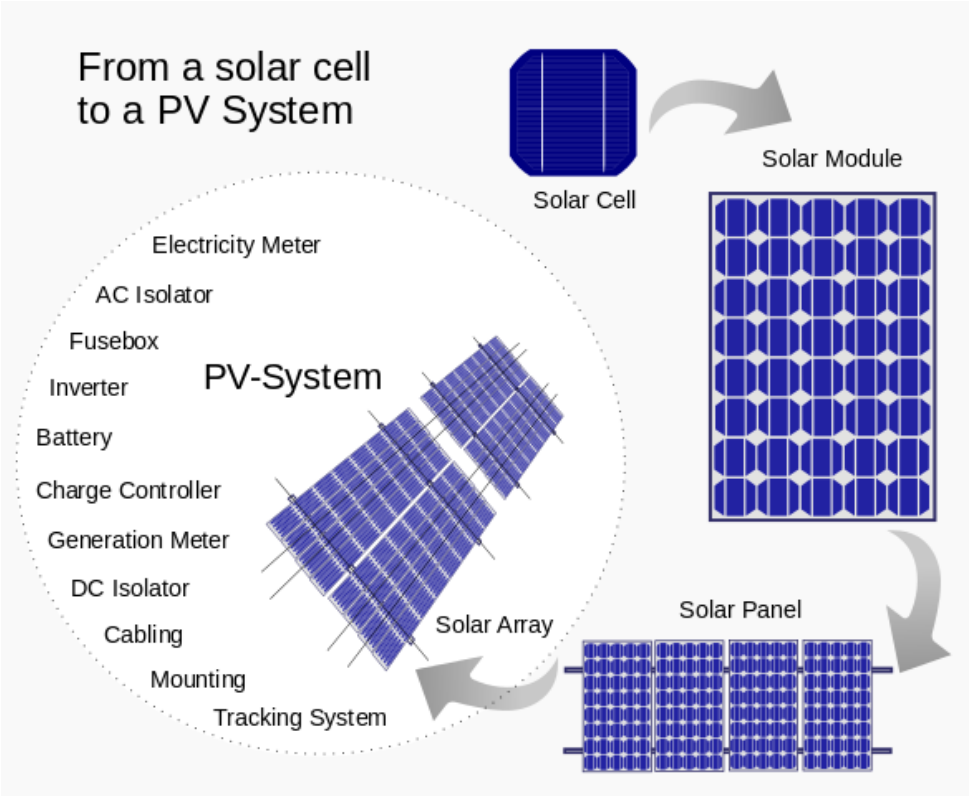

Figure 2.17: *Illustration of the connection between single cell to PV system [47].*

PV arrays are only part of a complete power-generating PV system. Solar cells generate DC current, whereas the grid and most other electricity consuming or transportation systems require AC current. This conversion is done by inverters. A complete PV system requires the use of related equipment, often electrical, some of which are listed on the left side of figure 2.17. Each individual part of the complete PV system is needed for safe and reliable distribution of PV power. A single line diagram of grid-connected PV systems is shown in figure 2.18 to illustrate the integration between PV modules and the grid. The technical details and devices covering the transportation of electricity from generation in the solar cells to delivery to the grid or other users are considered outside the scope of this thesis and are therefore not further explored.

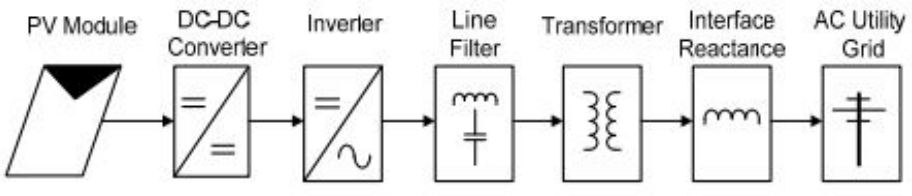

Figure 2.18: *Single line diagram of a grid-connected PV system [48].*

The standard measurement unit for the power modules can deliver is watt-peak, often given as Wp or for larger installations kWp. It corresponds to the maximum power output for a PV module under standard test conditions in a laboratory, given the following conditions: Temperature of 25°C, solar radiation of 1000 W/m^2 and AM factor of 1.5. [49]

2.3 Influencing Factors on Performance of PV Panels

Energy production from solar panels is influenced by several different factors, with the most influential presented in this section. Focus is primarily set on environmental factors, in addition to some mechanical factors. The suns position relative to the earth and the properties of solar radiation is introduced first, being the clearly most influential factor. Furthermore, additional environmental factors such as temperature and soiling are explored.

2.3.1 Solar Radiation and Position of the Sun

The most influential factor in solar panels' performance is solar radiation, also known as solar irradiance, which is the output of light energy from the sun registered at the earth's surface measured in W/m^2. Solar irradiance can be integrated over a given period of time to obtain solar irradiation, measured in kWh/m^2 or J/m^2. The amount of available light energy at the earth's surface depends on factors as geographic location, time of day, season, atmospheric conditions and weather. [18]

The suns position relative to the earth is the main factor in determining available irradiance. Every 24 hours the earth makes one full rotation about its own axis, and one full revolution around the sun every 365.25 days. The revolution is not fully circular but slightly elliptical with an eccentricity of 0.01673, resulting in a difference of 3,3% between the longest and shortest sun-earth distance. In addition, the earth's axis of rotation is tilted at axis of 23.45° to the plane of the elliptic. These relationships are shown in figure 2.19, and is the reason the earth has four different seasons, with different positions of the sun. [18]

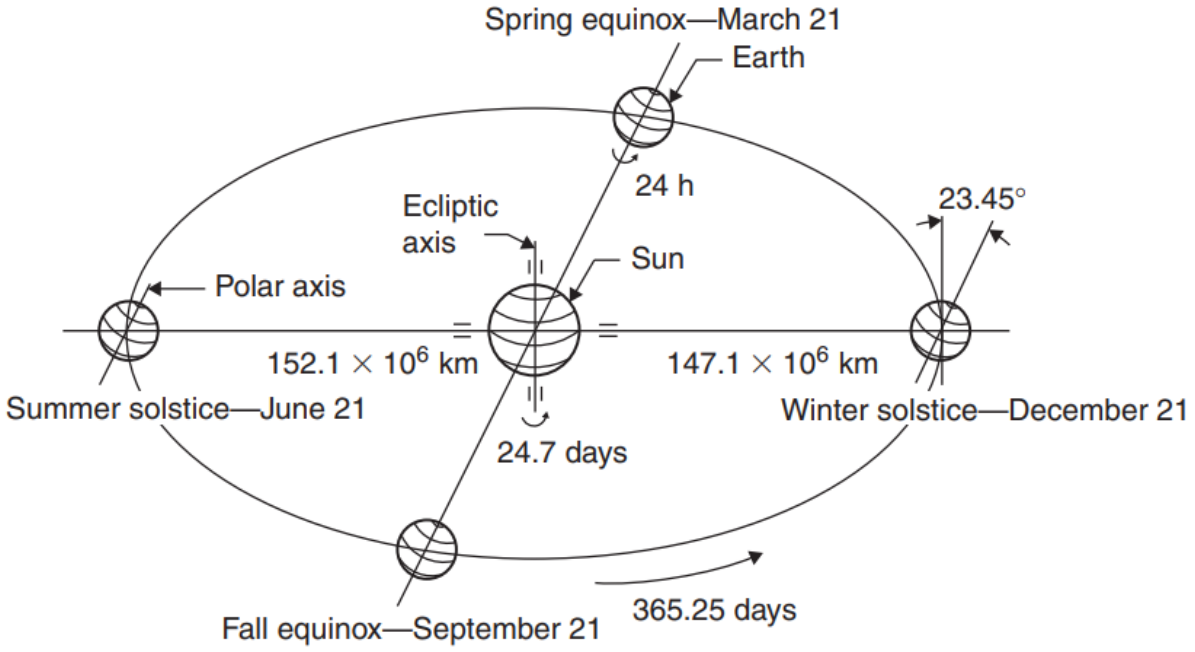

Figure 2.19: *Sun earth relationship [18].*

When winter moves towards spring and eventually summer, the points of sunrise and sunsets moves northwards along the horizon. In the Northern Hemisphere, the sun rises earlier and sets later, with the sun reaching a higher point each day. 21. June marks the summer solstice and is when the sun reaches its most northerly position related to the earth, in addition to being the longest day of the year. Winter solstice occurs half a year later, with the sun being at its most southerly position. In the middle of this six-month period, at 21. March and September, the length of day and night are equal and marks the spring and fall equinoxes. For the Southern Hemisphere, winter and summer solstices take place on opposite dates. [18]

2.3.2 Properties of Solar Radiation

Being an enormous fusion reactor where four hydrogen atoms are melted into one helium atom, the sun creates temperatures of around 15 million K. The created energy is scattered into all directions of space in the form of radiation with a value of $P_sun = 1367 * 10^26W$, with only a small fraction actually reaching the earth. This value is calculated assuming there is a sphere around the sun with a radius equal to the sun-earth distance, and dividing the suns radiation power with the area of the sphere. The result is the power density, or radiance at the earth's position, also called the solar constant of $1367W/m^2$. [50]

Planck's law of radiation states that the surface temperature of a body determines the spectrum of radiation. With a surface temperature of 5778K, the suns idealized black body spectrum is displayed as the dashed line in figure 2.20. Measured spectrum outside the Earth's atmosphere is displayed in red and roughly follows this line. Measured spectrum outside of the atmosphere is called AM 0, which stands for Air Mass 0 and indicates that the light has not passed through the atmosphere. Adding up all individual amounts of spectrum in figure 2.20 will result in an irradiance of 1367 $/m^2$, the solar constant. [50]

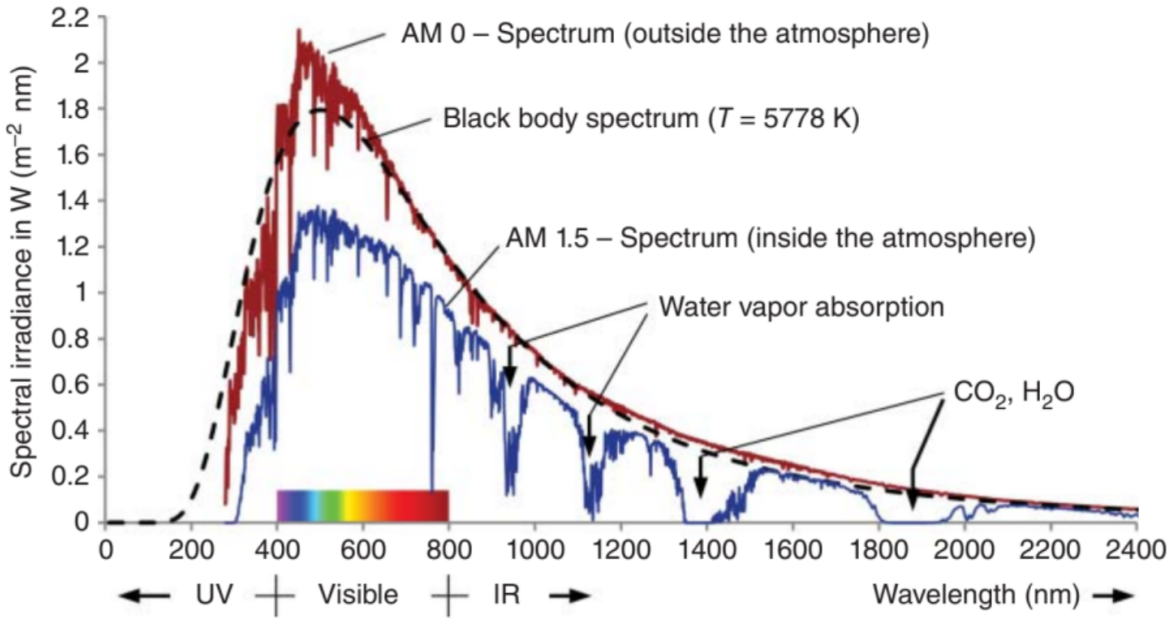

Figure 2.20: *Solar spectrum outside and inside of the atmosphere [50].*

When sunlight passes through the atmosphere, the spectrum changes due to several reasons: Reflection of light, light being reflected by the atmosphere and reducing the radiation striking earth. Absorption of light, molecules at a certain wavelength absorbing radiation. This effect can be seen in figure 2.20 by the gaps viewed in the AM 1.5 spectrum. Furthermore, scattering of aerosols and dust particles has an impact, mostly concerning particles large compared to wavelength of light, typically found in industrial and highly populated areas [50]. A measurement describing the water vapour contents and aerosols can be used in this respect, named the Linke turbidity coefficient. The coefficient ranges from 2.0, for dry and clear sky, to 5 or 6 in humid and/or very polluted conditions.[51]

The effect of changes in the spectrum when passing through the atmosphere is increased with a longer path of light. According to this, a different spectrum is appointed with regards to the path of sunlight through the atmosphere, as seen in figure 2.21. AM 1.5 means that sunlight has travelled 1.5 the distance compared to the vertical path, AM 1.

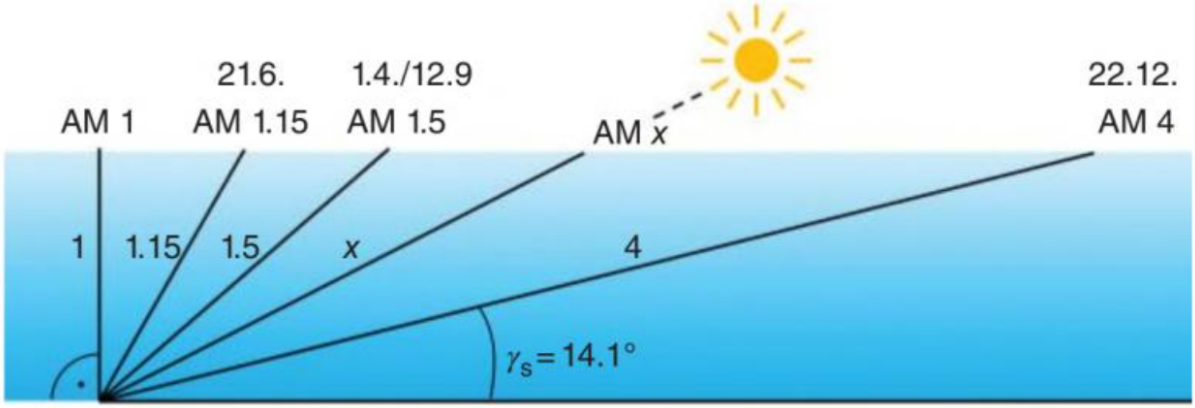

Figure 2.21: *Visualization of Air Mass. The number following AM indicates the elongation of the sunlight path compared to the vertical distance through the atmosphere. X is calculated by dividing 1 with the sine of a known sun height angle [50].*

As solar radiation passes through the atmosphere, its value can generally be composed of two components; direct and diffused radiation. The direct component is the energy from direct solar beams striking an area perpendicular to the beam on Earth's surface. The secondary component, diffused radiation, is obtained from sunlight passing through the atmosphere being reflected and scattered by air molecules, clouds, dust and other materials in the atmosphere, often referred to as aerosols. When measuring irradiance the term global horizontal irradiance (GHI) is used, being the sum of direct and diffuse radiation. For tilted surfaces, such as solar panels, which are often installed with an angle to the horizontal, a third component is added; reflected radiation. For a tilted surface, the sum of radiation is calculated using equation 2.1, with each component visualized in figure 2.22. [18, 52]

$$GHI = R_{Dir} + R_{Dif} + R_{Ref} \tag{2.1}$$

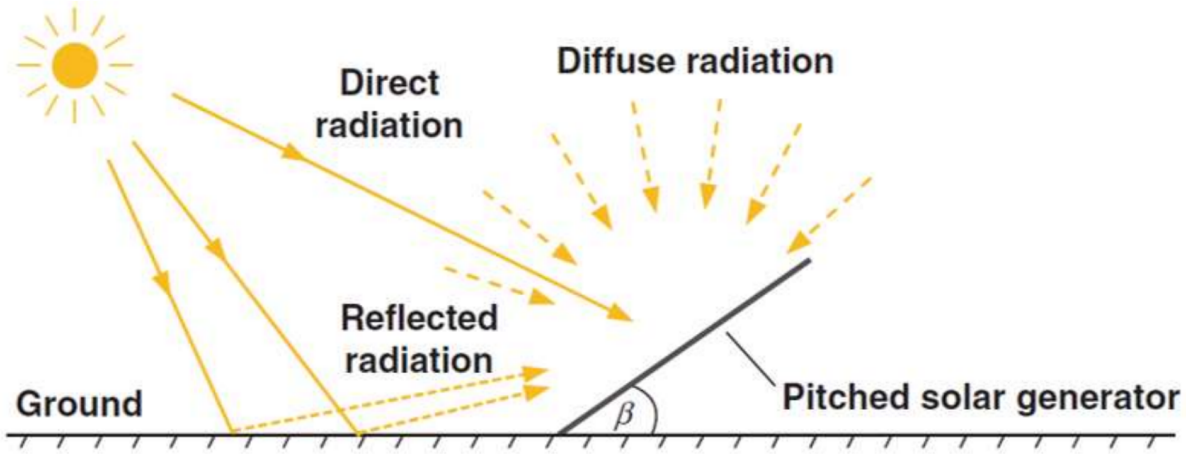

Figure 2.22: *Components of solar irradiance. [50]*

The reflected component is derived from solar radiation reflected from the earth's surface onto the inclined surface. The amount of reflection heavily depends on the properties of the struck surface and has a *reflection, or albedo coefficient* of 0-1.0. A completely white surface has an albedo of 1.0, while a completely black surface has 0.0. Vegetation, bodies and surfaces in nature have very different albedo coefficients, with snow around 0.85, grass around 0.26 and water around 0.05. [53]

When mounting a PV system, there are two main angles to consider: The tilt and azimuth angle. The tilt angle is the angle of deviation from the horizontal plane, while the azimuth angle is the deviation from true south in the northern hemisphere. Both angles are visualized in figure 2.23. The consideration of azimuth angle has an effect on what time of the day the system reaches maximum production and can be optimized for electricity demand on its connected system. Setting the azimuth angle west of true south will maximize production in the afternoon, sacrificing production in the morning. [18]

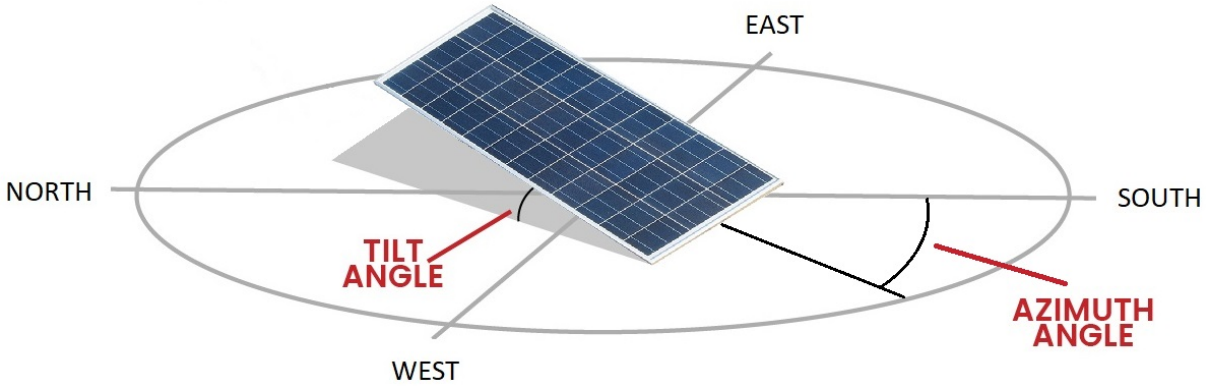

Figure 2.23: *Azimuth and tilt angles. Figure is edited from its original [54].*

Tilting the module can be performed at an angle equal to the local latitude in a practice latitude tilting. In reality a smaller tilt angle is often used to reduce self-shading to adjacent modules, lessen wind exposure and take advantage of summer months when the sun is higher in the sky. In general, the benefit of optimal tilting increases as one moves further away from the equator as the sun is lower in the sky. This increase reaches its maximum at a latitude of 65° and decreases towards the poles. [18]

2.3.3 Temperature

Operating temperature plays a significant role in the efficiency and power output of solar panels. As modern panels convert approximately less than 20% of the irradiance into electrical energy, the remanding is mainly converted into heat. Heat caused by excessive solar radiation and high ambient temperatures can lead to overheating and high operating temperatures of the panels. Studies performed on the subjects like *"Temperature Dependent Photovoltaic (PV) Efficiency and Its Effect on PV Production in the World"*, by Dubey, Sarvaiya and Seshadri conclude with a linear negative dependency of operating temperature and power output. Results vary with environmental, system and material variables, thus applying a particular expression for the dependency is difficult. The effect of wind velocity can be related to temperature, as increased wind will have a cooling effect on panels. [43, 55]

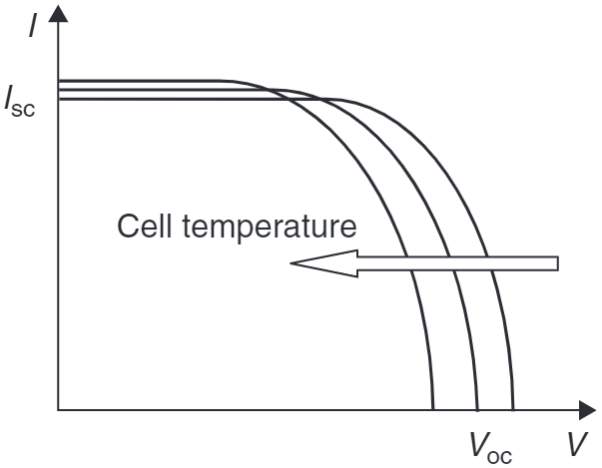

Figure 2.24: *I-V curve of solar panels with the arrow indicating effect of increased temperature [18].*

I-V curves for solar cells are often used to display the interrelationship between current and voltage and their respective effect on power. If the cell's terminals are connected to a variable resistance, the intersection of current and voltage determines the operating point and power can be calculated as the product. In figure 2.24, the effect of increased temperature is displayed. With increased cell temperature, the open-circuit voltage decreases linearly, leading to a drop in efficiency. The effect of decreased temperature naturally causes an opposite effect of higher efficiency. [18]

2.3.4 Soiling

Soiling refers to power loss from PV production due to the accumulation of snow, dust, dirt or other particles that cover the surface of solar panels. The effect can be categorized into two main types: hard and soft shading. Hard shading is caused by solids like bird droppings, leaves or dirt patches on the module, while soft shading is caused by smog or dust in the air. Naturally, rainfall will clean the panels regularly in some areas, but cleaning systems might be necessary in dry areas to improve efficiency. In residential areas and climates with regular periods of rain, the effect is usually low and can be neglected, being less than 1 % according to PVsyst. In more rural environments with typical agricultural activities, or industrial areas, the effect is on the other hand considered non-negligible. [51, 56]

What separates Norwegian conditions from large parts of the world, is the soiling effect caused by snow. The effect is very difficult to foresee and account for, as it has a significant impact with several variations, both negative and positive. For horizontally mounted modules, snow coverage are more of a problem, as the snow will remain on the panels until melted or removed. With a larger tilt angle, panels become less exposed to soiling from snow, and will in addition, be more exposed to ground reflected radiation, the albedo effect. [51]

2.3.5 Miscellaneous Factors

Power output from PV panels is decreased due to the effect of shadowing. This is relevant for the cell exposed to shading and the whole module since cells are connected in series. Following, shading half of a cell would lead to the entire power output from the module being cut in half. Shading can be caused by trees, buildings, ventilation systems or other objects blocking the sun. Leaves, birds and bird droppings can also cause shadowing. [55]

Degradation in PV modules is another factor that influences performance, with manufacturers considering a PV module degraded when its power reaches a level below 80% of its original power. Degradation factors include degradation of packaging materials, adhesion loss, corrosion caused by moisture intrusion, wiring and cables and semiconductor degradation [55]. Several reports are published on the subject displaying a wide range of yearly loss factors, with recent literature reviews concluding with a loss factor of around -0.5%/year. [57]

Under normal conditions solar systems require no operation costs as sunshine is a natural source of energy. However, the system might need lubrication, oil or other costs. Cleaning of panels might be required, as a thin film of dust can considerably degrade the modules' performance. It is although normal to include a certain yearly percentage of initial investment cost in the range of 0.5 - 1.0 % to cover unforeseen maintenance expenses and replacements costs. [55, 58]

3 Meteorological Conditions of Norway

This section will explore the meteorological conditions in different regions in Norway that impact power generation from solar panels. Solar irradiance will undergo the most research as it is the factor with the most substantial influence, but also temperature, precipitation and more precise, snow will be explored.

3.1 Potential of Power Generation

Figure 3.1 is an estimate of potential annual solar production in selected cities, provided by a WWF report. The values in the graph are based on a 1 kW system accounting for irradiance, temperature in addition to other factors. While measured irradiance in Norway is lower than Central-Europe, lower annual temperatures contribute to reducing system loss. As a result, the potential of power production from solar power in Kristiansand or Oslo is on the same level as cities in Germany, the largest solar power producer in Europe. [34]

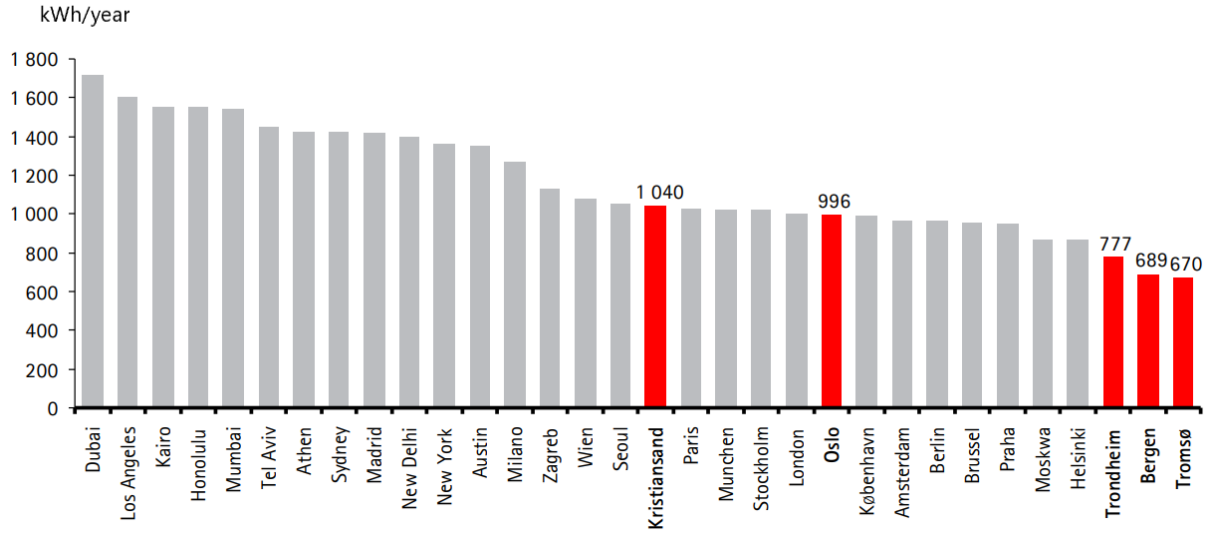

Figure 3.1: *Yearly production of solar power. Results based on a 1 kW system with 14% loss and 35° inclination. Figure is edited from its original [34].*

3.2 Latitude and Solar Irradiance

Being located between latitudes of 58.0° - 71.2°, differences in solar radiation across the country is one of the main characteristics of the Norwegian climate. These differences are shown with the big variation in daylight across latitudes at summer and winter solstices. At latitude 58° North (Kristiansand), the longest days are 18:11 hours, while the shortest days are 6:10 hours. At 63° North (aprox. Trondheim) daylight times varies from 20:19 hours to 4:42 hours, and at the Arctic Circle (66.5° north) it ranges from 24-0 hours, excluding twilight. In the summertime, regions in the north experience more than two months with constant daylight. In winter, the opposite occurs, experiencing two months of darkness. In these winter months, latitudes in the north receive no direct solar irradiance, but twilight from refraction and reflection of sunlight takes place until the sun is 18° below the horizon. [59]

In general, the intensity of solar radiation decreases further north due to factors as sun hours, cloudiness and aerosols, but also the angle of incidence (AOI), which decreases towards the poles. AOI is the angle between a horizontal plane and direct radiation and can be visualized in figure 2.22. [59] Summed up Norway receives irradiance in the region of around 600-1000 kWh/m^2 per year, with its distribution visualized by figure 3.2. [60]

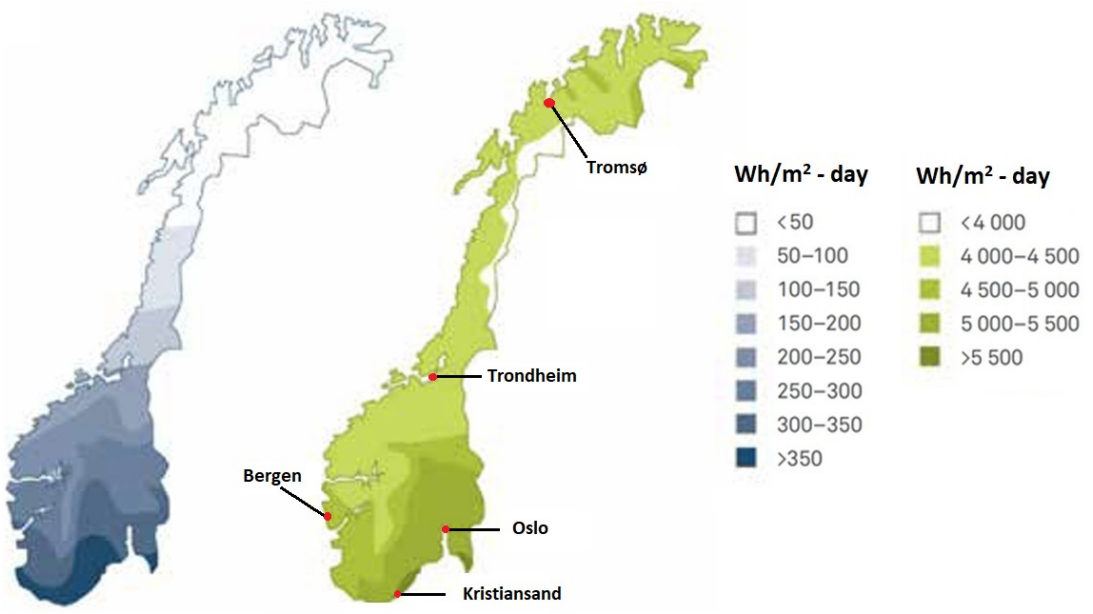

Figure 3.2: *Daily irradiance for a horizontal plane across Norway in January(left) and July(right). In addition, the location of each city is shown on the map. Figure is edited from its original [60].*

Irradiance does not only decrease northwards, but also westwards. Norway is located in a zone of westerly winds, that in combination with the increased elevation along the coast, causes the rise of humid air masses. As a result, the Norwegian south-west coast experiences increased cloudiness and precipitation, resulting in decreased annual solar irradiance. Due to a lack of reliable sources for measured irradiance in selected cities, sun hours is used to display this factor. Figure 3.3 show average monthly sunshine hours for selected Norwegian cities, where a general increase southwards can be observed. Spring and summer months in Tromsø also yields results both equalling and exceeding those of Bergen, and reaches close to Trondheim in late summer. [59]

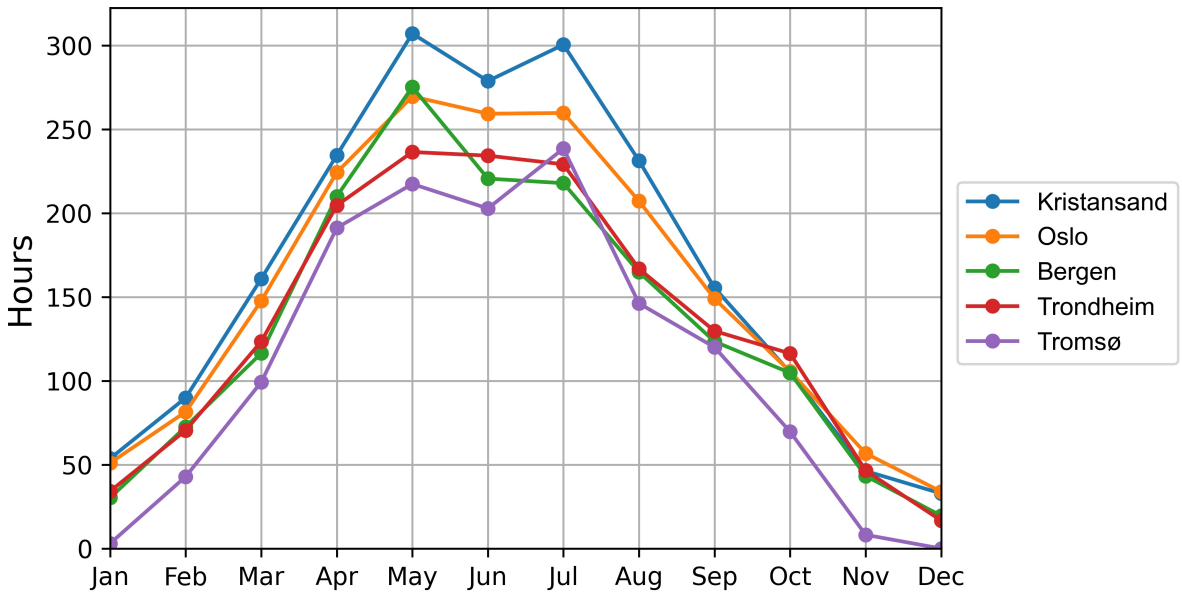

Figure 3.3: *Average monthly sunshine hours for 2016-2020. Data is imported and plotted from Norwegian Climate Service Service [61].*

3.3 Temperature

Average monthly temperatures for selected cities across the whole year is displayed in figure 3.4 and shows the relatively mild winter months and cool summer months typical for the Norwegian climate. The general trend is a temperature increase further south, but long periods of below zero temperatures in Tromsø is also noteworthy.

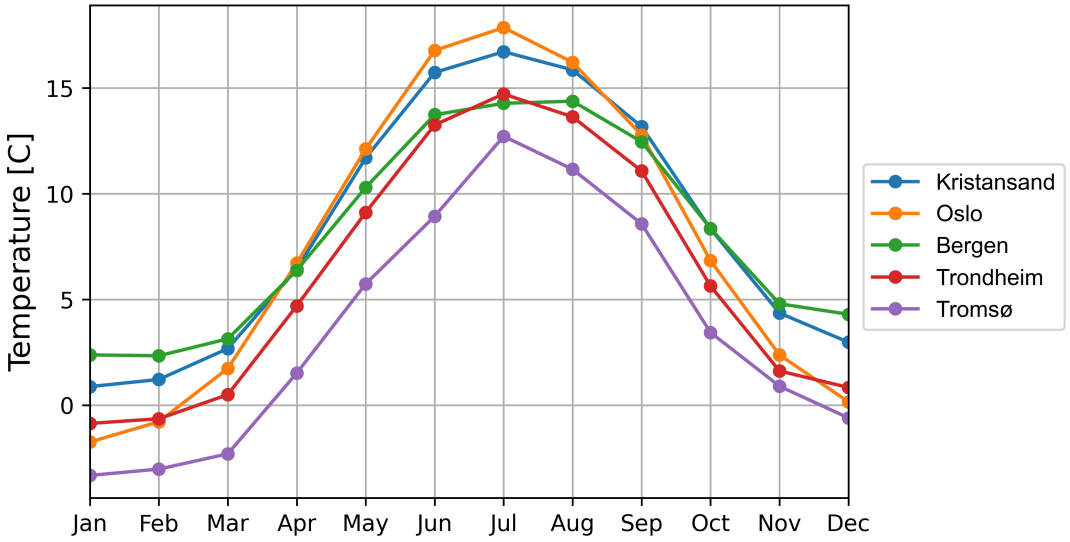

Figure 3.4: *Average monthly temperature 2016-2020. Data is imported and plotted from Norwegian Climate Service Service [61].*

3.4 Precipitation

Figure 3.5 displays average monthly precipitation for selected Norwegian cities. The general trend is a higher grade of precipitation along the coast, with Bergen receiving multiple times more precipitation as cities further inland.

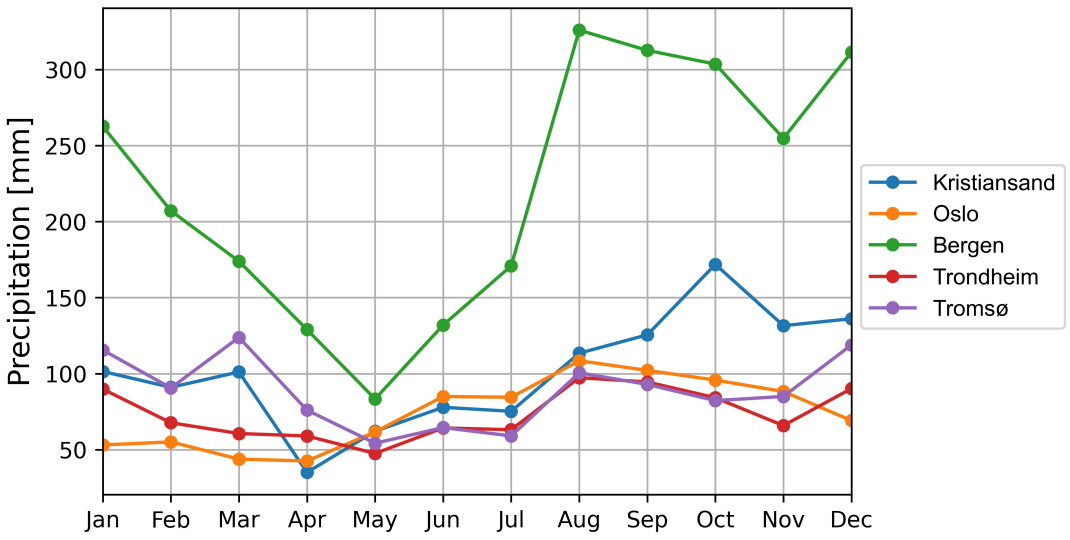

Figure 3.5: *Average monthly precipitation for 2016-2020. Data is imported and plotted from Norwegian Climate Service Service [61].*

3.5 Snow

As explained in section 2.3.4 the effect of snow has a huge impact on the performance of solar panels. Figure 3.6 displays average monthly snow cover in selected Norwegian cites. Snow cover is registered using a code of 0-4, where 4 indicates complete snow coverage and 0 represents snow-less conditions. Due to a lack of measured snow-data in Kristiansand, close by Lindesnes is selected to represent its values. [61]

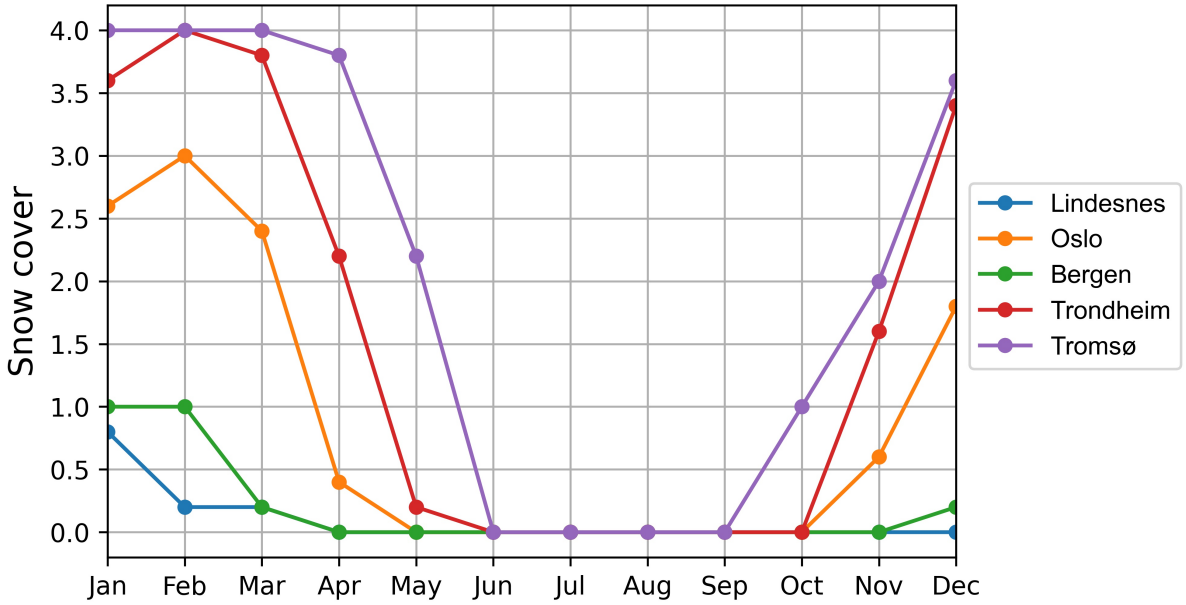

Figure 3.6: *Average monthly snow cover for 2016-2020. Data is imported and plotted from Norwegian Climate Service Service [61].*

4 The Electricity Market

This chapter will cover all the factors that together form the foundation of the electricity price. Hereinafter, the organization and infrastructure of the Norwegian power grid are explored, followed by information on the power market, where electricity is bought and sold. The division of regional bidding zones is introduced, including historical price differences between them. Furthermore, information on the contents of the electricity bill is presented with definitions of different shares and price variations across bidding zones. Finally, information on relevant regulations and future electricity costs is presented.

4.1 Electricity Grid

Electricity production and consumption rarely occur at the exact location, making a well-developed electricity grid essential for the transportation of power from producer to consumer. The electricity grid is interconnected between different geographic regions, allowing power trade across borders. The grid must be able to handle vast variations in consumer demand, production availability and exportation. The Norwegian grid consists of three levels: The transmission, regional and distribution grid. [62]

The transmission grid connects large producers and consumers in a nationwide system, as well as including international connections. In Norway, the designated transmission system operator (TSO) is Statnett. The regional grid connects the transmission grid to the distribution grid, which acts as the local electricity grid that supplies the consumer with power. The distribution grid carries voltage up to 22kV and separates into two categories: High and low voltage, divided at 1kV, where the low-voltage distribution to customers usually carries 400V or 230V. Large-scale electricity producers are connected to the transmission or regional grid, and smaller producers to the regional or distribution grid. [62]

The majority of the transmission grid in Norway is owned by Statnett, a company under state control by the Ministry of Petroleum and Energy. The primary responsibility for the grid is to secure a steady balance between generation and consumption of electricity, as well as the operation, maintenance and development of the central grid. Statnett owns about 94% of the transmission grid, while the rest is owned by regional grid companies also engaged in both trading and production. Most of the regional and distribution grids are owned by the local municipalities and counties, in addition to some private ownership. [62, 63]

4.2 The Power Market

The introduction of The Energy Act in 1990, based on the principle of marked based energy production and trading, gave Norwegian energy consumers the option of purchasing power from the supplier of their choice based on factors as price or other considerations. The introduction created a new state within the market, where suppliers had to compete for customers. Succeeding The Energy Act, the Nord Pool Spot power exchange was established in 1996 and served as the worlds first power exchange where power could be traded across borders. Today, Norway is linked with the other Nordic countries both by physical interconnectors and financial connections. These are in turn connected to the European power market through, amongst others, Germany, the Netherlands and the Baltic states. [64, 65]

Because of these interconnectors, power can be consumed where its demand is highest and its value greatest. During periods in Norway with little rain and low temperatures, the demand is often high while the energy production is low. Due to the high demand, domestic energy prices are high, and importing energy from foreign countries is a cheaper solution. Therefore, the prices are increased, and power is imported. In periods with high production and low demand, the situation will lead to power being sold to areas with greater demand and lead to lower domestic prices. [65]

The Nord Pool spot power exchange sets the power price each day, based on the market's supply and demand. The price can vary greatly in both 24-hour periods and throughout the seasons due to variations in factors such as precipitation, temperature and transmission conditions. Power distributed throughout the grid follows rules of physics and flows through the path of least resistance. As a result, power cannot be traced, or different sources separated from each other. This means that the consumer has no way of knowing the origin or path of the power consumed. To form the basis for settlement, grid companies keep track of how much power is delivered by the producers and how much is consumed by the end-user. [65]

4.2.1 Organisation of the Power Market

The power market can be divided into two main sections; the wholesale and end-user market. In the wholesale market large volumes and quantities of power are bought and sold by brokers, different industrial companies and customers as well as power producers and suppliers. The wholesale market consists of different markets where bids for power are submitted and prices are determined: [65]

- The day-ahead market
- The continuous intraday market
- The balancing markets

The primary market for power trading in the Nordic region is the day-ahead market. Here, contracts with deliverance of physical power hour-by-hour for the next day are bought and sold by making bids and offers to the Nord Pool trading system each day between 08:00 and 12:00. The TSOs for each bidding area publishes trading capacities before 10:00 every day, and the auction closes at 12:00. Prices for each hour of the following day are then calculated with basis on received purchase and sell orders, together with available transmission capacity. The day-ahead market plays a vital role in ensuring balance between supply and demand, but due to events that may occur after the auction in the day-ahead market has ended, for example vast changes in weather forecast, there is need for intraday market. In the intraday market it is possible to trade closer to the delivery of power, providing the customer and supplier with a greater chance of achieving balance between supply and demand. [65]

Even with the balance created in the day-ahead and intraday markets, events will occur that disturb the balance within the hour of operation. This is where Statnett utilizes the balancing markets to adjust production and consumption in order to maintain instant balance at a frequency of 50 Hz. In the Nordic region, the balancing markets are divided into primary, secondary and tertiary reserves. Primary and secondary reserves are automatically activated upon changes in frequency, while tertiary reserves are manually activated. [65]

4.3 Electricity Prices

Every day, Nord Pool power exchange calculates the system price for the following day. The system price is used for the whole Nordic market and serves as a reference price when setting prices in the financial sector in the Nordic region. The price is based on the assumption that there is no congestion in the transmission grid and is therefore counted as theoretical. The system price is strongly influenced by the Nordic regions high trading capacity, and therefore highly affected by each countries respective power markets consisting of energy sources like thermal power plants, reliance on the price of coal, natural gas and emissions costs. Production and consumption of renewable energy in the region also affects the price. [65, 66]

Other influential factors are precipitation and water inflow. This is due to a big portion of the Nordic power market being supplied by hydropower. Lots of rainfall, or high temperatures leading to snow melting, will result in high production capacity and lower prices. On the other hand, low temperatures will lead to a higher demand for heating and following higher prices. In addition, the price is influenced by a wide variety of factors that the scope of this assignment does not cover. [67]

4.3.1 Bidding Zones

As well as setting the system price, Nord Pool sets area prices that are made based on congestion in the grid. The area prices create a balance between purchase and sales bids from contributors in the different bidding zones in the Nordic region. By 2021, Norway has five bidding zones, Sweden four, Denmark two, while Finland accounts for one bidding zone. The bidding zones are shown in figure 4.1. Norway's five bidding zones are named NO1-NO5, and their division reflects physical structural congestions (transmission constraints) in the grid. The main reason for congestion and variations in power prices across bidding zones is the difference in power situation across regions. Some regions might experience a power surplus, and others a deficit at the same time, leading to power being imported to deficit areas and power exported from surplus areas. Congestion arises when the transmission grid lacks the capacity to handle the demand. [65, 68]

Bidding zones/area prices are mainly an essential tool for short term balancing, but the prices also indicate where there might be a need for longer-term measures in the power system. Price differences across zones indicate and will make producers and consumers aware of where new generation capacity or large consumers should be located. The separation into individual bidding zones does not necessarily result in different prices. With no constraints in capacity across zones, prices will remain and correspond to the system price. [65] Historically, price differences across bidding zones are similar but figure 4.2 shows some differences, with section NO3 (Trondheim) sticking out with the historical higher prices.

Figure 4.1: *Map of bidding zones in the Nordic region [69].*

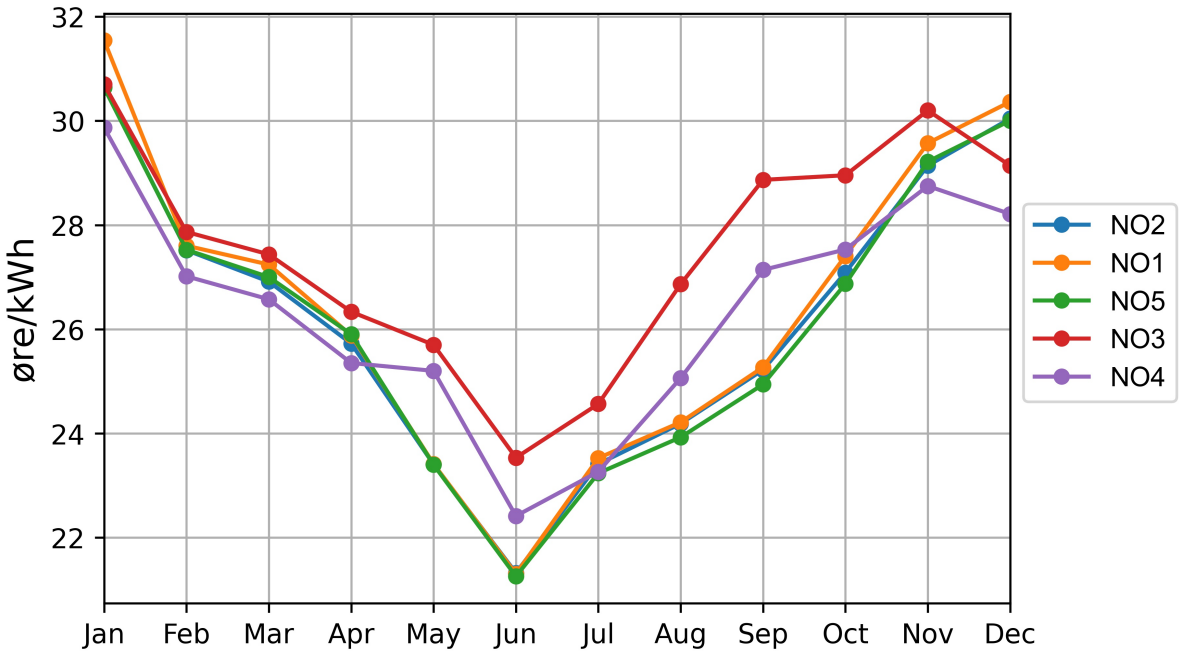

Figure 4.2: *Average price differences across bidding zones for 2013-2020. Data collected from NordPool [70].*

4.3.2 Contents of the Electricity Bill

The complete electricity bill can generally be divided into three main parts. The first part is the price of electricity, which varies with not only bidding zones but also the kind of contract signed. End users, consumers who purchase power for their own consumption, are in Norway free to choose their supplier of power, who offers a different kind of contracts. What separates the different types of contracts is the degree to which they follow the spot price of electricity for the region, using a fixed or variable price, including a markup. [65]

Grid tariff is the second part and covers expenses of power transportation and operation, in addition to usage and development of the grid. The grid tariff is set by the power company itself, but its sizing is controlled by NVE. For business customers, grid tariff is again divided into three shares: A yearly fixed share, a share based on monthly used energy and a share based on the hour with the highest power consumption during each month. The fixed share is set at the start of the year and varies with regions in the range of 1-21 thousand NOK per year. The energy share is based on total monthly energy usage and is calculated from a price usually in the region of 3-7 $øre/kWh$. The price may vary slightly with the seasons, as some companies operate with separate prices for the summer and winter months. The last part, the power share, varies substantially with different regions and power companies. As mentioned, it is based on the hour of each month with the highest consumption of power. The price is generally divided into summer and winter months, in addition to varying with the amount of energy used per month. The price is given in $NOK/kW/mnth$. [71, 72]

In order to use grid tariff as part of the final calculations, tariff prices were gathered from each bidding zones main grid company and presented in table 4.1. All companies have a wide range of price categories depending on what type of grid the consumer is connected to, the sizing of the fuse and consumption. In order to select relevant prices, a few assumptions had to be made: The designed system is connected to the low-voltage grid and fuse in the range of 125-330A. Each company has different methods of calculating the final price and defines summer and winter months in different methods. Additional information on the structure and season definitions for each region is found listed below the table.

Table 4.1: *Structure of grid tariff in each bidding zone. Sum = summer and win = winter. All of this information was public on each of their respective websites, and sources can be found listed below table.*

	Fixed [$NOK/year$]	**Energy sum.** [$øre/kWh$]	**Energy win.** [$øre/kWh$]	**Power sum.** [$NOK/kW/month$]	**Power win.** [$NOK/kW/month$]
Agder Energi (NO2)	750	4.1	4.1	0-50 kW: 37.80 50-200 kW: 28.36 200-1000 kW: 18.91 1000 + kW : 9.47	0-50 kW: 113.42 50-200 kW: 94.51 200-1000: 74.60 1000 + kW: 56.69
Elvia (NO1)	3280	3.9	7.0	22.0	120.0 67.0
BKK Nett (NO5)	21000	4.3	4.9	0-200 kW: 53.9 200 + kW: 47.3	0-200 kW: 62.7 200 + kW: 52.8
Tensio (NO3)	8000	5.0	5.0	0-99 kW: 39 100-399 kW: 33 400 + kW: 27	0-99 kW: 59 100-399 kW: 49 400 + kW: 30
Arva (NO4)	10400	3.6	3.6	May: 16 Jun: 16 Jul: 16 Aug: 16 Sept: 30 Oct: 43	Nov: 56 Des: 71 Jan: 71 Feb: 56 Mar: 43 Apr: 30

- Agder Energi defines their summer period from May through October and their winter from November through April. Additionally, it sets the power share price based on how much power is consumed, with four different categories for each period. The attached source displays prices from 2020 but is unchanged for 2021. [73]

- Elvia defines their summer period from April through October and their winter period from November through March. The company also separates the winter power share into two periods; December through February and March and November. [74]

- BKK Nett sets their summer period from April through September and winter period from October through March. They only separate between two levels of power usage in both periods. [75]

- Tensio has the same summer and winter periods as Agder Energi, with summer from May through October and winter from November Through April. Tensio sets their power share in three categories of sizes. [76]

- Arva has different power shares for each month and does not separate by the amount of power used. [77]

Setting of the grid tariff varies from regions as grid companies have different grid costs determining the grid tariff. The cost is determined by local climate and topography, age of the grid and cost compared to competing companies. Additionally, grid companies to some extent have freedom when it comes to the outline of the grid tariff. This leads to variation in how grid companies decide to distribute their income from fixed tariff, energy or power share. [73, 78]

The third and final part is made up out of taxes & fees. In recent years, this part has consisted of the Enova levy, electricity tax, VAT(value added tax), and the newest addition: the electricity certificates, introduced in 2012. This composition and its historical development are visualised in figure 4.3, where all included taxes & fees are located in the middle of each bar for every year, placed in between the power price and grid tariff. [65]

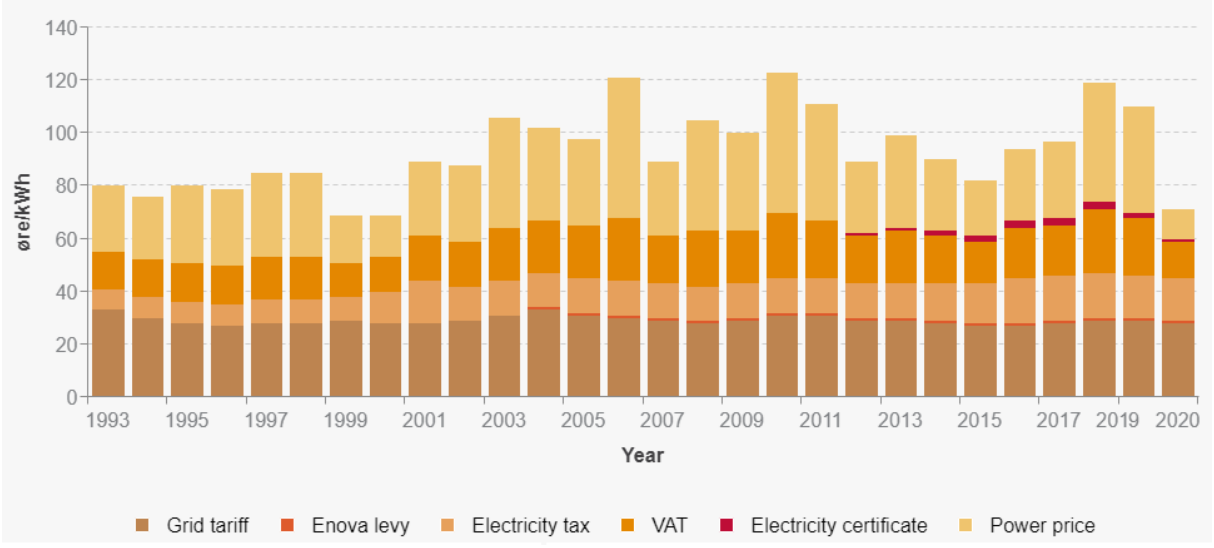

Figure 4.3: *Composition of end-user prices for households. Figure is edited from its original [65].*

For business customers, the electricity tax for 2020 was set to 16.69 $øre/kWh$, but it has a few exceptions. Large parts of business customers in Troms and Finnmark are except due to political reasons, having to pay a reduced fee of 0.546 $øre/kWh$. [79] Once Enova levy of 800 $NOK/measuring-ID$ and electricity certificates are included, the VAT rated at 25% comes on top. Most business customers are although eligible to get this refunded.

4.4 Prosumers

A prosumer is a customer of the power grid that both delivers and consumes electricity. Prosumers do not pay for electricity delivered to the grid because of the Norwegian prosumer arrangement (Plusskundeordningen). The arrangement requires that the point of connection measure both the electricity in and out of the grid. The arrangement does not change the fact that the grid company still have to provide delivery- and voltage quality, connection, delivery and plant cost. The plant cost is a fee from the grid owners when someone wants to be connected, increased capacity or increased quality on their grid connection [80]. As long as the prosumer does not surpass the limit of 100 kW delivered to the grid or increases the overload protection, the grid company can not bill them for plant cost even if the increased load on the grid would demand an upgrade or expansion of the existing network. [81]

Prosumers have to agree with their respective grid company to ensure that the grid company can ensure that the grid can handle the load and aligns with the applying regulations. In addition, the prosumer has to agree with an electricity provider that can handle both selling and buying of electricity. The prosumer can not sell their production to other users or participate in the electricity market under the rules of the prosumer agreement. If the prosumer surpasses the limit of 100 kW delivered to the grid, the prosumer will not qualify for the prosumer arrangement. Additional costs like plant fees and fee for providing electricity to the grid would be billed to the prosumer. [81]

4.5 Future Electricity Costs

2020 saw the lowest price for electricity in Norway since 2012, with the average price for electricity for service industries dropping as much as 62 % lower than 2019 [82]. The electricity prices in the South of Norway even became negative in the summer due to negative prices in both Denmark and Germany. In the annual electricity market report published by the Norwegian Water Resources and Energy Directorate (NVE), the decrease in electricity price was mainly explained due to record amounts of snow in the mountains during the winter of 2019/2020, in addition to a hydrological surplus in 2020. [82, 83].

The electricity prices are expected to increase in the future. According to NVE long-term power market analysis from 2020, the prices are expected to increase from 0.38 NOK/kWh in 2022 to 0.41 NOK/kWh in 2040, with an average electricity cost between 0.38NOK/kWh and 0.42 NOK/kWh. Figure 4.4 illustrate the trajectory of electricity prices in Norway according to NVE. [83]

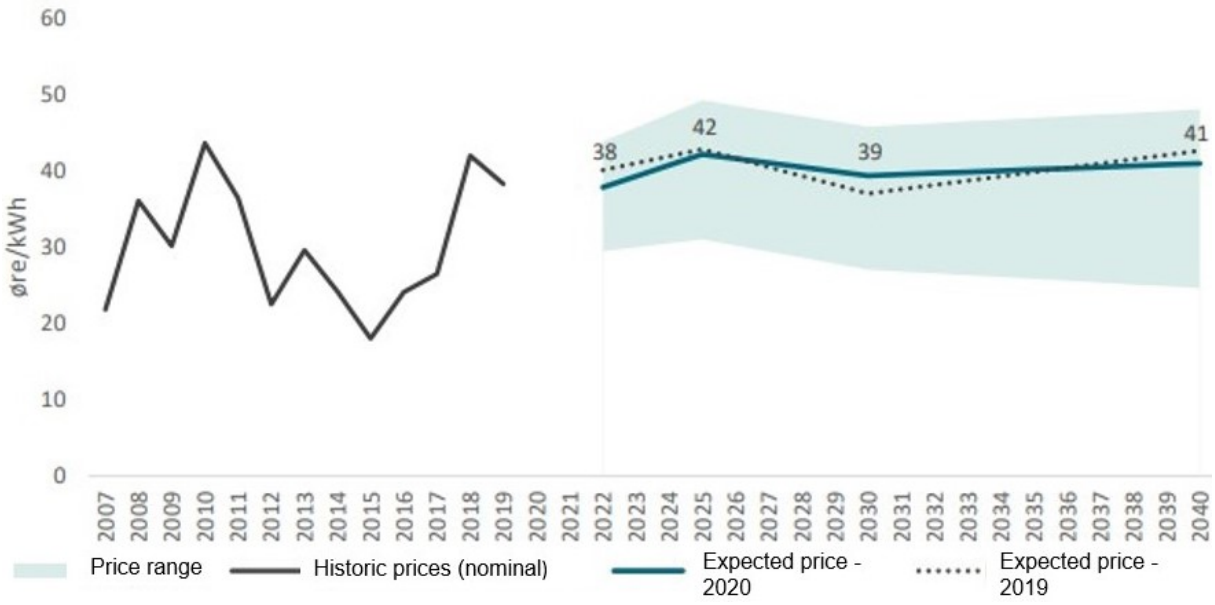

Figure 4.4: *An overview of the previous electricity prices and NVEs estimated future electricity prices [83].*

In the short term, the electricity prices will mostly depend on weather conditions. Rain and warm weather will decrease the electricity price, while warm and dry weather will increase the electricity cost. The future electrifying of industry and the Norwegian shelf will increase the future electricity costs, while new production from wind, solar and hydro will contribute to a lower electricity price in the future. The report from NVE also stresses that the market will adapt, and the electricity prices will determine whether investments in new energy production and energy efficiency will be profitable. [83]

Figure 4.4 has a wide price range for the future, which ranges from 25 $øre/kWh$ to 48 $øre/kWh$ in 2040. The price range is dependent on the future CO_2-fees and fossil fuel. While the amount of rain in Norway impacts the electricity prices in the short term, the CO_2-fees and price of fossil fuels have a higher impact on the long term electricity prices. [83]

The grid tariff is also expected to increase, at least up to 2026. With the electrifying in the communities, the grid owners have to increase their investments in the grid and use more funds on operation and maintenance. There are expected increases in all grid parts, with the most significant investments in the regional and central grid. If the inflation is considered, the prices will increase less and start a slight decline after 2023, according to Energiinorge.no in 2018 [84]. The decline will be caused by an expectation of smaller investments in the central grid after 2013.

Methodology

The analysis for this report was divided into three main sections: The gathering and selection of data, the simulation and modelling of a PV s system in the simulation software PVsyst and the financial analyses performed in the programming language Python. The purpose of the analysis was to examine the impact of geographical differences when installing solar panels on refrigerated warehouses and the correlation between the load of refrigerated and PV-cells. Therefore, the emphasis was on the parameters that deviate when location in Norway changes. The five cities selected for the analysis were Kristiansand, Oslo, Bergen, Trondheim and Tromsø, which each represent the largest city in their bidding zone.

First, an appropriate load profile was selected from a sample of load profiles collected. A PV system was then designed and modelled in the proportion of the load profile selected. The same PV system and load profile were used for the five selected locations. In every city, the PV system was simulated for the lifespan of the designed system based on data provided by Meteonorm. The lifespan was set to 25 years because most PV retailers guarantee this lifespan of their sold PV systems. After the simulations, the cost-benefit analyses for the system in the selected city was calculated based on the load profile, energy production, grid rent, electricity prices and fees & taxes.

5 Data Gathering

This section explains the collecting and selection of load profiles. A collection of multiple load profiles were gathered and presented below. Based on the data quality, data adequacy and trends, one load profile was selected for the rest of the analyses. This profile is illustrated with monthly energy consumption and hourly average values for each month.

5.1 Collection of Load Profiles

Initially, a load profile was required to represent the refrigerated warehouse. Multiple companies were contacted in the process to gather a load profile. This included ASKO, Login Eiendom and Trondheim Havn, which willingly shared their data and experience. ASKO is a distributor of groceries in Norway, while Login Eiendom manages logistics and industrial properties. Trondheim Havn manages bay areas on behalf of the municipality and facilitates infrastructure for transport, personal traffic, and tourism [85]. A total of seven yearly load profiles from six different warehouses were collected, mainly from 2020. The purpose of collecting multiple load profiles was to get an overview of different load profiles to identify trends and select one deemed representative.

Many refrigerated warehouses have already installed PV systems on their roof, including those who provided data to this thesis. The data provided from the refrigerated warehouses were mostly the bought energy from the grid. However, the energy production from the PV systems had to be considered as well. Therefore, the PV production had to be added to the bought energy from the grid to get the total energy consumption of the refrigerated warehouses where PV systems already were installed.

All the collected load profiles with complete data sets can be found in figure 5.1-5.5. The data provided from Trondheim Havn and one instance of data from Lgin Eiendom were not sufficient enough and are therefore not presented. The refrigerated warehouses with load profiles illustrated in 5.1, 5.2, 5.4 and 5.5 have PV systems on their roofs. As explained, to get the load profile of these refrigerated warehouses, the bought electricity had to be added with the amount of production at their facility. The figures 5.1, 5.2, 5.4 and 5.5 were therefore created assuming that the produced PV system energy is used at their facility.

However, when the PV production leads to a surplus of energy, some of the PV production can be sold. Most refrigerated warehouses did not distinguish the amount of production sold and used at their facilities in the provided data. ASKO Midt-Norge's refrigerated warehouse was the only one that distinguished their PV production between used and sold. Their load profile, illustrated in figure 5.1, does therefore

not include sold energy to the grid, while ASKO Vestby, figure 5.2, Login Vagle, figure 5.4 and Login Vinterbro, figure 5.5, might do. This leads to some uncertainty of the precision of the load profiles 5.2, 5.4 and 5.5. In addition, Login Eiendom has implemented energy storage solutions, which leads to even further uncertainty of the energy consumption to the load profiles illustrated in figure 5.3, 5.4 and 5.5.

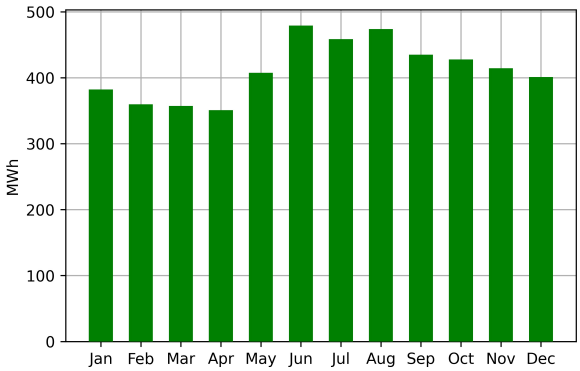

Figure 5.1: *The load profile for ASKO Midt-Norge in 2020.*

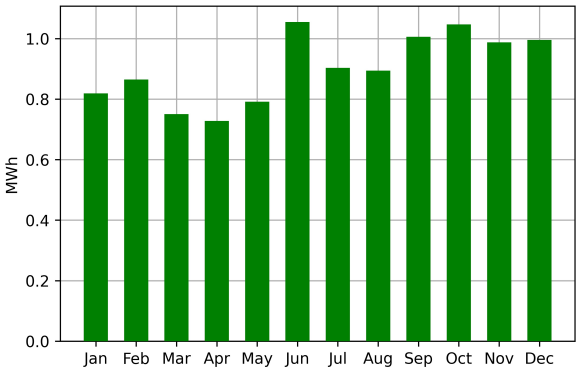

Figure 5.2: *The load profile for Asko Vestby in 2020.*

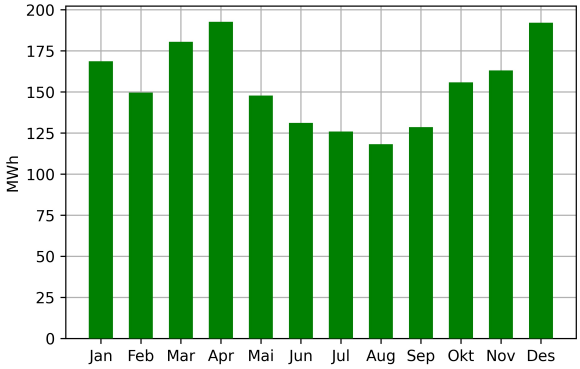

Figure 5.3: *The load profile for Login Bergen in 2020.*

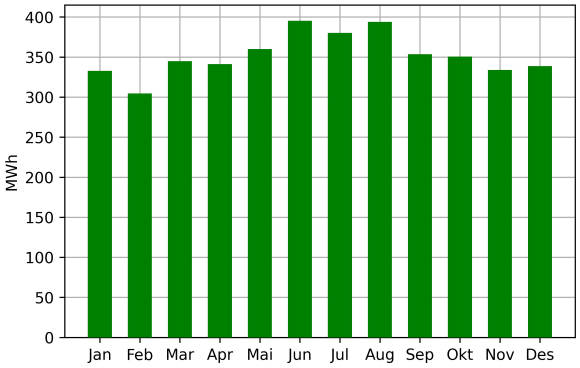

Figure 5.4: *The load profile for Login Vagle in 2020.*

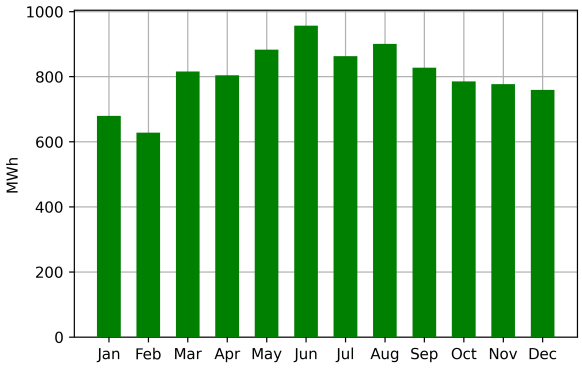

Figure 5.5: *The load profile for Vinterbro in 2020.*

Unlike the other refrigerated warehouses, the refrigerated warehouse with a load profile presented in figure 5.3 does not have PV systems on their roofs. This load profile is the clear distinction of the collected load profiles. This is not because the warehouse lacks a installed PV system, but this refrigerated warehouse has a dysfunctional heat recycling system, leading to increased energy consumption during the winter. The load profile is therefore not representative and excluded in the further selection progress.

5.2 The Selected Load Profile – ASKO Midt-Norge

ASKO Midt-Norge's load profile was selected, with the main reason being the distinction between PV system energy production sold to the grid and used at the facility. Even though the impact of including all the produced solar energy is small, there will be an effect on the hourly values used in the analyses. ASKO Midt-Norge also approved using their data without any anonymization and had the highest quality of the data. There was essential to find a load profile representative of a refrigerated warehouse. All except load profile 5.3 and to a certain degree load profile 5.2 have a flat curve with a peak during the warmest months of the year. The shape of these load profiles is in line with the fact that transmission- and infiltration load is temperature-dependent. Data suffiency and quality was also important. For instance, the production added on the bought load in figure 5.5 are monthly production data. For the analyses in this report, hourly values were required, so the sufficiency of data excluded this load profile.

Because ASKO Midt-Norges load profile had a characteristic shape for a refrigerated warehouse based on the sample in this paper, high quality of their data and sufficient data, their load profile was used in the analyses. ASKO Midt-Norge's load profile is presented in figure 5.1 with monthly intervals. The raw data from the load profile used in calculations are hourly and includes peaks and lows of energy consumption during the year 2020, which is not visible in figure 5.1. The 29th of February was removed from the data because the analyses do not consider leap years.

Even though ASKO Midt-Norge's load profile was considered the most certain load profile, there are some uncertainties. Because only one year with energy consumption was collected, uncertainties related to the weather were not considered. There will be changes in weather every year, which leads to a different energy consumption every year. In addition, the same selected load profile is used in the analyses for all five cities. To a certain extent, this will be imprecise because different temperatures in Norway will affect the energy consumption of refrigerated warehouses. Higher temperature during the summer in Kristiansand will possibly lead to a higher power peak demand, while colder winters in Tromsø might lead to lower peaks. These differences disappear when the same load profile is used for all five cities.

6 PVsyst

This section will go through each step from start to end in the process of designing a PV system at a selected location and generating production results. As one of the two main purposes of this assignment is the comparison of influencing factors in five different cities in their respective bidding zones, individual system optimization and considerations in PVsyst has for the most part been disregarded. In order to produce more precise results, consideration in regards to both local climatic conditions and surrounding environment would have to weighted more precisely. The final design can therefore be viewed as rudimentary.

Decisions made, components selected, and explanation of program functionality will to a varying degree be explored, with the purpose to provide the reader with an insight of final system specifications and understanding of each factors influence. The section will begin with an explanation of how PVsyst uses and generates meteorological data.

6.1 Meteorological Data

Horizontal global and diffuse irradiation are required as an external input in order to perform the simulation, as there is no good way to simulate them just based on geographical location. The other points are not required as an external input to the simulation, as they can be estimated using established models in PVsyst. [86] Figure 6.1 shows an example of monthly meteo data gathered from Oslo.

	Global horizontal irradiation	Horizontal diffuse irradiation	Temperature	Wind Velocity	Linke turbidity	Relative humidity
	kWh/m²/mth	kWh/m²/mth	°C	m/s	[-]	%
January	8.3	5.8	-1.5	2.39	2.763	80.3
February	23.2	15.2	-1.9	2.40	2.841	77.3
March	63.5	31.1	0.8	2.50	2.958	68.7
April	100.8	53.4	6.1	2.80	3.327	65.6
May	150.9	64.1	11.7	2.80	3.207	60.2
June	159.3	80.8	15.2	2.80	3.001	59.9
July	153.2	67.9	17.9	2.39	3.096	66.8
August	113.0	65.5	16.9	2.50	3.056	68.1
September	71.8	37.0	12.1	2.60	2.871	72.8
October	31.3	19.6	6.5	2.39	2.867	79.8
November	10.5	7.4	2.6	2.50	2.830	79.7
December	4.5	3.7	-1.1	2.38	2.756	81.7
	890.3	**451.6**	**7.1**	**2.5**	**2.964**	**71.7**

Figure 6.1: *Screenshot of monthly meteo data for Oslo in PVsyst. Numbers at the bottom represent summed yearly irradiation values for the two first columns and average values for the final four.*

Simulations of solar system performance in PVsyst are performed in hourly steps over a whole year, while the built-in meteo data comes in monthly values. Consequently, PVsyst needs hourly meteo data in order to simulate performance. This is done by generating synthetic data based on the monthly values, using special algorithms. For irradiance, synthetic data is generated using stochastic models developed by the Collares-Pereira team in the 1980's [86]. The model starts by generating a set of daily values, followed by a sequence of 24 values per day, using Markov transition matrices. For temperatures, no model exists for predicting temperature evolution as a function of irradiance, as temperature mainly follows atmospheric conditions. Following, temperature generation is primarily random while correlated to the irradiance. In general, it should be noted that the whole process of generating hourly values is a fully random process. Performing two generations with identical data sets may produce variations of 0.5 - 1.0 % in yearly results. [86]. The result of hourly gata generation can be seen in figure 6.2.

Interval beginning File beginning	GlobHor W/m²	DiffHor W/m²	T_Amb °C	WindVel m/s	RelHum ratio
06/06 02h00	0.0	0.0	12.8	1.5	0.801
06/06 03h00	4.2	4.2	12.9	2.6	0.801
06/06 04h00	56.2	48.3	13.6	1.9	0.801
06/06 05h00	117.6	96.7	14.3	0.7	0.747
06/06 06h00	192.5	159.4	15.2	0.5	0.709
06/06 07h00	280.0	227.2	16.2	1.0	0.661
06/06 08h00	344.8	275.8	17.2	0.9	0.619
06/06 09h00	412.9	330.6	18.2	1.7	0.578
06/06 10h00	460.7	359.1	19.0	1.9	0.524
06/06 11h00	446.9	359.7	19.6	1.7	0.520
06/06 12h00	369.6	345.3	19.9	1.5	0.505
06/06 13h00	342.2	319.1	20.0	1.7	0.492
06/06 14h00	324.9	304.7	20.1	3.0	0.490
06/06 15h00	282.6	267.2	20.0	3.0	0.623
06/06 16h00	208.8	202.6	19.7	2.8	0.499
06/06 17h00	154.5	150.6	19.3	3.0	0.509
06/06 18h00	105.5	104.5	18.8	4.0	0.533
06/06 19h00	62.6	62.1	18.2	3.3	0.516
06/06 20h00	20.2	20.2	17.5	1.5	0.562
06/06 21h00	0.3	0.3	16.8	2.2	0.599

Figure 6.2: *Screenshot of generated hourly meteo data for Oslo in PVsyst. The values displayed are from the 6. of June, from 02:00 in the morning to 21:00 in the evening.*

6.1.1 Meteonorm

Meteonorm uses several different international databases in combination to ensure a single reliable database for worldwide simulation of solar energy systems. The database consists of all required parameters for further processing such as global radiation, temperature, wind, humidity and precipitation. Global radiation data is gathered from GEBA (Global Energy Balance Archive), and is thoroughly controlled using six separate procedures. These quality controls include physical probability, time series analysis and comparison of cloud data. Temperature, humidity, wind data, sunshine duration and precipitation, is taken from the WMO (World Meteorological Organization) climatological normal 1961–1990. In total, the database contains information from 8350 weather stations. The resulting monthly average radiation values are calculated for periods of at least 10 years, with variations in final 10-year period depending on available data. [87]

In addition to databases of measured data, satellite data is used for radiation interpolation in all locations. At locations where no radiation data is available nearer than 200km (50km for Europe), satellite data is exclusively used. For sites with radiation data further away than 30 km (10 km for Europe), a combination of satellite and measured ground data is used. [87]

6.1.2 Visualization of Hourly Data

Examples of hourly generated data can be seen in figure 6.3, displaying the variation of irradiance in Oslo from two different selected days. The graph on the left is from the 5. May, a clear and sunny day, while the graph on the right is from the 21. June, showing the result of clouds emerging just before noon. The bold line shows the curve of global irradiation, while the thinner line shows diffused irradiation. The figure clearly visualizes the difference in how PVsyst generates irradiation data for clear and cloudy days.

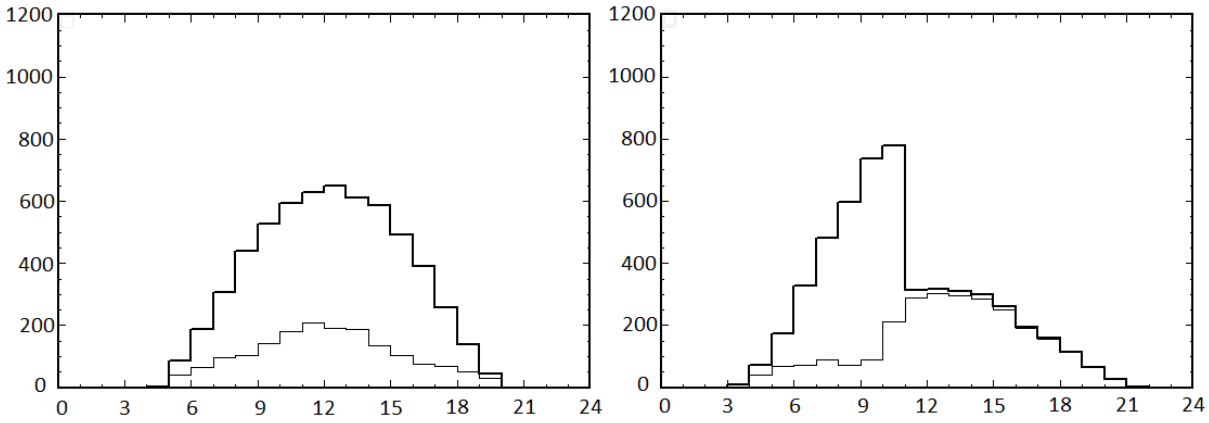

Figure 6.3: *Screenshot from PVsyst displaying the difference in generated data between clear and clouded conditions from 5. of May and 21. June in Oslo.*

6.1.3 Uncertainties

One of the primary sources for uncertainty in PVsyst the quality of monthly meteorological data, which is used to generate hourly data. Early investigations on the subject discovered that actual measured data for locations at Norwegian latitudes is scarce, and satellite data is only available for longitudes up to approximately 65° North, just north of Trondheim. Monthly data for locations at these longitudes, like Tromsø, is generated by interpolating between the nearest stations, but these can in reality be far away. As the amount of actual measured data is in short supply, validation of interpolated results is difficult. To an extent, the uncertainty remains unknown but is certainly larger compared to central Europe. This has been confirmed through contact with Meteonorm customer support.

Alternative approaches include importing actual measured data from weather stations or solar plants outside of the Meteonorm database, an option that to a large extent was investigated but eventually disregarded due to several challenges. The PVsyst manual states: *Self-measured data should only be used if the measurements were performed with the proper equipment that has been installed, carefully calibrated and the results analyzed by qualified experts [86].* This can be difficult to validate. Imported data from five different locations would have to include all required parameters from the same meteorological period in order to be used for comparison. In addition, the potential technical difficulty of implementing five different formats in Python seemed like a huge obstacle. The conclusion was made to stick with meteorological data in PVsyst provided by Meteonorm.

6.2 Project Design

The process of designing a complete PV system suitable for the purpose of this thesis assignment involved many separate stages with different levels of both difficulty and complexity. Information on components and meteorological conditions have been explored, discussed and decided on with the help of available theory and guidance from experts on the field. After opening the program, the first decision to be made is to define the system-type. PVsyst separates between grid-connected, stand alone and pumping systems. For the purpose of our assignment, grid-connected is chosen.

6.2.1 Site Specification

Once system type is decided, the project requires site specification and ensuing meteorological data. The selection is performed using the interactive map function in PVsyst, by searching for one of our chosen cities and moving the selected point to the desired location within the city. As each city requires a precise location chosen for the placement of the PV system, individual considerations were made in order to place the PV system in a realistic location that would provide us with reliable simulation results.

The precise system placement in each of the cities was a decision made with the intention of selecting a realistic placement that had no major challenges like nearby mountains or other constrictions. For Trondheim, Oslo and Bergen this meant that the locations were decided by placing the system on the exact location as ASKO's refrigerated warehouse in those cities. For Trondheim this is Tiller, an industrial area 10 kilometres south of the central city. For Oslo this meant Vestby, an area 40 kilometres south of the city centre. Both of these locations already have existing solar systems and were deemed as a safe and realistic placement option. The refrigerated warehouse in Bergen is placed in Arna, east of the city centre. There were some initial concerns regarding this placement due to mountainous areas in the vicinity. Therefore, simulations were performed with exact conditions in close-by areas with more optimal conditions in order to discover differences. The results discovered only minor differences, therefore the placement was kept.

In Tromsø the initial idea was to follow the procedure of choosing locations based on existing refrigerated warehouses from ASKO. In Tromsø this is located in Ramsfjordbotn, around 20 kilometres south-east of the city centre. Also here concerns regarding nearby topography were risen, and later confirmed when performing simulations in nearby areas with more optimal conditions. Eventually, the location was set to Sydspissen, an area at the southern tip of the Tromsø island and deemed a more realistic placement option for solar systems. In Kristiansand we had discovered very limited information of already existing refrigerated warehouses and accordingly the location was set to an industrial area just west of the city centre called Rigedalen. The finals locations chosen were:

- Trondheim: ASKO Midt-Norge, Heimdal
- Bergen: ASKO Vest, Arna
- Oslo: ASKO Vestby, Vestby
- Kristiansand: Rigedalen
- Tromsø: Sydspissen

Once the location is decided and set, PVsyst creates an .SIT-file with monthly meteorological information based on the best available data. At this point, a .MET-file with synthetic meteorological data is also generated.

6.2.2 Field Type and Orientation

With system type and site specification selected, the first step in actual project design is selecting desired field type and orientation for the solar panels. PVsyst separates between three main categories of *field types*, or variations of plane orientations, with more specific underlying alternatives. These are fixed orientation planes and one/two-axis tracking planes. Based on information from already existing systems in Norway presented in chapter 2.1.3, a fixed east/west field type with 10°tilt was selected. Figure 6.4 shows a screenshot of this selection step.

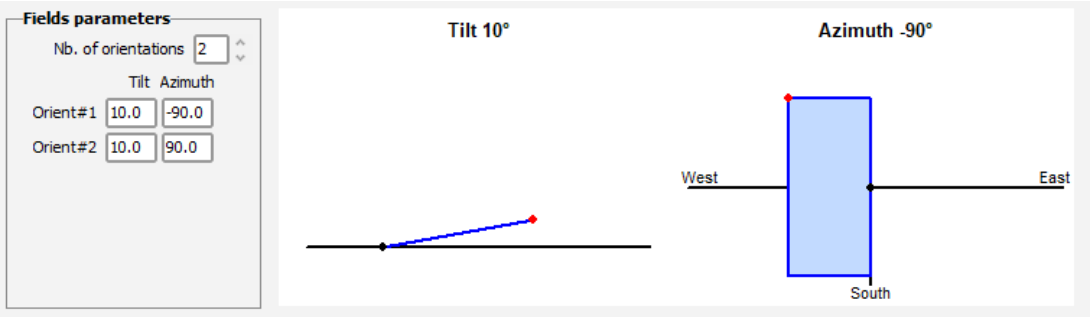

Figure 6.4: *Screenshot from PVsyst of orientation selection.*

The panels' orientation and tilt were decided based on already existing installations in Norway and guidance from experts on the field. The solution of using an east-west fixed orientation with a tilt of 10°is deemed the best arrangement for maximum utilization of available area due to being exposed to solar irradiation both morning and evening. This solution also removes the issue of self-shading of the panels. On the other hand, due to the low tilt angle, these kinds of systems do not produce maximum energy when the sun is at its highest. Using panels with a close to horizontal tilt angle can also lead to a higher chance of snow setting on the panels, compared to a higher tilt where snow can slide off.

Other potential solutions include installing panels mounted directly to the south in order to take advantage of the position of the sun in the northern hemisphere. This solution would create a production curve with higher peaks but less production on morning and evening. Additionally, the option of installing tracking systems is included in PVsyst, either on one or two axis. This option has not been explored, as a literary review indicated that this solution is seldom seen at installations in Norway. The option does, on the other hand, instinctively seem like an area where implementation could lead to improvements.

6.2.3 System Parameters

Setting the system parameters includes defining a desired nominal power or available area for installing modules, in addition to selecting a module model and inverter model from the database. After multiple tests, the PV system area was set to 6000 m^2 with a capacity of 1181 kWp. As explained in section 4.4, current regulations of overproduction would lead to increased costs with larger sizing. The first simulations with an area of 10000 m^2 lead to over 10% of the hours resulting in overproduction for Kristiansand. As it was in our greatest interest to model a system with a small amount of overproduction while still having a considerable amount of production, the area could be adjusted to a small size with no overproduction. However, for the examinations in this report, the amount of production close to real PV systems on refrigerated warehouses was desired. After multiple adjustments, the size of 6000 m^2 was therefore selected.

Comparing the simulated system to the one actually installed at ASKO Midt-Norge, the simulated system is around 3000 m^2 smaller in size, with 267 kWp less capacity. This is mainly due to the simulated system being equipped with more modern and efficient components, in addition to the real system having systems for utilizing overproduction. These systems could include storage of produced energy or other consumption options such as charging of electric vehicles or hydrogen production. These solutions were, although not in the scope of our assignment, thus left unexplored.

The selection of components was performed with the intention of selecting modern, realistic and well-performing modules and inverters that would stay relevant in the coming years. Implications of component selection are challenging to predict as simulations exploring this subject was not performed. It is though possible to predict that less expensive, lower-performing components would lead to reduced initial costs but decreased performance. The selected solar panel were Trina Solar TSM-DE15M(II), a 400Wp mono-crystalline modern type of panel, and lastly the inverter type was set to Sungrow SG80KTL, an 80 kW inverter suitable for conditions in our assignment.

Once these three parameters are set, the program will select the required number of inverters based on pre-defined ratios. It will then propose the number of modules in a series, as well as the number of strings in order to obtain the planned power or utilize the available area. Decisions taken in this automatic process is made on the basis of defined requirements of maximum/minimum voltage in both high and low temperature conditions, taking into account restrictions from selected components. In the case of incompatibilities between components, warming messages on different levels will be displayed. An overview of the final selected system parameters are displayed in figure 6.5.

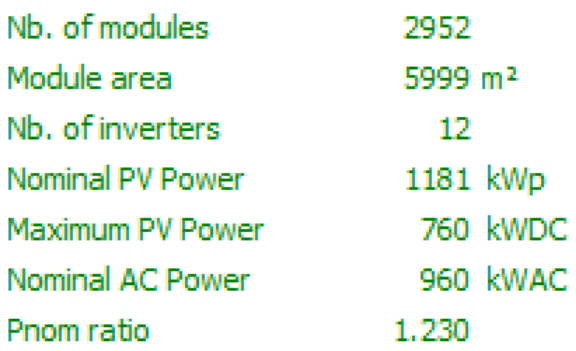

Figure 6.5: *Screenshot of system summary in PVsyst.*

6.2.4 Detailed Losses

PVsyst provides a large array of possible minor detailed losses. These losses include thermal, ohmic, module quality, soiling, IAM (Incidence Angle Modifier), auxiliaries, aging, unavailability and spectral correction. All of these parameters are initially set to reasonable default values by PVsyst, and after evaluation of values, most of them are left untouched throughout simulations. Investigation, exploration and iteration of each setting to find the most optimal conditions were though deemed excessive and too time-consuming for the scope of this task and consequently left to their initial default values. Degradation and maintenance settings were slightly adjusted and set uniform for all locations, but soiling in the form of snow was considered too relevant and individual for each location. Adjusted factors are specified below:

- Unavailability was set to 1% to cover expected maintenance, resulting in 3.65 days of unavailability distributed over three random periods across the year.
- Ageing is a factor that covers degradation of the modules and inverters, increasing mismatch between modules and elements of wiring etc. The degradation results in a progressive loss of efficiency, and is characterized by an average degradation factor, and is set to 0.2% pr. year, as recommended by Thor Christian Tuv at FUSen.
- Soiling is initially defined as a yearly loss factor, but due to the significant effect snow has in winter months, monthly soiling values are set for each city based on measured data presented in figure 3.6, and displayed in table 6.1.

Table 6.1: *Soiling values set for each city for every month.*

	Jan	Feb	Mar	Apr	May	Jun	Jul	Aug	Sep	Oct	Nov	Dec
Bergen	50	25	25	0	0	0	0	0	0	0	0	25
Kristiansand	50	25	25	0	0	0	0	0	0	0	0	25
Oslo	75	75	50	0	0	0	0	0	0	0	25	50
Tromsø	100	100	100	50	25	0	0	0	0	0	50	100
Trondheim	100	75	50	25	0	0	0	0	0	0	25	75

Implemented soiling factors has been a large factor for consideration as their effect is both extensive and very hard to predict. Once the snow sets on the panels, it is possible to either manually remove the snow, but this leads to a risk of damaging the panels. Additional options include systems for melting the snow, but this has been disregarded. The decision was made to use measured snow cover data presented in figure 3.6 as a basis for soiling factors.

For all locations, numbers presented in figure 6.1 are manually imported in PVsyst as soiling factors. The only exception is Tromsø, where snow cover data indicates 75% snow cover in April and 50% snow cover in May, but this has been adjusted down to 50 and 25 with the assumption that there will be measures taken to remove the snow in these months. Leaving snow on the panels during large parts of these months would be considered inadvisable due to the amount of potentially unused solar radiation these months experience.

This can be observed in figure 6.6, displaying columns of monthly produced energy, divided into three different categories. The dark red section shows actual useful produced energy and green snows system losses from inverters and other components. The purple column shows a collection of PV-Array losses, and this is where the effect of soiling can be observed. Especially March, April and May show has huge losses of produced energy, indicating that some for of snow-removing system should be considered in areas where long periods of snow cover are typical.

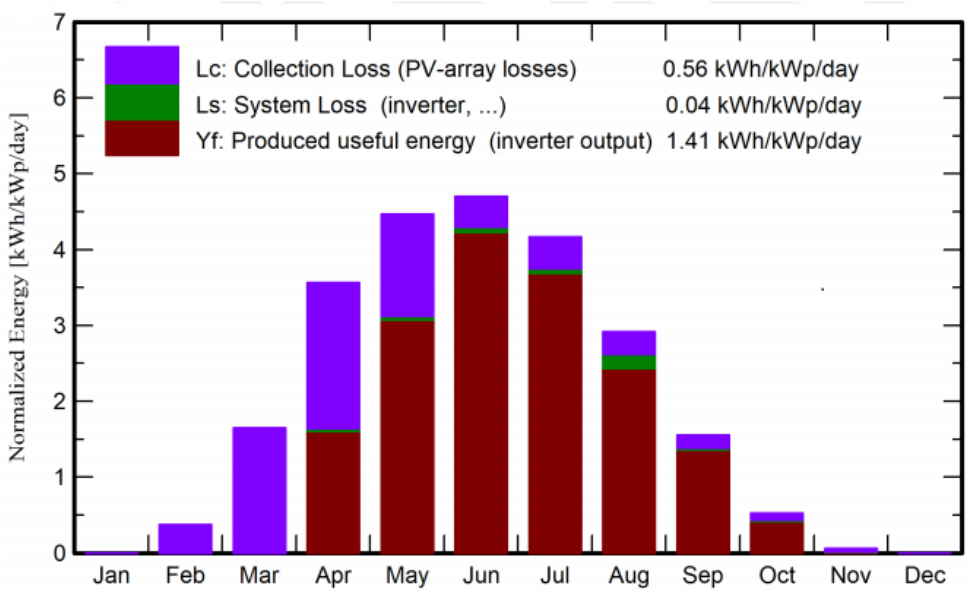

Figure 6.6: *Screenshot from PVsyst report displaying production results in Tromsø. Red bar indicates produced energy, while green and purple show losses.*

PVsyst provides the user with optional system design additions and specifications like shaping the horizon and setting near shadings. Horizon settings is relevant with concern to nearby topographic conditions like distant mountains or other objects potentially blocking the irradiance. When using near shadings the user is provided with the option of designing the building in order to include shading from nearby conflicting components such as trees, ventilation systems on the roof or other hindrances. For the purpose of this assignment, both these options were left out in order to not disturb the basis for comparison. This could potentially lead to simulated results being unrealistic.

6.2.5 Simulation Results and Extraction

Once all the above mentioned factors are included, an individual simulation over 25 years for each location is performed. For every simulation, PVsyst provides the user of generating output files for each year with desired data. The result is 25 Excel files for each location, meaning a total of 125 separate Excel files containing production data for every hour, for every year in five different cities. These files were then imported into Python in order to perform calculations. The same data is also provided in the form of a 10-page report for each city, also containing loss diagrams, system summary, graphs on performance ratios and other interesting results and data. The full report can be found in appendix E.

7 Financial Analysis

The financial analysis was executed in Python once simulations in PVsyst were complete. Parameters included in the financial analysis were: Grid tariff, electricity prices, taxes & fees, the load profile, installation costs and operation- and maintenance costs. The financial values calculated are the net present value (NPV) and internal rate of return (IRR). NPV was calculated using all future costs and incomes with and without PV systems, including the total investment. The calculations were based on yearly cash flows with a discount rate of 4%. IRR, the discount rate to get at an NPV of 0, was also calculated based on the yearly cash flows. Pearson correlation factor is calculated to determine the correlation between solar energy production and load profiles in the five cities. This section explains how these three results were calculated for one of the five case studies. In order to recreate the results in this report, the methods below must be repeated for all five cities.

7.1 Calculation of Electricity Prices and Overproduction

As figure 4.3 illustrates, the electricity prices have been very volatile for the last 18 years. Therefore the electricity prices were implemented such that the uncertainty of their prices was represented. The electricity prices are the only contribution to the standard deviations presented in this thesis. Multiple methods of implementing the electricity prices were considered because of their significant impact on the financial results and their volatility. The chosen implementation was selected because of its simplicity and to be able to present a standard deviation.

From Nordpool, hourly electricity prices from 2013 to 2020 are available. Because eight years of electricity prices were available, eight separate analyses were executed for each case study, one for each year with recorded prices. As a result, the 25-year extended analysis was calculated eight times. After the eighth analyses, the mean and standard deviation of the electricity cost, sold electricity income, IRR, and NPV were calculated based on the eighth analyses of each case study.

There were multiple files of different formats that were necessary to import to Python. The library Pandas in Python was used to import, visualise and manipulate the data imported. Firstly the load profile and production data from PVsyst were imported. The load profile was repeated 25 times, making it a 2 by 219000 row long data frame, each row representing an hour of the 25-year span. The PVsyst and the load profile data were then merged into a 2 by 219000 data frame. Figure 7.1 illustrates an extract of this data frame. The production and load are from 09:00 to 14:00 on the 5th of July in Oslo's first year of simulation.

Table 7.1: *Row 4474 to 4478 of the 2 by 219000 data frame containing the load and production from Oslo.*

	Production $[kWh]$	**Load** $[kWh]$
4474	744.28	728.75
4475	855.06	736.85
4476	911.32	692.10
4477	879.24	1005.54
4478	811.40	1123.98

The load and production data frame was saved and used for the eight financial analyses using the eight different years of electricity prices. A for-loop in the main function was used to run a single analysis for each year of electricity prices. Each year the new electricity prices are imported, starting with 2013. The electricity prices were implemented the same way as the load profile. It was repeated 25 times and added to the data frame illustrated in table 7.1.

When production values exceeded load values, referred to as overproduction, the analysis had to consider the possibility to sell up electricity up to 100 kW. The costs of exceeding 100 kW delivered to the grid are higher than the income due to the added costs when the prosumer arrangement no longer applies. In

the analysis, all energy was set to zero if the overproduction exceeded the 100 kW limit. This means that no energy was sold or used at the refrigerated warehouse to save costs during these hours. For example, in table 7.1, the production in row 4477 and 4478 needed to be reduced to zero because the production exceeded the load plus 100 kWh in these hours. 100 kWh is equivalent to an average effect of 100 kW each hour. However, in row 4474 there are less than 100 kWh in surplus. This means that the surplus energy is sold, while the PV production in the frame is set equal to the load. This was done to prevent the load after PV were considered to never go below zero.

In order to implement this in Python, all hours with overproduction had to be located and examined. These hours were identified by looping over all the hours. If the overproduction was greater than the energy consumption of the refrigerated warehouse + 100 kWh per hour, the production was set to zero. For hours where this was not the case, the amount of overproduction was subtracted from the production and sold for the corresponding electricity price at that specific hour. The rows production and load in table 7.2 illustrates how the production was changed from table 7.1 depending on the difference between the load and production. The curtailed electricity was saved in a sum to examine the match of the PV system and load profile. The yearly income from overproduction was saved and used later in the analysis to calculate the IRR and NPV. As the electricity prices are implemented eight times, the number of earnings from sold electricity are calculated eight times. Therefore, the mean and standard deviation of the eight earnings from overproduction were calculated at the end of the analysis.

The next step was to calculate the electricity costs for each hour, with and without production from PV systems. The electricity was calculated by multiplying the bought load with the imported electricity prices hour for hour. For the scenario without production, the imported load from ASKO Midt-Norge was multiplied by the imported electricity price. For the scenario with production, the load minus the production was multiplied with the corresponding electricity prices. Table 7.2 is an extract of the data frame for Oslo after the electricity costs for each hour was calculated.

Table 7.2: *Row 4474 to 4478 of the 5 by 219000 data frame used for the financial case study of Oslo using the electricity prices from 2019.*

	Production [kWh]	**Load** [kWh]	**Electricity prices** [NOK/kWh]	**Electricity cost** [NOK]	**Electricity cost(PV)** [NOK]
4474	728.75	728.75	0.27476	200.231350	0.000000
4475	0.00	736.85	0.26503	195.287355	195.287355
4476	0.00	692.10	0.26166	181.094886	181.094886
4477	879.24	1005.54	0.25819	259.620373	32.609397
4478	811.40	1123.98	0.25318	284.569256	79.139004

By calculating the difference between the columns electricity cost and electricity cost(PV), the savings in electricity are calculated. The yearly savings are viewed as an income cash flow and are used to calculate the IRR and the NPV of the investment later in the analysis. Since the electricity prices are implemented eight times, these cash flows are calculated multiple times and will give a mean value with a standard deviation.

7.1.1 Inflation and Price Increase

The electricity prices, grid tariff and taxes & fees used in the analyses neither account for inflation nor the expected price increase in the future. Subsection 4.5 explains why the the electricity prices and grid tariff are expected to increase. As figure 4.4 illustrates, the electricity prices from 2013 to 2019 are at average lower than the expected future electricity prices according to NVE. 2020, which not is a part of the figure, also had record-low electricity prices. Because the expected increased electricity costs were not considered in the financial analyses, this does impact the NPV and IRR to have lower values than in reality. There will also be inflation in prices, increasing future electricity costs. When the costs are lower, the potential savings from installing PV system also becomes lower. Accounting for this was not prioritized, as the focus was on relative differences between regions, which is largely unaffected.

7.2 Grid Tariff and Taxes & Fees

As explained in section 4.3.2, grid tariff is separated into three cost sectors: Fixed cost, energy cost and power cost. The fixed cost is paid once a year with a predetermined cost, and independent of the amount of energy used and peak power. Therefore, the fixed cost was added to the bottom line without further calculation necessary in the grid tariff functions for each year. The energy costs are fixed rates that are multiplied by the energy consumption. Some of the cities have multiple consumer cost rates depending on the season, like Oslo and Bergen, which have to be considered in their grid tariff functions. The last and most complicated fee was the power cost. This is the cost that gives incentive to reduce the power peaks. The maximum energy consumption during a single hour, called the peak power consumption, over each month was located and multiplied with a rate depending on the month. As figure 4.1 shows, the rate changes multiple times a year. To calculate the power cost, two things have to be examined for each month. Firstly, the peak power consumption has to be found. Secondly, the function has to keep track of which month it is and its rate. These challenges were solved by looping over the months in a year, checking the maximum energy consumption and using if statements to select the right rate depending on the month.

Taxes & fees are separated into two categories, electricity tax and energy fund cost (Enova levy). The electricity tax is similar to the energy cost and is a rate multiplied by the energy consumption. This rate is constant for the whole year at 16.69 $øre/kWh$ for Bergen, Oslo, Kristiansand and Trondheim, but 0.546 $øre/kWh$ for Tromsø. The energy fund cost is similar to the fixed cost and is 800 NOK per year for the five cities. The energy fund cost is added to the total sum of taxes & fees without further calculations.

The grid tariff and taxes & fees was calculated twice for each analysis, with and without PV system energy production in consideration. In both cases, the costs were calculated for each year using a function logically built up by the rules explained in table 4.1. This function was repeated 25 years, the estimated lifespan of the system. The function returns lists containing every year's cost in grid tariff, and taxes & fees. Four lists were created, both without and with PV system energy production for both grid tariff and taxes & fees. These lists were later used to calculate IRR and NPV of the investment.

7.3 Maintenance and Installation Costs

In section 2.1.3 installation and maintenance costs are presented. The selected cost for the installation in these analyses were 10 NOK/Wp, the cost presented from Solenergiklyngen. This estimate origins from 2018 but are the cheapest of the two estimates presented and consider larger facilities than the report from WWF. While the price from the WWF report is for facilities greater than 10 kWp, the estimate for Solenergiklyngen is for facilities over 100 kWp to 1 MWp. As figure 6.5 displays, the system modelled in PVsyst deliver 1181 kWp, which is a large facility on the Norwegian scale. It would be imprecise to have a linear estimate from 10 kWp up to 1181 kWp, therefore the price estimate from the WWF was dismissed. A linear price increase from 100 kWp to 1181 kWp is still unlikely. However, in lack of public reports on prices on this size PV system, the estimate of 10 NOK/kWp from Solenergiklyngen was selected. The price of the PV system was therefore $10NOK/kWp \cdot 1181kWp = 11.81MNOK$.

The price estimate from 2018 could be outdated. Figure 2.2 illustrate a learning curve of all commercially available PV technologies, and it is safe to assume that with continuing growth in the PV technology market, prices will decrease. For each doubling in cumulative production, the price of PV modules went down by 25 % on average between 1980 and 2019. With the recent development explained in section 2.1.2 the installed Wp has increased since 2018. Therefore, the price of PV systems has likely decreased since 2018, and the estimate could be too expensive.

7.4 Calculation of NPV and IRR

The NPV is the net present value of and an investment using future cash flows with a discount rate. The NPV in this paper has five different cash flow considerations: The grid tariff, electricity cost, taxes & fees, income from sold electricity and operation- and maintenance costs. In addition, an investment of 11.81 $MNOK$ is added at year zero. The grid tariff, electricity cost and taxes & fees are technically not incomes but saved money. However, when the NPV and IRR were calculated, the cost difference between with and without PV system was viewed as an income cash flow. These three incomes were calculated yearly and used as income cash flows. The maintenance cost was fixed at 0.075% of the installation cost yearly, while the income from sold electricity was also yearly calculated.

Based on an official report from the Norwegian government, the risk-free rate for use in cost-benefit analyses are set to 2% [88]. In addition, an additional risk premium of 2% should be added. The discount rate was therefore set to 4%. Using all the created lists of yearly cash flows, the NPV was calculated. Because of how the electricity prices were implemented, the NPV will have a standard deviation with contributions from the electricity costs and income from sold electricity.

The IRR is the discount rate that makes an investment of zero NPV. The two algorithms are very much alike, but the IRR solves the discount rate when the NPV is 0, while the NPV solves the present value of future cash flows given a discount rate. Therefore, the IRR uses the same cash flows as the NPV. The IRR will also get a standard deviation with contributions from the electricity costs and income from sold electricity. Both the NPV and IRR algorithms are imported from numpy_financial, which is a collection of elementary financial functions available in Python.

8 Pearson Correlation

The Pearson correlation between the load and production was calculated to examine the initial assumption that refrigerated warehouses and PV systems are a good fit. Pearson correlation measures how linear two variables are compared to each other. If the data is illustrated as a scatter plot and a regression line is drawn, the Pearson correlation, r, indicates how far away from the line the scatter points are. The correlation factors range from -1 to 1, where 1 is a perfect correlation, -1 is a perfect negative correlation, and 0 is no correlation. Figure 8.1 contains three plots which illustrate scatter plots with positive, negative and no correlation. [89]

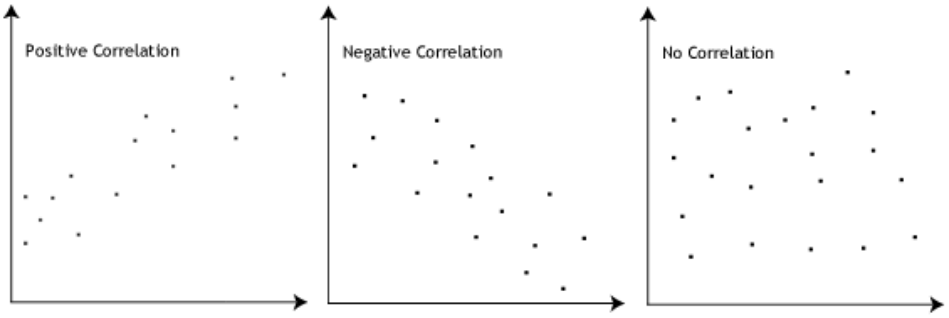

Figure 8.1: *An illustration of three scatter plots and their correlation. [89]*

The stronger the association of two variables are, the closer to $\pm$ 1 the correlation will be. A perfect correlation would mean that no points on the scatter plot will be outside a regression line. It is also important to know that the Pearson correlation does not tell the difference between dependent and independent variables. This means that the Pearson correlation only tells the association between two variables. If the number of sun hours and PV system energy production have a correlation of 0.7, the same correlation would be true between PV system production and the number of sun hours. However, it is certain that the the PV system production does not affect the number of sun hours, and the correlation could therefore be misapprehended. The awareness of data is important, and blindly relying on the Pearson correlation could make the results misleading. [89, 90]

Using pandas' function .corr() the Pearson correlation coefficient were calculated. The correlation was calculated over 25 years, meaning production and load profile data over 25 years were used. This means that the production and load data illustrated in table 7.2 were used to calculate the correlation. The correlation was calculated over the whole 25-year span to make sure the degradation of the PV system impacted the results.

Because of a mismatch between the simulated PV system and a real PV system, and the same load profile being used for all locations, the Pearson correlation in this thesis might be weaker than in the real world. In real world, the climate would be the same at the same time for both the refrigerated warehouse and PV system. However, the Metonorm data and real world weather are not equal. Because the energy consumption of refrigerated warehouses are temperature dependent, the difference in climate will likely impact the Pearson correlation in this thesis to being lower than real-world data would indicate.

Results

This part presents the results from the PVsyst simulations and Python calculations and is split into two chapters. The first chapter presents results related to correlation, while the second chapter presents results regarding regional differences in production and finance. The results consist of key findings from analyses done using the selected refrigerated warehouse load profile from ASKO Midt-Norge 2020 and a simulated PV system at five cities dispersed across Norway. The key findings presented are the correlation coefficient between load and production, total and yearly energy production from the simulated PV systems, and the financial results.

9 Correlation

Table 9.1 shows the Pearson correlation coefficients for five cities in Norway. The correlation is between simulated PV production after curtailing and ASKO Midt-Norge's energy use. The production values are over 25 years, while the load values are ASKO Midt-Norge's energy use in 2020, repeated 25 times. All correlation coefficients are based on hourly values.

Table 9.1: *Pearson correlation coefficient between the load profile and production for the five cities.*

	Correlation coefficient
Kristiansand	0.4036
Oslo	0.4209
Bergen	0.3894
Trondheim	0.3780
Tromsø	0.3553

The correlation coefficients for the five cities in table 9.1 imply a moderate positive correlation between energy demand at a refrigerated warehouse and simulated PV production. Oslo has the highest correlation coefficient of 0.4209, followed by Kristiansand, Bergen, Trondheim and lastly Tromsø, with 0.3553. The correlation coefficients decrease from south to north, except for Kristiansand, which has a lower correlation coefficient than Oslo despite being further south. Oslo also has a significantly higher correlation coefficient than Bergen, despite being located only about 0.5° latitude further south.

Figure 9.1 displays the load of ASKO Midt-Norge for 2020 in green and the average monthly production of the simulated PV system for Kristiansand in red. The production curve has clear tendencies with low production ($< 10MWh$) in November, December, January and February. The production then increases in March and April, before reaching peak values in May, June and July. The curves are similar for all five cities, as shown in appendix A, figures A.1 – A.5, with slight differences which is further described in chapter 10. The green load graph is the same for all five cities.

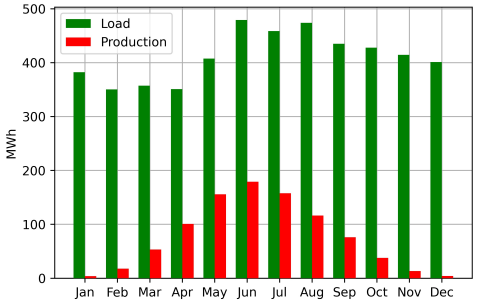

Figure 9.1: *Bar plot of average yearly production and load from 2020 in Kristiansand.*

The load profile shown in figure 9.1 has peak values during the summer months, which is similar to the production values. The relative differences between months are, however, significantly smaller for the load values than the production values. The monthly values only display the total load an production throughout the month, while the actual correlation is dependant on hourly values and intradaily trends.

Figure 9.2 and 9.3 shows the average load of ASKO Midt-Norge's refrigerated warehouse and average PV production in Kristiansand respectively, for each hour in the day for each month throughout the year. The load values are generally stable between 400 and 550 kWh per hour between 20:00-05:00. After 05:00, the energy demand increases for the next few hours to values about 150-200 kWh per hour higher for the low-demand months, and between 200-350 kWh per hour for higher demand months. The demand remains high during the day before decreasing between 14:00-20:00.

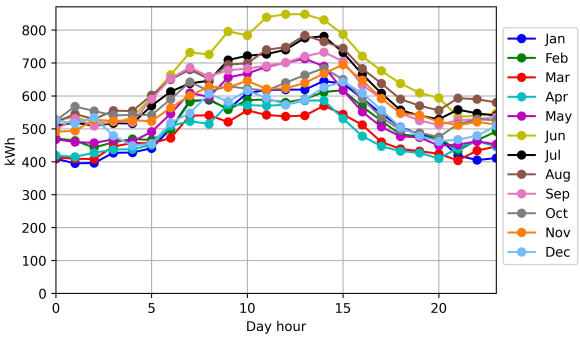

Figure 9.2: *The hourly average energy demand throughout the day for each month.*

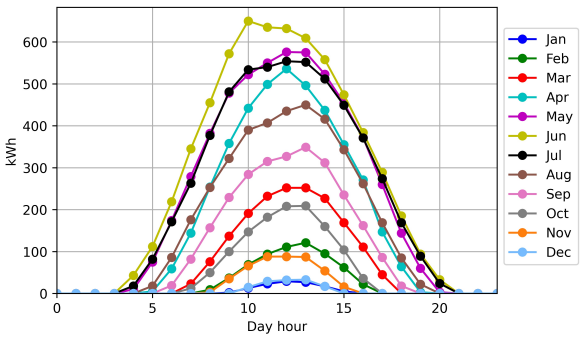

Figure 9.3: *The hourly average production throughout the day for each month for Kristiansand.*

The production graph in figure 9.3 show the same trends as the energy demand graph, but the relative differences from hour to hour and between months at the same hours are way more significant. Between 20:00 and 05:00, there is no or low production for every month. After 05:00, the production increases consistently, reaching peak values between 10:00 and 14:00. The summer months, led by June, peaks at over 600 kWh per hour. Winter values are minuscule in comparison, peaking at about 25 kWh per hour in December and January and about 90 kWh per hour in November. The spring- and autumn months peak somewhere in between, with higher production values closer to summer months.

Similar graphs to the graph displayed in figure 9.3 can be found in appendix B, figures B.1 – B.5. The curves are similarly shaped for all cities, with the biggest difference being the amplitude of the curves. While Kristiansand peaks at over 600 kWh per hour, Oslo peaks at about 525, Bergen at 475, Trondheim at 500 and Tromsø at 420 kWh per hour.

10 Regional Differences

This section will present two main results – the PV simulation results with regards to production and the calculated economical accounts of PV installations. Both results will be presented for all five cities. The differences between each city will be highlighted and commented.

10.1 PV Production

Figure 10.1 shows the average yearly energy production and energy distribution for each city without curtailing. Kristiansand has the highest average production with 977 MWh, followed by Oslo, Trondheim, Bergen and at last Tromsø, with 580 MWh. The Sold energy and curtailed energy columns displays how much of the total produced energy that is sold and curtailed respectively. The sum of sold and curtailed energy is the total overproduction and does not contribute in reducing the warehouse's energy demand from the grid.

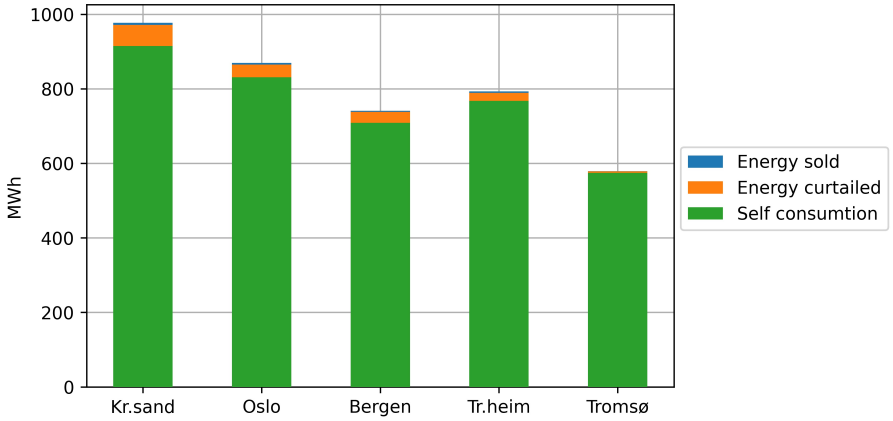

Figure 10.1: *Average yearly production of the simulated PV system divided into energy sold, energy curtailed and energy used for self consumption.*

Kristiansand both sells and curtails the most energy, as can be seen in table 10.1. This curtailing reduces the amount of potential produced energy used by almost 6 %. Tromsø has the least overproduction, selling 0.76 MWh and cutting under 4 MWh each year. This reduces energy available for self consumption only by 0.7 %, a significantly smaller fraction than in Kristiansand. Trondheim has more energy sold than Bergen, but Bergen has significantly higher energy curtailed, despite Bergen having lower total production than Trondheim. This means that the PV production in Trondheim is more often in the range of 0 - 100 kW above the demand at the refrigerated warehouse, while PV production in Bergen more frequently surpasses 100 kW above the demand.

Table 10.1: *Yearly average energy production and distribution for all five cities. w.c. means without curtailing.*

	Production [MWh]	**Production w.c.** [MWh]	**Energy curtailed** [MWh]	**Energy sold** [MWh]	**Self consumption energy** [MWh]
Kristiansand	920.16	977.26	57.10	5.46	914.70
Oslo	835.20	869.67	34.48	4.31	830.89
Bergen	710.85	740.82	29.96	2.31	708.54
Trondheim	771.07	792.89	21.84	3.52	767.55
Tromsø	575.35	579.32	3.98	0.76	574.59

Figure 10.2 shows a comparison of the average monthly production of all five cities. Kristiansand has the highest production every month besides August and September, in which Oslo has slightly higher production. Tromsø has the lowest production every month but two of the summer months, June and July, in which Bergen has slightly lower production. Bergen has higher production than Trondheim from November till April. Trondheim has markedly higher production than Bergen from May till August and slightly higher production in September and October.

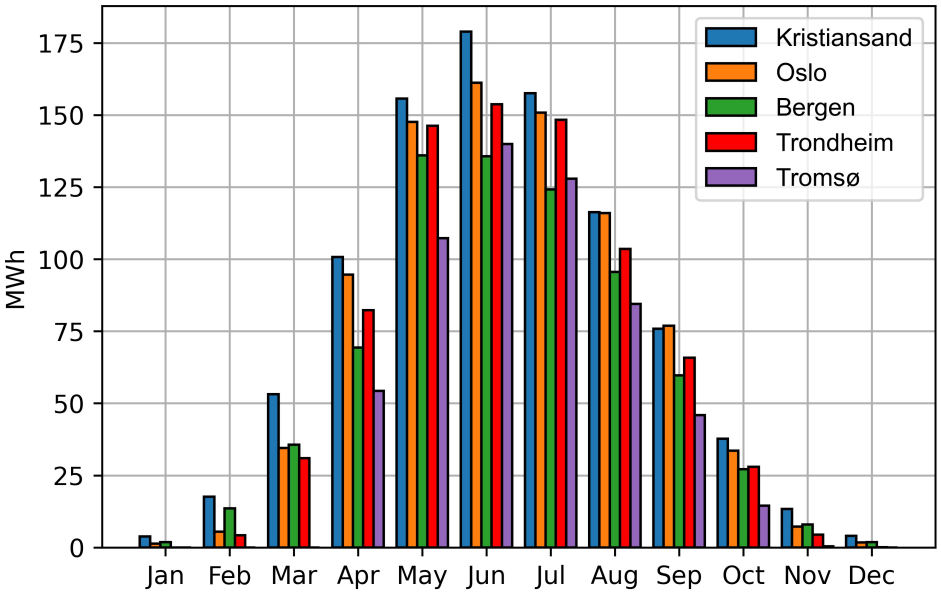

Figure 10.2: *Average monthly energy production from the five cities compared.*

The summer months have the highest production for all cities, but the monthly differences between May, June and July differ from city to city. Both Kristiansand and Tromsø has clear peaking values in June, as can be seen in figure 10.2. Production in Oslo and Trondheim also peak in June, but for both cities, the production in June is very similar to both May and July. Bergen is the only city with peaking production in May, as shown in figure A.3, but the production is almost equal in June before decreasing in July.

All simulations are based on the same load profile and consequently have the same total demand before PV of 4937.25 MWh per year, as can be seen in table 10.2. The remaining demand column displays the remaining yearly energy demand that needs to be covered through alternative sources or by purchasing power from the grid with a PV system installed. The demand covered as a percentage is shown in the rightmost column of table 10.2. The covered demand is highest for Kristiansand at 18.53 % and lowest for Tromsø with 11.64 %. The demand covered can also be considered as the degree of self-sustainability or as the portion of the energy used that is self-acquired.

Table 10.2: *Yearly average energy account with and without PV system installed.*

	Total demand [MWh]	**PV contribution** [MWh]	**Remaining demand** [MWh]	**Demand covered** [%]
Kristiansand	4937.25	914.70	4022.55	18.53
Oslo	4937.25	830.89	4106.36	16.83
Bergen	4937.25	708.54	4228.71	14.35
Trondheim	4937.25	767.55	4169.70	15.55
Tromsø	4937.25	574.59	4362.66	11.64

10.2 Financial Calculations

The internal rate of return (IRR) for building PV systems on refrigerated warehouses in the five different cities is shown in figure 10.3. All IRRs are negative, which from a strictly monetary point of view implies that the investment will result in a loss and should not be realized. Kristiansand has the highest IRR (least negative), followed by Oslo, Trondheim, Bergen and Tromsø. Tromsø's IRR is significantly lower than the others at -10.16 (σ = 3.05) %. The standard deviations for Bergen and Trondheim are quite similar, at 2.08 and 2.02 % respectively, while the standard deviations for Kristiansand and Oslo are slightly higher, at 2.26 and 2.20 %. Tromsø has the highest standard deviation of 3.05 %. The standard deviation reflects variation in electricity prices.

Table 10.3: *Internal rate of return (IRR) for all cities.*

	Kristiansand	**Oslo**	**Bergen**	**Trondheim**	**Tromsø**
IRR [%]	-2.96 ± 2.26	-3.41 ± 2.20	-4.50 ± 2.08	-3.52 ± 2.02	-10.16[1] ± 3.05

Ordering the cities from best to worst with regards to IRR will result in the same ranking as if ordered by total production, as can be seen by looking in the graph of figure 10.1 and the IRRs in table 10.3. However, the relative differences in production between cities do not directly reflect how good an investment the selected city is. For instance, Trondheim has 73 MWh lower yearly production than Oslo and 53 MWh higher yearly production than Bergen, but the IRR of Trondheim is only 0.11 %-points lower than Oslo while being 0.98 %-points higher than Bergen. This implies that production alone is not enough to decide which city is most suited, but the electricity prices, grid tariff and fees & taxes also needs consideration.

Table 10.4 shows the financial results of the investments in each city. All cities have the exact same initial installation cost of 11.81 $MNOK$. The maintenance cost is 0.75 % of installation cost yearly, which with a discount rate of 4 % gives a total NPV of 1.38 $MNOK$ after 25 years. This covers both maintenance and operations. The differences between each city comes primarily from the cost reduction. The cost reduction is money saved due to reduced energy costs with a PV system installed and will be further explored in table 10.5. The overproduction is different from city to city, as shown in table 10.1, but is very low compared to the differences in total cost reductions. The result shows the NPV of the investment.

Table 10.4: *Economic account for all five cities. All values in MNOK given in NPV using a discount rate of 4 %.*

	Kristiansand	**Oslo**	**Bergen**	**Trondheim**	**Tromsø**
Installation (−)	11.81	11.81	11.81	11.81	11.81
Maintance (−)	1.38	1.38	1.38	1.38	1.38
Cost reductions (+)	6.50 ± 1.67	6.16 ± 1.56	5.44± 1.31	6.07 ± 1.37	2.79 ± 1.07
Overproduction (+)	0.02 ± 0.01	0.02 ± 0.01	0.01 ± 0.00	0.01 ± 0.01	0.00 ± 0.00
Result (NPV)	-6.68 ± 1.69	-7.02 ± 1.57	-7.74 ± 1.32	-7.10 ± 1.38	-10.40 ± 1.07

The differences between the results of each city and the cost reductions of each city in table 10.4 are two sides of the same coin, as the differences in results are almost entirely due to differences in cost reduction. Therefore, they will for the remainder of this chapter be collectively referred to as the results. The result for each city is negative, which means that the investment will loose money. The results range between 6.68 (σ = 1.69) and 7.74 (σ = 1.32) $MNOK$ for Kristiansand, Oslo, Trondheim and Bergen, while Tromsø's result is 10.40 (σ = 1.07) $MNOK$. This means that of the 11.81 $MNOK$ initially invested, only 5.13 (σ = 1.69) $MNOK$ in NPV (11.81 - 6.68) will be returned for Kristiansand and only 1.41 (σ = 1.07) $MNOK$ in NPV (11.81 - 10.40) will be returned for Tromsø, after 25 years of production.

[1] When using the 2020 electricity prices for the case study of Tromsø, is was not possible to calculate the IRR, because the yearly maintenance costs exceeded the saved money. An exclusive negative cash flow will not lead to any IRR. The IRR presented are the average from using the seven other years of electricity prices.

Table 10.5 shows the total costs of electricity for the refrigerated warehouse before and after installing a PV system. The costs are separated by the categories grid tariff, taxes & fees and electricity costs, while the total costs are displayed in the rightmost column. The difference row for each city displays the difference in cost with and without PV installed. The most significant contributor to the total cost difference is the difference in electricity costs. The second-largest contributor is the taxes & fees for all cities but Tromsø, which only has a difference of 0.05 $MNOK$ due to its low taxation. The biggest difference in grid tariff can be found in Bergen, with a difference of 0.85 $MNOK$ before and after PV installation, while the slightest difference in grid tariff is for Tromsø, with 0.46 $MNOK$ before and after PV installation.

Table 10.5: *Power costs with and without PV system installed by cost segment for all five cities. All values are in MNOK and are the NPV of costs after 25 years of operation. Values after the ±-signs represent one standard deviation (σ).*

		Grid tariff	Taxes & fees	Electricity costs	Total costs
Kristiansand	None	11.07	12.88	20.19 ± 8.14	44.13 ± 8.14
	PV	10.52	10.48	16.64 ± 6.48	37.64 ± 6.48
	Difference	0.55	2.40	3.55 ± 1.67	6.50 ± 1.67
Oslo	None	15.70	12.88	20.36 ± 8.18	48.94 ± 8.18
	PV	14.93	10.70	17.14 ± 6.63	42.77±6.63
	Difference	0.76	2.18	3.22 ± 1.56	6.16±1.56
Bergen	None	14.92	12.88	20.13 ± 8.15	47.93 ± 8.15
	PV	14.07	11.02	17.40 ± 6.84	42.48 ± 6.84
	Difference	0.85	1.86	2.73 ± 1.31	5.44 ± 1.31
Trondheim	None	10.27	12.88	21.31 ± 7.91	44.46 ± 7.91
	PV	9.48	10.86	18.04 ± 6.56	38.38 ± 6.56
	Difference	0.79	2.01	3.27 ±1.37	6.07 ± 1.37
Tromsø	None	11.44	0.42	20.37 ± 8.12	32.23 ± 8.12
	PV	10.98	0.37	18.09 ± 7.06	29.43 ± 7.06
	Difference	0.46	0.05	2.28 ± 1.07	2.79 ± 1.07

Kristiansand has the biggest difference in both electricity costs and taxes & fees, with 3.55 ($\sigma = 1.67$) and 2.40 MNOK respectively. Oslo has slightly higher difference in taxes & fees than Trondheim, with 2.18 versus 2.01 MNOK, but slightly lower difference in electricity costs, with 3.22 ($\sigma = 1.56$) versus 3.27 ($\sigma = 1.37$) $MNOK$. The total cost reduction is marginally higher in Oslo than in Trondheim, with a difference of about 0.09 $MNOK$. Tromsø has a significantly lower total cost reduction of 2.79 ($\sigma = 1.07$) $MNOK$ compared to between 5.44 ($\sigma = 1.31$) and 6.50 ($\sigma = 1.67$) $MNOK$ for the other cities. The standard deviations for the cost reductions are higher for cities with higher PV production.

Curtailing the entire production when producing more than 100 kW above the warehouse's energy demand accounts for only a tiny fraction of the total production, as shown in table 10.1. However, as table 10.6 shows, the impact curtailing has on total energy costs is way more significant than the total amount of energy curtailed would indicate. Bergen has the most considerable difference in total costs with 2.39 ($\sigma = 0.00$) $MNOK$, which is almost entirely due to the reduction in grid tariffs of 2.31 $MNOK$. This would put the total cost reduction for Bergen from 5.44 to 7.83 ($\sigma = 1.31$) $MNOK$, increasing almost 44 %.

Table 10.6: *Potential reduction cost lost due to curtailment.*

City	**Grid Tariff** [$MNOK$]	**Taxes & fees** [$MNOK$]	**Electricity costs** [$MNOK$]	**Total costs** [$MNOK$]	**Above 100kW energy** [MWh]
Kristiansand	1.72	0.12	0.16 ± 0.07	2.01 ± 0.07	201.83
Oslo	1.09	0.08	0.11 ± 0.05	1.28 ± 0.05	91.79
Bergen	2.31	0.07	0.08 ± 0.04	2.46 ± 0.04	120.07
Trondheim	1.47	0.06	0.07 ± 0.03	1.60 ± 0.03	57.66
Tromsø	0.47	0.00	0.01 ± 0.01	0.48 ± 0.01	6.36

Almost all costs reductions are due to changes in grid tariff. This shows that the energy demand of the refrigerated warehouse has some monthly peak values at the same time as the PV system produces the most energy. After Bergen, Kristiansand has the biggest difference in grid tariffs with 1.72 $MNOK$, followed by Trondheim, Oslo, and at last Tromsø with 0.47 $MNOK$. The above 100 kW energy column results from the energy produced above the curtailing point of 100kW. For Kristiansand, only about 202 MWh of energy is produced by power above curtailing point. This is a minuscule amount compared to the total production of 24 432 ($977.26 \cdot 25$) MWh over 25 years. The 202 MWh of energy would only result in an income of about 31 $KNOK$[2]. The energy above curtailing point is way less for the other cities, as seen in table 10.6, and the income would be even smaller.

[2] 31 $KNOK$ is the NPV using an average energy cost of 25 $ØRE/KWh$ and a discount rate of 4 %, assuming a yearly production of 8.08 ($202 \div 25$) MWh.

Discussion

This part will provide further analysis of the results presented in the previous chapters. The discussion will follow the same structure as the results. First, the correlation will be discussed. Afterwards, regional differences in PV production and financial impact will be covered. Each part will be discussed in depth to understand the underlying factors, as well as understanding what the results mean. This will be done in accordance with relevant theory and through the use of figures extracted from the results.

11 Correlation

This chapter will discuss the results regarding the first part of the thesis statement – *What is the correlation between load at a refrigerated warehouse and power output from a PV system? If such a correlation exists, how suitable are PV systems as a measure to reduce energy costs?* In addition to discussing the general correlation, as well as the suitability, between PV systems and refrigerated warehouses, factors that distinguish refrigerated warehouses from other potential contenders for the use of PV systems will be discussed in accordance with relevant theory.

The correlation coefficients presented in chapter 9 show a modest correlation between 0.3553 and 0.4209. A correlation coefficient alone shows only part of the picture, so this chapter is divided into three subchapters to get a better grasp of the meaning of the correlation. Firstly, the month-to-month correlation between load and production will be discussed. Secondly, the intradaily correlation will be discussed. Both monthly and intradaily correlation will be discussed through the use of graphical displays of real- and simulated data. Finally, the correlation will be explored with regards to financial impact.

11.1 Monthly Correlation

As shown in figures 9.1 and 10.2 in chapter 9 and 10 respectively, as well as appendices A and B, the production profile of a PV system follows a characteristic curve of low or no production during winter months, increasing production during spring, peaking production during summer before decreasing again during autumn. This is coherent with the theory presented in chapter 2.3.1, which states that solar radiation is the dominant factor in PV production, in combination with available sunshine hours presented in figure 3.3. The characteristics of the production curve of PV is well known and consistent. Therefore, looking at the load profile is crucial in deciding how well the PV systems fits the load profile.

Judging by the load versus production profile shown in figure 9.1 in chapter 9, there seems to be a decent fit between energy need and PV production based on monthly values. The high yielding summer months of PV production can contribute to reducing the summer load peaks, which depending on the amount of energy produced can lead to either a flattening of the monthly loads, making the energy demand more stable month to month, or even making the load profile U-shaped.

A good fit between PV production and load av refrigerated warehouses alone does not necessarily answer an important question – *is refrigerated warehouses particularly suited for utilizing PV systems, in comparison with other building or industries?* Refrigerated warehouses energy demand deviates from general energy use in Norway. This deviation is apparent when comparing the average monthly energy use in Norway, shown below in figure 11.1, and the energy demand of a refrigerated warehouse, shown below in figure 11.2. The energy demand profile for Norway is U-shaped, with high energy demand during winter, lower during Autumn and Spring, and low demand during Summer. This is due to the cold climate of Norway and the subsequent high required energy use for heating.

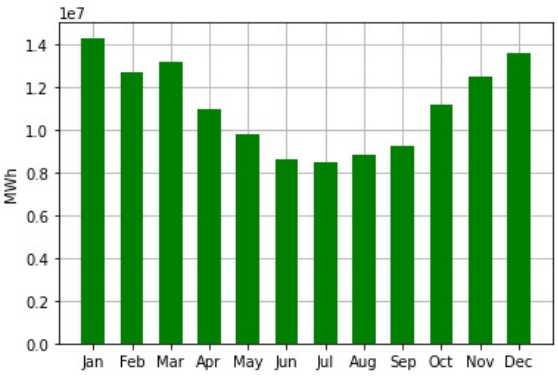

Figure 11.1: *Average monthly load in Norway from 2016 to 2020.*

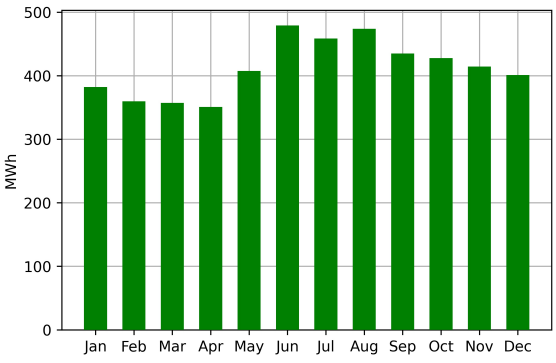

Figure 11.2: *The load profile of ASKO Midt-Norge in 2020.*

The refrigerated warehouse's load profile tells a contrasting story. The highest energy use is clearly during the summer months, which is the opposite of Norway's average. The energy use then decreases towards winter. For the particular load profile displayed in figure 11.2, the energy use steadily decreases during spring before spiking in May. The energy use of refrigerated warehouses Login Vagle and Login Vinterbro, as displayed in figures 5.4 and 5.5 in chapter 5, show a steady increase in energy use from winter throughout the spring till summer.

The load profiles of refrigerated warehouses can be characterized as having a slight reverse U-shape. The energy is generally relatively stable, only varying about $\pm$ 15 % from the average monthly values, as can be seen by looking at figure 11.2, with monthly load values ranging from about 350 to 475 MWh, while the mean value is 414 (4937 $\div$ 12) MWh. The PV production values however, as can be seen in figure 9.1, using Kristiansand as an example, deviate from the average with $\pm$ 100 %, with close to no production during winter months and over 150 MWh during May, June and July.

While the refrigerated warehouse's load profile might not fit perfectly with the production profile of PV systems, the load profile has a positive correlation that might be significantly better than other options. This is supported by looking at the average monthly energy use in Norway in figure 11.1, which indicate a negative correlation with PV production on month by month basis. While PV systems have close to no production during winter, the average monthly demand is peaking. During summer, when the PV system produces most of its energy, the average monthly load in Norway is at its lowest. Considering this, the load profile of refrigerated warehouses might constitute a particularly good fit for PV systems in comparison.

Explaining why refrigerated warehouses' load profiles are shaped the way they are can contribute to understanding why refrigerated warehouses constitute a good fit with PV production. While other buildings', industries' and other energy consumers' energy demand might be highly dependant on heating, most of a refrigerated warehouse's energy demand come from cooling. Assuming that the activity with regards to running refrigerated warehouses stays relatively similar throughout the year, which is reasonable to believe as goods are needed all year round, there is likely some other factor that makes the energy demand spike during summer.

One such factor may be the ambient temperature, or more specifically the difference between internal and ambient temperature, which as presented in chapter 1 cause a larger cooling need when the ambient temperature is higher. This cooling need is characteristic for refrigerated warehouses and argues that refrigerated warehouses are a good fit for PV systems. This does not exclude the possibility that there are other industries, buildings, or other big consumers that could benefit from PV, but it does distinguish refrigerated warehouses from most other large consumers positively with regard to PV production.

Regardless of whether the temperature is the defining factor that gives a refrigerated warehouse its characteristic consumption profile, the fact remains that refrigerated warehouses load profile does constitute a good fit with PV production, judging by monthly values. This fit is particularly strong compared to the average energy consumption in Norway. Analyzing monthly values does give implications that are important in understanding the fit between PV production and load at refrigerated warehouses. However, as PV energy in Norway is best utilized for reducing self-consumption of energy, it is important to check whether the actual production and consumption occur simultaneously. This requires analysis at smaller time intervals, such as hour by hour.

11.2 Intradaily Correlation

As the main advantage of installing PV systems on refrigerated warehouses is to reduce energy consumption from the grid, it is essential that PV production occurs simultaneously as when the refrigerated warehouse has high energy demand. PV is an intermittent energy source with high production during sunny days and none or low production during night and cloudy days. Additionally, the production is directly dependant on the solar radiation and the AM-coefficient, as described in chapter 2.3.1, which causes the production to peak during midday when the sun is closer to perpendicular to the earth, causing the characteristic intradaily reverse U-shape PV production curve as shown in figure 9.3. In order for refrigerated warehouses to correlate well with PV production, the refrigerated warehouse's energy consumption should optimally increase during sunny days when PV production is high and follow a similar intradaily curve as PV production.

The correlation coefficients presented in chapter 9 show a modest correlation of about 0.3553-0.4209 between the production of a PV system and load at a refrigerated warehouse. Considering that refrigerated warehouses have significant energy demand at all times, and PV systems produce no energy when the sun is not up, the sky is cloudy, or when the panels are covered in snow, the correlation coefficient indicates that the changes in consumption likely follow similar trends as the production curve when the PV system produces energy.

Comparing intradaily monthly averages in figures 9.2 and 9.3 shows that both consumption and production follow similar trends. Both curves have the lowest values at time intervals between 20:00 and 05:00. After 05:00, the load increases significantly for the next 2-3 hours. Thereafter, the load increases slightly different depending on the month. For low load months, such as March, April, February, January and December, the load has a slight increase or stays relatively stable for the next 7-8 hours. For medium load months, such as October and November, the load is relatively stable from about 08:00 till 12:00 before increasing for the next 4 to 5 hours. For the highest load months, May, June, July, August and September, the graph shows a generally stable increase in load for the next 6-7 hours.

After 14:00 or 15:00, all months have a significant decrease until 20:00. The decreasing rate is most prominent for the first 3-5 hours after 14:00 or 15:00. Most months reach bottom values within 20:00, with a few exceptions such as June, January and March, which experience lower values after 20:00. Although there are some deviations from month to month with regards to rates of increase and decrease at specific intervals for the intradaily curves, and when they peak and when they have their lowest values, looking at the graph in figure 9.2 as a whole show similar trends for all months. The load is lower during the night, increasing load during the morning, higher mid-day load and decreasing load towards evening, as detailed in chapter 9.

Some of the same trends are clear in the production graph shown in figure 9.3. One of the most significant differences between the load curve and the production curve is that the production curve experiences stronger rates of increase and decrease from morning till midday and midday till evening, respectively, compared to the load curve. Additionally, the intradaily production is substantially more month dependant, with peak power production reaching values as high as 600 kW for peak hours for summer months, whereas some winter months have peak production below 50 kW for peak hours, based on monthly averages.

Considering the unique intermittency of PV production, it is hard to find a perfect correlated energy-consuming source that is consistent, has high enough energy consumption such that installing a PV system is impactful with regards to reducing both total energy demand and energy costs. Therefore, a moderate correlation coefficient, as found with refrigerated warehouses, might be particularly strong.

In the intradaily load profile graph in figure 9.2 and the monthly load profile graph in figure 11.2, June stands out as having particularly high load. As can be seen in appendix C June 2020 was a warm month, significantly warmer than May and July. This indicates that temperature is indeed a pivotal contributor to the energy consumption of a load profile. Also taking into considerations the similarities between the average monthly sunshine hours in figure 3.3 and the average monthly temperature graph in figure 3.4, in combination with the fact that solar radiation is a defining factor in PV production, as detailed in chapter 2.3.1, the found positive correlation between PV production and load at refrigerated warehouses is coherent with theory.

Judging by graphs in figures 9.2 and 9.3 and the correlation coefficients in chapter 9, there is a clear positive correlation between PV system production and load at refrigerated warehouses. As described in chapter 11.1, refrigerated warehouses might have a better fit with PV systems than other large energy consumers with regards to monthly values. Monthly values alone can be misleading, and hourly values are a more reliable way of analyzing correlation as it considers intradaily variations. Table 11.1 shows a comparison of the correlation coefficient of PV production and load at the refrigerated warehouse presented in the results, and the correlation coefficient between PV production and the consumption in Norway, 2016-2020.

Table 11.1: *Correlation coefficient between PV production and load profile of refrigerated warehouse, and PV production and consumption in Norway 2016-2020*[3] *[11]. Refrigerated warehouse values retrieved from table 9.1.*

	Correlation Refrigerated Warehouse	**Correlation Consumption Norway**
Kristiansand	0.4036	-0.2603
Oslo	0.4209	-0.2880
Bergen	0.3894	-0.2640
Trondheim	0.3780	-0.3061
Tromsø	0.3553	-0.3635

While the refrigerated warehouse's correlation coefficient is categorized as moderately positive, the correlation coefficient of the total energy consumption in Norway is moderately negative. Both coefficients are based on hourly values and are consequently sensitive to intradaily changes. Using total consumption as a point of reference might be grossly misleading, as there exists a myriad of different sources for energy consumption, each with different yearly-, monthly- and intradaily load profiles that are not shown in the total consumption values. Drawing definite conclusions from comparing must therefore be done with great caution.

The differences in correlation coefficients displayed in figure 11.1 show that refrigerated warehouses have a positive correlation, whereas the total energy consumption in Norway is negatively correlated. This is coherent with what the monthly load profiles displayed and supports the aforementioned notion discussed in chapter 11.1, that refrigerated warehouses may be particularly suited for PV production compared to other large energy consumers. This does not exclude other contenders as viable for using PV technology, but this would require further analysis, which is not part of this thesis.

[3]The correlation was calculated using the 13th year of PV production five times VS hourly energy consumption in Norway 2016-2020.

11.3 Cost Implications of the Production-Load Correlation

For most businesses considering PV installations, the main factor may not be the amount of energy saved but rather how much money the energy saved results in. Due to fluctuations in electricity prices and the monthly max power dependant grid tariff structure in Norway, when the energy costs and power reductions caused by PV production occur, it is of huge importance with regards to the financial aspect of PV installations.

Figure 11.3 compares the percentage reduction in energy demand from the grid for the refrigerated warehouse and the resulting percentage reduction in total energy costs. The total portion of energy saved is consequently higher than the portion of energy costs cut for all cities. This highlights that a partial reduction in energy demand is not necessarily transferable to an equally big reduction in costs.

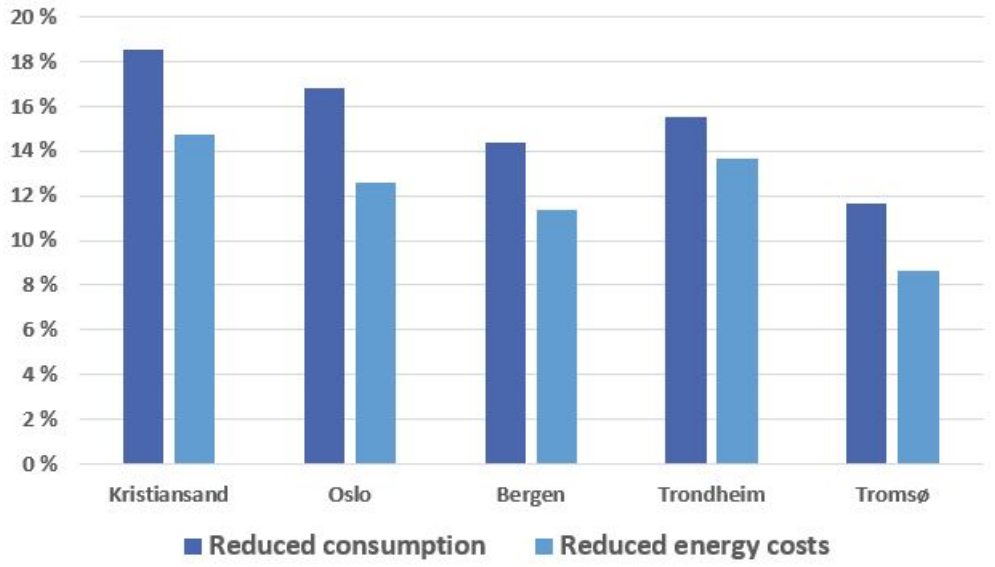

Figure 11.3: *Reduction in energy demand from grid versus reduction in total energy costs. Values retrieved from tables 10.2 and 10.5.*

For large consumers, energy can be considered as its own currency as it has a significant impact on operation costs. Many businesses focus on reducing their energy demand from the grid as a way to reduce costs, but as figure 11.3 shows, not all energy is worth the same from a financial viewpoint. It is therefore essential to discover what causes the discrepancy between energy reduction and cost reduction – *Is it the electricity, grid tariffs or taxes & fees?*

Figure 11.4 shows the cost of electricity without PV system installed by segment for Kristiansand. Similar figures for all cities can be found in appendix D, figures D.1 – D.5, which are all based off of values from table 10.5. In Kristiansand, electricity account for the largest part of the electricity bill, with 45.7 %. Taxes & fees and grid tariff account for 29.2 % and 25.1 % respectively. Tromsø sticks out since it has a significantly lower consumer cost, as explained in chapter 4.3.2. Tromsø's taxes & fees only account for 1.3 %, while electricity account for 63.2 % and the remaining 35.5 % are from grid tariff costs. The percentages reflect where there is most potential for cost reductions.

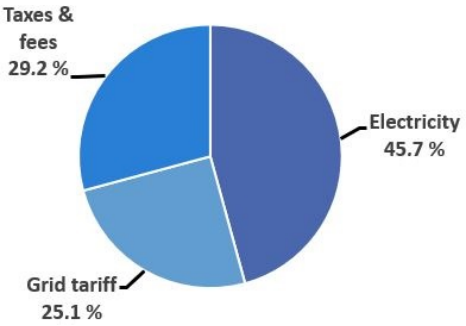

Figure 11.4: *The percentage costs for Kristiansand by segment. The total cost is 44.13 MNOK. Values retrieved from table 10.5.*

11.3.1 Electricity Prices at Times of Production

As shown by the average monthly prices in Norway from 2013-2020 in figure 4.2, electricity prices are generally lower in the summer. The electricity prices adapt to energy production and consumption, so the electricity prices show a similar curve to the average Norwegian energy consumption in figure 11.1. The monthly electricity curve is U- or V-shaped, whereas the production curve, as presented in figure 9.1 is reverse U- or V-shaped.

So electricity prices are, judging by monthly values, generally higher when PV has low production and lower when PV has high production. This could mean that the total reduced energy costs might not be as significant portion as the total reduced energy might indicate. This is, however, not unique to refrigerated warehouses but rather a general concern with PV production. Regardless of where a PV system is installed in Norway, the characteristic PV production curve will look similar, with more production during midday and no production at night and low production during winter and higher production during summer. For any PV applications where PV is used to reduce energy consumption from the grid, the problem would remain to some degree.

How big of an impact the varying electricity prices have on the relation between the amount of energy saved and the amount of money saved is not obvious. Assuming that the average monthly electricity prices as shown in figure 4.2 are representative of electricity prices each month, electricity prices during winter months are up to 50 % higher than electricity prices during winter. As a significant portion of PV production occurs during summer, it might be expected that the reduction in electricity costs for PV production on refrigerated warehouses is significantly lower than the energy reduction might indicate. This, however, is not the case, as can be seen in figure 11.5.

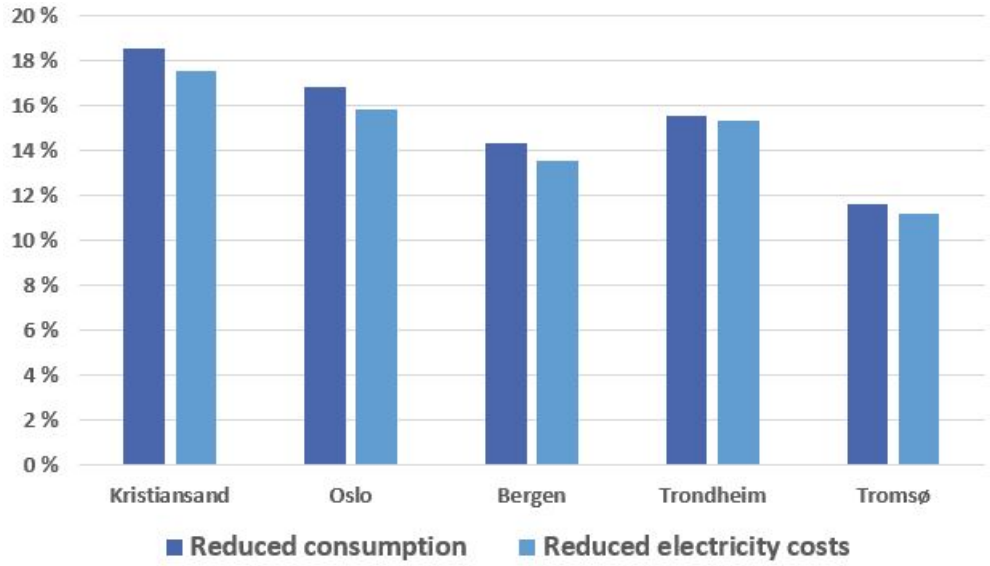

Figure 11.5: *Reduction in energy demand from grid versus reduction in electricity costs. Values retrieved from tables 10.2 and 10.5.*

Figure 11.5 shows that the percentage reduction in electricity costs is lower than the percentage reduction in energy consumption. It is, however, not nearly as big of a difference as what might be expected by looking at average monthly electricity prices in figure 4.2 in combination with the PV production curve in figure 9.1. In fact, the percentage reduction in electricity costs is markedly higher than the percentage reduction in total energy costs. This indicates that the relatively lower portion of money saved compared to energy saved is not mainly due to electricity costs.

Furthermore, as the reduction in electricity costs is almost equal to the reduction in energy demand, the indications shown by the monthly electricity prices and monthly PV production are misleading. Although it is true that electricity prices are higher during winter months and lower during summer months, whereas

the PV production is low during winter months and higher during summer months, it is not the case that electricity prices are consequently lower at times of PV production. What monthly values do not show are the fluctuations in energy prices from day to day and hour to hour.

Since the percentage reduction in electricity costs is similar to the percentage reduction in energy demand, the average electricity cost of the energy covered by PV production must be similar to the average electricity cost of the entire refrigerated warehouse's consumption. Considering the significantly higher energy costs during winter months, where PV production is minimal, the electricity prices at production times probably have a good fit with the intradaily electricity prices. That is, during the day, when production is high, the electricity prices are also higher. Furthermore, when production is low at night, the electricity prices are also low.

Higher electricity prices during the day and lower electricity prices during nighttime are reasonable, considering that the power market works by supply and demand. During the day, the energy demand is higher due to daily activities. The electricity consumption is probably higher during the day. Further analysis on this subject has not been done in this thesis, as it is not directly relevant to refrigerated warehouses. It is a more relevant study for PV systems in general regarding electricity costs.

Since electricity prices are not the leading cause of the lower percentage of total energy costs compared to the reduction in energy consumption after PV production, either grid tariffs or taxes & fees must be the main factors.

11.3.2 PV Production's Impact on Taxes & fees

The taxes & fees have an equal portion of reduction as the energy consumption. This is expected as the consumer cost is calculated based on energy consumption. In addition, the energy fund cost of 800 NOK remains both with and without PV production. The reduction in taxes & fees is always proportional to the reduction in electricity consumption, and therefore has no impact on the discrepancy between between reduced energy consumption and reduced energy costs, displayed in figure 11.3.

11.3.3 PV Production's Impact on Grid Tariff Costs

Since electricity prices and taxes & fees do not make up the discrepancy between the percentage of reduced energy consumption and the percentage of the reduced energy costs, grid tariffs must account for the significant difference. As can be seen in figure 11.6, the reduction in grid tariff costs is only about 5 % for Kristiansand, Oslo and Bergen, slightly higher at almost 8 % for Trondheim and close to 4 % for Tromsø.

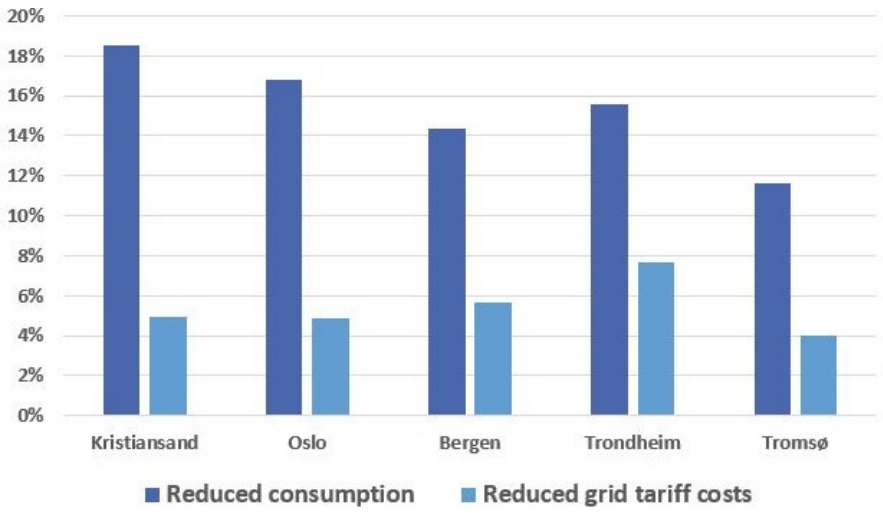

Figure 11.6: *Reduction in energy demand from grid versus reduction in electricity costs. Values retrieved from tables 10.2 and 10.5.*

Discovering why the reduction in grid tariff costs is so much lower requires looking at the model by which the grid tariff is set. The fixed sum of the grid tariffs remains the same with and without a PV system. This means that the fixed sum will not reduce energy cost with a PV system installed. This does make it such that the reduced grid tariff costs do not decrease as much as the total consumption. However, considering that the fixed sum is only a tiny portion of the total costs, its significance is not that big, and it does not explain the significant difference between the percentage reduced energy consumption and the percentage reduced grid tariff costs.

The energy part of the grid tariff is directly proportional to the energy consumption. This part is only 3.9 - 5.0 $øre/KWh$ during summer and 3.6 – 7.0 $øre/KWh$ during winter, as displayed in table 4.1, which is only a fraction of the electricity price. This part of the grid tariff costs will always have a similar percentage reduction as the reduced consumption with a PV system installed and does therefore not contribute to the large differences displayed in figure 11.6.

The power peak share of the grid tariff are the defining factor. As explained in chapter 4.3.2, this share is a monthly value depending on the single peak power value during that month. Since there is close to no PV production during the winter, a PV system will contribute very little, if any at all, to reducing the peak power consumption during winter.

As can be seen in table 4.1, the power part of the bill is higher per KW during winter than summer. Oslo, supplied by Elvia (NO1), is almost six times higher during winter than summer months. This relative difference between months is higher than the consumption differences shown in figure 9.1, and the power peak part of the bill during winter likely makes up the largest portion of the total power peak part of the bill throughout the year.

However, during spring, summer, and autumn, PV production is quite strong. Judging by the correlation between the load profile and the PV production curve, it seems that the PV production is high at peak consumption times. This is logical, assuming that when the temperature is high, the refrigerated warehouse's consumption increases due to increased energy use to cool wares and the fact that temperature is higher when the sun is up, which means there is more radiation and subsequently high production.

The findings discussed in chapters 11.1 and 11.2 indicate that PV production might reduce power consumption significantly at times of peak demand for refrigerated warehouses during spring, autumn and especially summer. However, a significant factor might reduce the potential impact of power peak reduction, namely curtailing of production. If it so happens that peak power consumption occurs at the time of peak PV production and that the PV production is sufficiently large (over 100 kW above demand), all PV production at that time will be curtailed.

Taking into consideration that curtailing is required quite often, as displayed in figure 10.1, it is likely that curtailing makes it such the peak power during some months is not lowered when it could have been. Figure 11.7, displayed on the next page, shows the difference in total grid tariff costs with and without a PV system installed with curtailing (Original difference) and without curtailing (Difference without curtailing) PV production.

As can be seen in figure 11.7, curtailing has an enormous impact on the grid tariff costs. Considering that the total amount of energy that curtailed, the lost potential reduction due to curtailed energy with regards to the energy part of the grid tariff is only about 58 $KNOK$[4] for Kristiansand. Considering that the fixed part of the grid tariff is the same, the difference in grid tariff costs due to curtailing is practically entirely due to the power share.

[4]Calculated using an energy price of 4.1 $øre/KWh$ from table 4.1, yearly curtailment of 57 MWh over 25 years. $0.041 \cdot 57000 \cdot 25 = 58425$ (NPV would be lower).

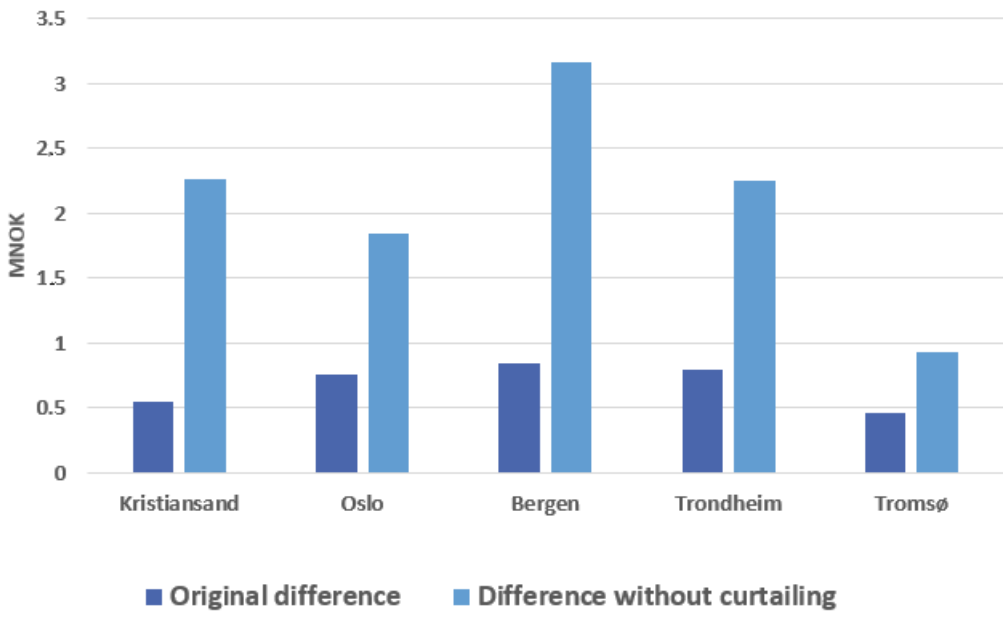

Figure 11.7: *Total reduction in grid tariffs costs with a PV system installed with and without curtailing. Values retrieved from table 10.5 and table 10.6.*

Other than displaying that the curtailment has a significant impact on cost reductions, figure 11.7 also has important implications regarding the correlation between load and PV production – *Peak power production for the PV systems occur, at least occasionally, at times of peak power demand at the refrigerated warehouse.* Since the power share of the electricity bill would be significantly lower if there was no curtailment, times of peak demand at the refrigerated warehouse occur when production is curtailed. This means that the power delivered by the PV system does not only meet the power demand of the refrigerated warehouse at times of peak demand but actually surpasses the power demand by over 100kW.

The impact curtailment has on the power share of the grid tariff costs further supports the aforementioned statement that there is a correlation between PV production and load at refrigerated warehouses. Additionally, it shows that the correlation is not perfectly utilized due to the 100 kW prosumer limit, which forces the curtailment of production. Furthermore, curtailment occurs at times of peak power demand, which causes lost potential in cost reduction with regards to the power share of the grid tariff costs.

12 Regional Differences

This chapter will discuss the results regarding the second part of the thesis statement – *What is the relative difference in installing PV systems on a refrigerated warehouse in five geographically different cities across Norway considering climatic and financial factors?* To answer this question, the regional differences in PV production is discussed by looking at climatic differences. Afterwards, the financial results are discussed, both considering differences in PV production and financial structure between cities.

12.1 Climatic Differences and Influence on Production Results

Production results can be seen in figure 10.1, displaying yearly average production results for each city and figure 10.2, displaying a monthly comparison. Kristiansand and Oslo produces the most energy per year, with average numbers of respectively 977 and 869 MWh, while northernmost city Tromsø has significantly lower production results of 580 MWh. Results in Trondheim and Bergen are placed in between, with results from Trondheim exceeding those of Bergen, despite being placed further north. Figures introduced in chapter 3 show a variation of meteorological factors across Norway. These figures indicate clear differences in conditions for solar power generation, and forms the basis of production results.

More specifically, figure 3.2 shows the difference in measured irradiance during summer and winter and indicates obvious variations. Cities located in the south-east part of Norway, like Kristiansand and Oslo, is on average exposed to more radiation from the sun compared to the other cities. This can also be observed in figure 3.3, where Kristansand and Oslo has a substantially higher number of measured sun hours. This is mainly caused by Kristiansand and Oslos southern latitudes and protection from cloud coverage by the mountainous region to their north-west. These locations are also less exposed to longer periods of precipitation, and snow cover is rarely an issue during months with high irradiance. These factors all contribute to Kristiansand and Oslo producing the highest yearly average of power compared to other cities investigated.

For the by far northernmost placed location in our assignment, Tromsø, located more than six latitudes, or 790 km further North compared to Trondheim, figures 3.2 and 3.3 indicate contrasting conditions to Oslo and Kristiansand. Figure 10.2 show the result of these conditions, as Tromsø has zero, or close to zero production from November through March. Tromsø's far north location leaves them without sunlight hours in large parts of winter, resulting in no measured irradiance and production. Summers in the North are on the other hand exposed to longer periods of sunlight, and in this period Tromsø experiences irradiation levels comparable to more southern regions, even exceeding those of Bergen during June and July. Another highly influencing factor is displayed in figure 3.6, showing that Tromsø is exposed to long periods with complete snow cover. It is noteworthy that this effect on results primarily coincides with months of darkness, thus making the effect insignificant in some months. The exemption is for March, April and May, where large parts of potential production is unused.

Despite Trondheim being around three latitudes further North, or 430 km in air distance compared to Bergen, the results show that Trondheim on average has higher production results. This can largely be explained by precipitation numbers presented in figure 3.5 The figure indicate just the one clear trend: Bergen is on another level compared to every other city, but due to their average monthly temperature seldom dropping below zero, precipitation is mostly in the form of rain. The effect from more frequent precipitation periods does coincide with more cloud cover, thus resulting in less direct sunlight and power generation. Rainfall does on the other hand have a cleaning effect on panels, which will result in a higher efficiency in ensuing periods, although the extent of this is hard to extract and remains unknown. For all other cities, precipitation numbers are very similar and any distinctive characteristics are hard to extract. Trondheim is like Tromsø, prone to large periods of snow during winter months, reducing the total production.

Average temperature across selected cities displayed in figure 3.4 indicates two contrasting factors. Higher average temperatures does indicate regions with potential for solar power generation as irradiance leads to higher temperatures, but at the same time solar panels efficiency drops with higher temperatures, and increases with lower. The figure shows that Oslo and Kristiansand has the highest average temperatures during summer months, but drops lower in Oslo during winter. In general, Tromsø has the lowest average temperature for all months, with Bergen and Trondheim in between.

As previously mentioned, for locations further North, Trondheim and Tromsø, precipitation often comes in the form of snow, as displayed in figure 3.6 The combination of large periods with below zero average temperatures and precipitation, leads to complete snow cover during some winter months, and has a significant effect on performance of solar panels as snow will completely block the panels. Solutions to issue this does exist, such as physically removing the snow, but this does on the other hand increase risk of damaging the panels. Heat generating systems is also an option, but comes with higher installation costs. The negative effect of snow is also noteworthy in Oslo, as temperature often drops below freezing during winter months.

12.2 Financial Differences

This chapter will discuss the financial differences with regards to installing PV systems on refrigerated warehouses in the five selected cities. There are two main factors that cause the financial differences, the PV production and the electricity bill structure. Both are accounted for in the financial analysis. The chapter is structured by first going through the three sections of the electricity bill, the electricity costs, taxes & fees and grid tariffs, before the impact of curtailing production is discussed. Finally, the regional differences in NPV and IRR is discussed, which accounts for both PV production and electricity bill structure as a whole.

12.2.1 Electricity Costs

The reduction in the electricity cost share of the total energy bill in table 10.5 display that Kristiansand has the largest reduction of 3.55 $MNOK$, followed by Trondheim and Oslo which are almost equal at 3.27 and 3.22 $MNOK$ respectively. Bergen has a lower reduction of 2.73 $MNOK$ while Tromsø has the lowest reduction at 2.28 $MNOK$. Since the electricity cost reduction is both dependant on total energy reduction and on the electricity prices, discovering how the regional electricity prices differs requires comparing the electricity prices while accounting for differences in PV production.

Figure 11.5 shows the relative differences between percentage reduced energy consumption and percentage reduced electricity costs for the five cities. If the electricity prices were constant, the percentage reduced electricity costs would be identical to the percentage reduced consumption. Therefore, the gap between the percentage reduced consumption and the percentage reduced electricity costs displays how much lower the electricity prices are at times of PV production, compared to the average electricity price per energy consumed at the refrigerated warehouse throughout the lifespan of the PV system.

Kristiansand, Oslo and Bergen have similar gaps between reduced consumption and reduced electricity costs, which indicate that each of their respective regions have similar electricity prices at times of production. Trondheim has the smallest gap, indicating higher electricity prices at times of production, compared to the other cities. Tromsø has a slightly larger gap, which indicates higher electricity prices at times of production than Kristiansand, Oslo and Bergen, but lower than Trondheim.

Each city represents its own regions electricity prices at times of production. As a whole, the electricity prices are generally quite similar at times of production in every region, with NO3 (Trondheim) and NO4 (Tromsø) having slightly higher electricity prices than the other bidding zones. This finding is perfectly coherent with the historical electricity prices during summer, which is when most of PV production occurs, as shown in figure 4.2. The figure shows that during spring, summer and autumn, NO3 (Trondheim) has the highest electricity prices, NO4 (Tromsø) has the second highest, while NO2 (Kristiansand), NO1 (Oslo) and NO5 (Bergen) have the lowest and almost identical electricity prices.

The standard deviations of the electricity costs saved, displayed in table 10.5 show some variation from region to region. The cities with the largest standard deviations are reflective of the cities with the most production. Considering the similarities in average electricity prices, the differences in the standard deviations is probably due to the production differences, rather than being reflective of yearly electricity variations between cities.

12.2.2 Taxes & Fees

The reduction in taxes & fees is proportional to the amount of reduced consumption. The only significant difference between the regions is for Tromsø (NO4), which has a electricity tax of only 0.00546 NOK/kWh which is 1/21 of the prices in the other cities at 0.1169 NOK/kWh. While Tromsø only saves about 0.05 $MNOK$ in taxes & fees throughout the lifespan of the PV system, the other cities save between 1.86 and 2.40 $MNOK$. The low taxes & fees reduction for Tromsø makes PV systems less suited as a measure to reduce energy costs. The differences between the other four cities are entirely due to differences in PV production. The VAT is not included in this analysis as most business-customers are eligible to get this refunded.

12.2.3 Grid Tariff

As can be seen in grid tariff column of table 10.5, Oslo and Bergen have significantly higher grid tariff costs, at 15.70 and 14.92 $MNOK$ before PV reduction, than the remaining three cities, with original grid tariff costs between 10.27 and 11.44 $MNOK$. The biggest differences in the electricity bills comes from the grid tariff costs, as each city's respective region have unique grid tariff structures, as shown in table 4.1. The power share of the grid tariffs makes the biggest impact between regions.

As shown in table 10.5 and illustrated in figure 11.7, Bergen, Trondheim and Oslo have the largest reductions in grid tariff costs at 0.85, 0.79 and 0.76 $MNOK$ respectively, while Kristiansand and Tromsø have the lowest reductions with 0.55 and 0.46 $MNOK$ respectively. The differences between the cities is caused by the differences between grid tariff structures, as well as the energy production differences.

The fixed sum of the grid tariff remains the same with and without PV production, and has no impact on the reduction in grid tariff costs. The energy share of the grid tariff costs makes up a significant portion of the reduction. This portion is the product of the reduced energy consumption times the energy prices in the region. As can be seen in table 4.1, there are differences in the energy cost per kWh of the grid tariff costs. As most of PV production occurs during summer, the summer energy prices are the most important. Trondheim has markedly higher costs at 5.0 $øre/kWh$, followed by Bergen at 4.3 $øre/kWh$, Kristiansand at 4.1 $øre/kWh$, Oslo at 3.9 $øre/kWh$ and at last Tromsø at 3.6 $øre/kWh$.

Trondheim's energy price is 22.0 % higher than the energy price in Kristiansand with regards to the grid tariff, during both summer and winter. Kristiansand's production is 19.2 % higher than Trondheim's production, which means that the reduction in grid tariff costs due to the energy share is about equal. Despite this fact, the total reduction in grid tariff costs is 0.24 $MNOK$ (43.6 %) higher in Trondheim compared to Kristiansand. This shows that the power share of the grid tariff costs reduction is an important factor which causes the differences between the cities. Additionally, the differences caused by the energy share of the grid tariff costs is relatively small considering that these costs are between 3.6 to 5.0 $øre/kWh$ compared to the electricity costs, which range between 21 to 27 $øre/kWh$ during summer months, judging by figure 4.2. Therefore, looking at the power share impact on the grid tariff costs is more interesting.

The reduction in the power share of the grid tariff costs is dependent on three factors – how often PV production effectively shaves the power peak of a month, how much the power peak is shaved by, and the price per kW each month. Since most PV production is occurs during summer, the regional differences in the price per kW for summer months is explored. As can be seen in table 4.1, Kristiansand (NO2) and Tromsø (NO4) has the lowest power share costs at 9.47 and 16 $NOK/kW/month$ respectively. Oslo (NO1) and Trondheim (NO3) are both significantly higher at 22 and 27 $NOK/kW/month$. Bergen has by

far the most expensive power share costs at 47.3 $NOK/kW/month$. All these prices are during summer months, which are slightly differently defined by each region.

Despite there being significant differences in the grid tariff reductions in each region, the total amount of money saved due to grid tariff reduction is low, compared to the reductions in taxes & fees and electricity costs, as displayed in figure 10.5. As described in the previous paragraph, there are significant differences in the power share costs of the grid tariff costs between the five regions. The impact of these differences, however, is very little if the PV system does not actually contribute in shaving power peaks. As established in chapter 11.3.3, a lot of cost reduction potential in the power share of the grid tariff is lost due to curtailing. The next chapter will explore exactly how much potential is lost for each region.

12.2.4 Curtailment's Impact on Cost Reductions

As shown in table 10.6 and further described in chapter 11.3.3, the lost reduction in grid tariffs due to curtailment is significant. Figure 12.1 displays the total cost savings with and without curtailing production. The upper part of the figure displays the percentage increased cost reduction without curtailing production. Even in Kristiansand, which curtails by far the most energy, as seen in table 10.4, the curtailment impact on the cost reductions is still almost entirely due to reduction in grid tariff costs, as shown in table 10.6. As most of the potential reduction without curtailing is due to the power share of the grid tariff, it is this factor that will be further discussed.

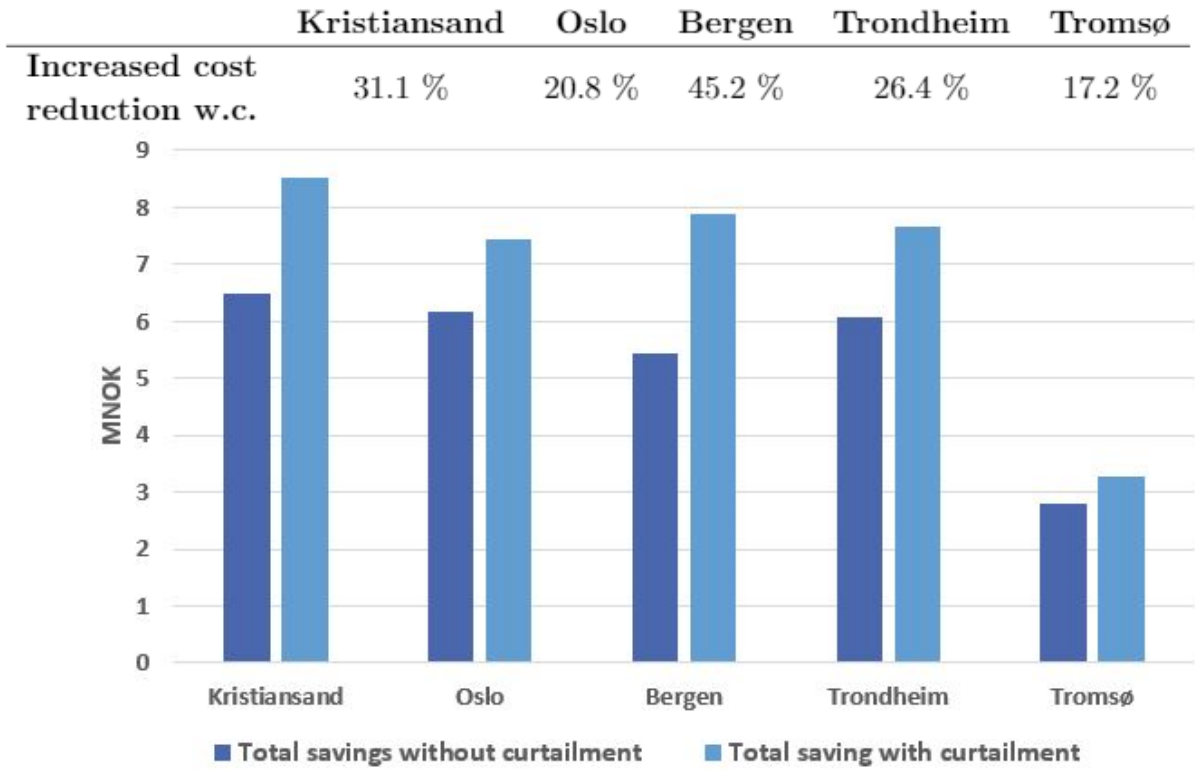

Figure 12.1: *Cost reduction with and without curtailing production, as well as the potential percentage increased cost reduction. w.c. means without curtailment. Values retrieved from tables 10.5 and 10.6.*

As shown in figure 12.1, Bergen has the highest potential increased cost reduction at 45.2 %. This change would make Bergen surpass both Oslo and Trondheim in total cost savings. Furthermore, as cost reduction is the only income of the cash flow analysis used to calculate NPV and IRR, and all cities have the same installation and maintenance costs, this change would cause Bergen to have a better NPV and IRR than Oslo and Trondheim. Kristiansand has the second highest increased cost reduction, and remains the city with the best NPV and IRR, due to having the largest total cost reduction.

Explaining the discrepancies between the five cities with regards to potential cost reduction lost due to curtailing requires going back to the three aforementioned factors that defines the power share of the grid tariff costs – how often PV production effectively shaves the power peak of a month, how much the power peak is shaved by, and the price per kW each month.

Bergen has by far the biggest potentially increased savings without curtailing due to the aforementioned expensive summer power share costs. The cost in $NOK/kW/month$ is about five times higher than that in Kristiansand, which has the lowest. The high cost reduction without curtailing in Bergen argues that a PV system could potentially shave peaks often, and furthermore shave the peaks by a considerable amount. Considering that Bergen has the second lowest production, as shown in figure 10.1, it is unlikely that the peaks are shaved during more months and by a bigger amount. However, Bergen's high power share cost during summer makes the shaved peaks have a much greater financial impact, if production is not curtailed.

Despite Kristiansand having the lowest power share costs per kW during summer, Kristiansand still has the second greatest reduced grid tariff costs that is lost due to curtailing. Initially, attributing this great reduction to the total curtailed energy might seem logical. However, considering that the reduced electricity costs are so low, as shown in table 10.6, and that the energy share of the grid tariff costs is lower than one fifth of the electricity costs[5], the impact of the energy share is not that big. Most of the lost reduction in costs due to curtailing is still the power share of the grid tariffs. But how come the power share of the grid tariff cost without curtailing make such a great impact on the total cost reductions when the power share prices per kW is so low?

Part of the explanation is that Kristiansand curtails energy the most often, and subsequently probably shaves a greater number of kW of the monthly peaks. This is however not sufficient to explain the great reduction in grid tariff costs lost due to curtailing. Kristiansand has higher production during both March and April than the other cities, which with regards to the power share of the grid tariff costs is considered as winter months, as described in chapter 4.3.2. During these months, the peak power cost is 56.69 $NOK/kW/month$, more than five times higher than the summer price. This indicates that significant peak shaving would occur during these months if production is not curtailed, and that this has a major impact on the potential savings in the grid tariff costs without curtailment for Kristiansand.

Trondheim and Oslo have the third and fourth most reduced savings without curtailing, with an additional 1.60 and 1.28 $MNOK$ reduced costs respectively. Trondheim's reduction potential is higher than Oslo's reduction potential, which is due to the slightly higher power share cost per kW during summer months with 27 vs 22 $NOK/kW/month$. Additionally, Trondheim (NO3) defines April as a winter month whereas Oslo (NO1) defines April as a summer month. This only has a slight impact on the total cost reduction as the power share cost only jumps to 39 $NOK/kW/month$ in Trondheim for winter months. The higher power share cost in Trondheim outweighs the fact that Oslo has higher production than Trondheim, as seen in figure 10.1. Oslo has significantly higher grid tariff costs without a PV system installed, but as this is mostly due to the expensive power share during winter months, this is unaffected by PV production.

Tromsø has the least lost potential due to curtailment, with only 0.48 $MNOK$ (0.47 of which is due to reduction in grid tariff costs). This would make the total cost reduction in Tromsø 17.2 % higher, as seen in the upper part of figure 12.1. Tromsø has consequently the lowest production, and it is so much lower than the other that curtailment occurs way rarer than with the other cities, as displayed in table 10.1. This fact, in combination with relatively low summer power share prices, as shown in table 4.1, results in curtailing having both the least total and relative impact on the cost reduction in Tromsø.

[5] 4.1 $øre/kWh$ is the energy share of the grid tariff costs vs the electricity price which averages monthly values between 21 and 27 $øre/kWh$ from March through October.

12.2.5 Regional Differences in IRR and NPV

Both IRR and NPV work as a total measurement of the profitability of the PV systems in the respective cities. The values are clearly negative for every single city, indicating that the investment is not worth it from a strictly financial perspective. Why the results might be too negative is described in sub chapters 7.1.1 and 7.3. As this thesis aims to answer the question – *What is the relative difference in installing PV systems on a refrigerated warehouse in five geographically different cities across Norway considering climatic and financial factors?* rather than answering if PV systems are suitable across Norway as a whole, the fact that the IRR and NPV values are negative will not be the main focus, but rather the relative differences between the cities will be emphasized.

Considering that all cities have the same installation costs, maintenance costs, as well as using the same load profile, the two factors that cause differences between the regions are firstly the differences in energy production, and secondly the difference in financial structure and costs between the regions. Therefore, the differences between the cities' IRR and NPV display the differences in utilizing a PV system on a refrigerated warehouse in the five cities, taking into account both aforementioned factors as a whole.

Kristiansand has the best IRR and NPV at -2.96 % and -6.68 $MNOK$. This is largely due to having the highest production, as shown in figure 10.1. The reduction in electricity costs and the taxes & fees makes up most of the cost reduction, and as these cost reductions are proportional to the produced energy, as well as the prices per energy consumed being quite similar between all cities, Kristiansand clearly comes out on top despite having a relatively low power share cost during summer months.

Oslo and Trondheim have similar IRRs and NPVs, with Oslo's values being slightly better. Trondheim has both slightly higher electricity prices and power share prices during summer, which results in Trondheim having marginally higher grid tariff and electricity costs reductions, as can be seen in table 10.5 and described in sub chapters 12.2.1 and 12.2.3. The taxes & fees reduction is the only part of the electricity bill that has a greater reduction in Oslo than Trondheim, and this is purely due to Oslo having 8.3 % higher PV production. As a whole, Oslo's higher production makes it slightly more suited than Trondheim, despite Trondheim having an electricity bill structure that benefits more from PV production.

Bergen has the second worst IRR and NPV. This is largely due to the low production in Bergen, which is only higher than Tromsø's production. Bergen has the highest power share costs during summer of all the cities, which results in Bergen having the highest grid tariff cost reduction. Bergen's high power share prices makes peak shaving by far the most effective in Bergen, but as this is poorly utilized due to curtailment, it is not enough to make up for the lower production. Therefore, Bergen comes out significantly behind Kristiansand, Oslo and Trondheim, at an IRR of -4.50 % and NPV of -7.74 $MNOK$. If production is not curtailed, however, the large reduction in power share of the grid tariff would make Bergen's IRR and NPV better than both Trondheim and Oslo, only beaten by Kristiansand.

Tromsø has by far the worst IRR and NPV at -10.16 % and -10.40 $MNOK$ respectively. The two main factors are that Tromsø has substantially lower production and extremely low taxes & fees, which lessens the benefit of reduced consumption. Additionally, Tromsø has the second lowest power share price per kW shaved during summer. The only positive for Tromsø is having slightly higher electricity prices during summer than Kristiansand, Oslo and Bergen. This, however, is insignificant compared to the other factors and Tromsø stands out as being worse suited for PV production compared to the other cities.

Conclusion and Further Work

13 Conclusion

The Norwegian PV industry is expected to experience a significant growth throughout the next decade. This section presents answers to the two questions raised in the thesis statement, which may contribute to the expansion of the Norwegian PV industry. Due to limitations in the scope of this thesis and simplifications made to the PV simulations and financial analysis, the financial results should only be considered as a tool to highlight how well the correlation between PV systems and refrigerated warehouses is utilized, as well as displaying the regional differences in PV systems on refrigerated warehouses.

Through data analysis between load at a refrigerated warehouse and production at a PV system, a moderate correlation from 0.3553 to 0.4209, depending on city, between load and PV production is found. PV production during summer constitutes a good fit with the increased energy consumption of refrigerated warehouses during summer months, considering that both production and load are significantly higher. Furthermore, the intradaily load and PV production show similar trends with higher load and production during the day, although production has higher relative peaks. Additionally, the intradaily curves are both affected in the same direction by monthly variations. Considering the intermittency of PV production, a moderate correlation can be considered as particularly good.

The percentage-wise reduction in financial savings is consequently lower than the energy savings. This is mostly due to the impact curtailing has on the power share of the grid tariff costs. The large difference in the power share of the grid tariff costs with and without curtailing shows that there is high production at peak power demand and that PV systems could effectively shave peaks during summer months. Without curtailing, PV systems are a suitable measure to reduce energy demand and costs at refrigerated warehouses.

Differences in production results stem solely from differences in climatic conditions. Locations in the south like Kristiansand and Oslo are exposed to more irradiation and more sunlight hours than other cities, resulting in the highest production. Moving north, the cities are exposed to less sunlight and have lower PV production. Bergen is the exception and has lower production than Trondheim as a result of cloud coverage due to topography, despite being located about 3° further south. Additionally, snow increases towards the North Pole which further decreases PV production.

From a financial perspective, Kristiansand is most suited for utilizing PV, which is entirely due to having highest PV production. Oslo and Trondheim are similarly suited for utilizing PV. Oslo has 8.3 % higher production than Trondheim, but Trondheim makes up for this by having higher electricity and power share prices during summer months, which makes the PV energy produced have a greater financial impact. Bergen is second worst suited for utilizing PV, mostly due to having the second-lowest PV production. Peak shaving has a greater financial impact in Bergen, but this is not fully utilized due to curtailing. Tromsø is significantly worse suited for utilizing PV, which is due to low production and lower taxes & fees.

Curtailing has a significant impact on the financial aspect of PV systems on refrigerated warehouses. Most of the potential cost reduction in the power share of the grid tariffs is lost. This is true for all cities, but especially in Bergen which have high power share prices per kW shaved during summer. Without curtailing, Trondheim would be better suited than Oslo, and Bergen would be better suited than both Oslo and Trondheim. The energy cost savings do not see the full benefit of the production-load correlation, and the energy cost savings could potentially be between 20.8 and 45.2 % higher without curtailing.

To summarize, there is a good correlation between load at a refrigerated warehouse and production from a PV system. PV systems have the potential to shave power peaks and reduce energy costs, but this potential is poorly utilized due to curtailing production. PV production increases northwards, with the exception of Bergen. Considering both PV production and electricity bill structure, ranking the cities from best to worth is, 1. Kristiansand, 2. Oslo and Trondheim, 3. Bergen and 4. Tromsø.

14 Further Work

This section will suggest areas uncovered during the thesis that were left unexplored and where further research on these subjects is recommended.

The correlations in this report were calculated over the whole 25-year span of the analyses. However, the correlation when there is no production is irrelevant and therefore influence the results. PV solar production is at its peak during the summer and very low during the winter. An examination looking more in-depth on the seasonal Pearson correlation could further uncover how good fit refrigerated warehouses and PV systems are.

One of the major discoveries in this report is the impact of curtailment. The timing of curtailment could be discovered even further. How often does curtailment occur at the time of peak demand, and what impact does this have? A quantitative analysis using large quantities of real-world PV production data and refrigerated warehouses' load data could provide valuable insights on this subject.

During the thesis, it was discovered that cost savings due to peak shaving are poorly utilized as a result of curtailing overproduction. Further analysis on how surplus energy can be used rather than curtailed could be interesting and have a significant financial impact. Some possible solutions are energy storage systems, interconnecting PV systems at refrigerated warehouses to other consumers, and smart systems which can predict production and only partly curtail production. Solutions to the curtailing issue can potentially allow significant up-scaling of new and existing PV systems. This could be beneficial as the marginal cost of adding new capacity decreases with size.

The environmental aspect of PV systems on refrigerated warehouses was not emphasized in this thesis, although being an important reason for looking at PV technology. An extensive life cycle analysis (LCA) of using PV systems, considering greenhouse gas emissions compared to alternative sources could be interesting.

Furthermore, the optimal size of a PV system could be examined. Finding the right size considering a precise installation cost model, electricity prices, and grid tariff is a difficult task. The PV system should not produce too much energy, but reducing the size of the facility would increase the relative installation costs. A more in-depth literature and market research with more precise financial parameters and multiple simulation and financial calculations could discover how an optimal PV system on a refrigerated warehouse should be designed.

Further research in PVsyst to determine both optimal location and system design would lead to more precise simulations that could potentially change the results. This would include defining all detailed losses to each individual location, settings near shadings and determining the horizon. In addition, and possibly most influential, gathering real measured meteorological data for every location for several years could significantly impact results.

The load profile used in the report origins from a refrigerated warehouse in Trondheim from 2020. There could be significant differences between refrigerated warehouses' load profiles from city to city. Neither a warehouse from Kristiansand nor Tromsø were collected. Therefore the impact of climate on refrigerated warehouses is to an extent unknown. The weather in 2020 could also have been unique, so collecting multiple years of load profiles would be advantageous. By collecting more load profiles from different years and additional locations, the correlation between refrigerated warehouses and PV solar energy production could be more precisely determined. In addition, the differences between installing PV solar cells on refrigerated warehouses in the different cities examined would also be more trustworthy because the load profiles would be affected by the cities' climate.

References

[1] PVsyst. *PVsyst - General Information.*
URL: https://www.pvsyst.com/help/index.html?general_descr.htm (visited on 05/16/2021).

[2] *What is Python? Executive Summary.*
URL: https://www.python.org/doc/essays/blurb/ (visited on 05/16/2021).

[3] *Introduction to Python.*
URL: https://www.w3schools.com/python/python_intro.asp (visited on 05/16/2021).

[4] NVE. *Kraftproduksjon - NVE.*
URL: https://www.nve.no/energiforsyning/kraftproduksjon/ (visited on 05/15/2021).

[5] Ingrid Endresen Haukeli et al.
"Elektrifiseringstltak i Norge - hva er konsekvensene for kraftsystemet?" In: (2020).
DOI: https://publikasjoner.nve.no/rapport/2020/rapport2020_36.pdf.

[6] Energifakta Norge. *Electricity production.*
URL: https://energifaktanorge.no/en/norsk-energiforsyning/kraftproduksjon/ (visited on 05/15/2021).

[7] Carl Andreas Veie et al. "Analyse og framskrivning av kraftproduksjon i norden til 2040".
In: (2019). DOI: http://publikasjoner.nve.no/rapport/2019/rapport2019_43.pdf.

[8] DNV GL. *Energy transition Norway 2020 - A national forecast to 2050.* 2020.
URL: https://www.norskindustri.no/siteassets/dokumenter/rapporter-og-brosjyrer/energy-transiton-norway-2020.pdf.

[9] NVE. *Solkraft - NVE.* Mar. 17, 2021.
URL: https://www.nve.no/energiforsyning/kraftproduksjon/solkraft/?ref=mainmenu (visited on 05/07/2021).

[10] NVE. *Effektuttak - NVE.* URL: https://www.nve.no/energibruk-effektivisering-og-teknologier/energibruk/effektuttak/?ref=mainmenu (visited on 05/10/2021).

[11] *Tall og data fra kraftsystemet.* Statnett. URL: https://www.statnett.no/for-aktorer-i-kraftbransjen/tall-og-data-fra-kraftsystemet/ (visited on 05/10/2021).

[12] Solenergiklyngen. *Bruk av solenergi i Norge.* 2015.
URL: https://static1.squarespace.com/static/597512eb579fb3d3de0207aa/t/59806508be65948aa727a108/1501586729727/Bruk+av+solenergi+i+Norge.pdf (visited on 05/19/2021).

[13] Jens Hetland. *Solenergi og kjøling av bygg - passer som hånd i hanske!* Mar. 27, 2019.
URL: https://blogg.fusen.no/solenergi-og-fryselager (visited on 05/17/2021).

[14] *Topp 10 - Norges største solcelleanlegg.*
URL: https://www.solenergi.no/nyhet/2017/9/25/norges-strste-solcelleanlegg (visited on 05/17/2021).

[15] ASKO. *Veien til fornybar energi.*
URL: https://asko.no/om-oss/fokus-pa-miljo/fornybar-energi/ (visited on 05/10/2021).

[16] Jørn Hindklev. *Rema Distribunal Østlandet.* Jan. 28, 2020.
URL: http://www.bygg.no/article/1421717 (visited on 05/10/2021).

[17] Solcellespesialisten. *Norges største solcelleinvestering setter standarden for fremtidens anlegg.* Aug. 31, 2020.
URL: https://www.tu.no/deltav/energi/annonse-norges-storste-solcelleinvestering-setter-standarden-for-fremtidens-anlegg/498350 (visited on 05/19/2021).

[18] Soteris A. Kalogirou. *Solar Energy Engineering : Processes and Systems.* Vol. Second edition. Academic Press, 2014. ISBN: 978-0-12-397270-5.

[19] REN21. *Renewables 2020 Global Status Report.* 2020.
URL: https://www.ren21.net/reports/global-status-report/ (visited on 02/15/2021).

[20] Lewis M. Fraas and Larry D. Partain. *Solar Cells and Their Applications.* Wiley, Oct. 2010.
ISBN: 978-0-470-44633-1.

[21] *This Month in Physics History.*
URL: http://www.aps.org/publications/apsnews/200904/physicshistory.cfm (visited on 02/03/2021).

[22] D. M. Chapin, C. S. Fuller, and G. L. Pearson.
"A New Silicon p-n Junction Photocell for Converting Solar Radiation into Electrical Power".
In: *Journal of Applied Physics* 25.5 (May 1, 1954), pp. 676–677. DOI: 10.1063/1.1721711.

[23] NASA. *Vanguard 1.*
URL: https://nssdc.gsfc.nasa.gov/nmc/spacecraft/display.action?id=1958-002B (visited on 02/08/2021).

[24] NASA. *Sputnik 1.*
URL: https://nssdc.gsfc.nasa.gov/nmc/spacecraft/display.action?id=1957-001B (visited on 02/08/2021).

[25] Lewis M. Fraas. *Low-Cost Solar Electric Power.* Springer, June 11, 2014. 186 pp.
ISBN: 978-3-319-07530-3.

[26] Harry Wirth, Karl-Anders Weiss, and Cornelia Wiesmeier.
Photovoltaic Modules : Technology and Reliability. De Gruyter, Sept. 12, 2016.
ISBN: 978-3110348279.

[27] Fraunhofer Ise. *Photovoltaics Report.* Sept. 16, 2020.
URL: https://www.ise.fraunhofer.de/content/dam/ise/de/documents/publications/studies/Photovoltaics-Report.pdf (visited on 04/06/2020).

[28] REN21. *Renawbles Global Status report.* 2019.
URL: https://www.ren21.net/wp-content/uploads/2019/05/gsr_2019_full_report_en.pdf (visited on 02/17/2021).

[29] Nora Holst Haaland. *Solenergibloggen - Hvilke typer solcelle-teknologier finnes?* Apr. 10, 2020.
URL: https://blogg.fusen.no/ulike-typer-solcelleteknologi (visited on 05/10/2021).

[30] *The Effect of Wavelength on Photovoltaic Cells.*
URL: https://sciencing.com/effect-wavelength-photovoltaic-cells-6957.html (visited on 05/19/2021).

[31] John F. Geisz et al.
"Six-junction III–V solar cells with 47.1% conversion efficiency under 143 Suns concentration".
In: *Nature Energy* 5.4 (Apr. 2020), pp. 326–335. DOI: 10.1038/s41560-020-0598-5.

[32] Solcellespesialisten. *Flate tak – Solcellespesialisten.no.*
URL: https://solcellespesialisten.no/flate-tak (visited on 05/10/2021).

[33] Soleneriklyngen. *Solenergi - Noe for din kommune?* June 11, 2019.
URL: https://solenergiklyngen.no/app/uploads/sites/4/bestiller-og-innkjoperkompetanse-om-solenergi-i-offentlig-sektor-1.pdf.

[34] WWF and Accenture. *Solkraft i Norge - Fremtidige muligheter for verdiskapning.* Apr. 2016.
URL: https://www.wwf.no/assets/attachments/solkraft_i_norge___fremtidige_muligheter_for_verdiskaping1.pdf (visited on 05/10/2021).

[35] *What is Material? - Types, Semiconductor & Band Gap.* July 11, 2017.
URL: https://electronicscoach.com/material.html (visited on 05/19/2021).

[36] C.B.Honsberg and S.G.Bowden. *Photovoltaics Education Website.*
URL: https://www.pveducation.org/pvcdrom/pn-junctions/semiconductor-structure (visited on 02/24/2021).

[37] Christiana Honsberg and Stuart Bowden. *Module Materials.*
URL: https://www.pveducation.org/pvcdrom/modules-and-arrays/module-materials (visited on 04/16/2021).

[38] *PN Junction Diode.* Jan. 29, 2020.
URL: https://lastminuteengineers.com/pn-junction-diode/ (visited on 02/24/2021).

[39] Adolf Goetzberger, Christopher Hebling, and Hans-Werner Schock.
"Photovoltaic materials, history, status and outlook".
In: *Materials Science and Engineering: R: Reports* 40.1 (Jan. 1, 2003), pp. 1–46.
DOI: 10.1016/S0927-796X(02)00092-X.

[40] Liam Nelson. *The Physics of Solar Cells.* Imperial Collage Press, 2003,
pp. 1–6, 127–130 186–198, 261–263. ISBN: 1-86094-340-3.

[41] Dricus De Rooij. *Anti Reflective Coating: usage for solar panels.* URL: https://sinovoltaics.com/learning-center/solar-cells/anti-reflective-coating-for-solar-panels/ (visited on 04/16/2021).

[42] Martin A. green. *Solar Cells – Operating Principals, Technology, and System Applications.* Prentice-Hall, 1982, pp. 161–165. ISBN: 0-13-822279-3.

[43] Swapnil Dubey, Jatin Narotam Sarvaiya, and Bharath Seshadri. "Temperature Dependent Photovoltaic (PV) Efficiency and Its Effect on PV Production in the World – A Review". In: *Energy Procedia*. PV Asia Pacific Conference 2012 33 (Jan. 1, 2013), pp. 311–321. DOI: 10.1016/j.egypro.2013.05.072.

[44] Jordon Layne. *Average Solar Panel Size,Weight and Dimensions (video).* Aug. 29, 2019. URL: https://www.ablison.com/average-solar-panel-sizeweight-and-dimensions/ (visited on 05/12/2021).

[45] *Multicrystalline Solar Panel Munchen Solar 250W MSP250AS-30.* URL: https://www.poweracu.com/photovoltaic/multicrystalline-solar-panel-munchen-solar-250w-msp250as-30.html (visited on 04/22/2021).

[46] *All Modules - IBC Solar AG Catalogue.* URL: https://shop.ibc-solar.de/products/en/shop/PV/pv_modules/all_modules/ (visited on 04/19/2021).

[47] Wikipedia. *From a solar cell to a PV system. Diagram of the possible components of a photovoltaic system.* Aug. 2014. URL: https://en.wikipedia.org/wiki/File:From_a_solar_cell_to_a_PV_system.svg (visited on 05/20/2021).

[48] Muhammad Hafeez Mohamed Hariri et al. "Grid-Connected PV Generation System—Components and Challenges: A Review". In: *Energies* 13.17 (2020), p. 4279. DOI: http://dx.doi.org/10.3390/en13174279.

[49] Knut A. Rosvold. *watt peak.* Aug. 30, 2019. URL: http://snl.no/watt_peak (visited on 05/18/2021).

[50] Konrad Mertens. *Photovoltaics: Fundamentals, Technology, and Practice.* John Wiley & Sons, May 29, 2018. 371 pp. ISBN: 978-1-119-40116-2.

[51] PVsyst. *PVsyst 7 Help.* URL: https://www.pvsyst.com/help/ (visited on 05/12/2021).

[52] John Boland, Jing Huang, and Barbara Ridley. "Decomposing global solar radiation into its direct and diffuse components". In: *Renewable and Sustainable Energy Reviews* 28 (Dec. 1, 2013), pp. 749–756. DOI: 10.1016/j.rser.2013.08.023.

[53] Tomislav Pavlovic. "Solar Energy". In: Green Energy and Technology (2020). DOI: 10.1007/978-3-030-22403-5_1.

[54] Kuga Electrical. *Optimum Solar Panel Angle: A Guide.* Sept. 16, 2019. URL: https://www.13kuga.com.au/solar-panel-orientation-vs-production/ (visited on 03/24/2021).

[55] M. M. Fouad, Lamia A. Shihata, and ElSayed I. Morgan. "An integrated review of factors influencing the perfomance of photovoltaic panels". In: *Renewable and Sustainable Energy Reviews* 80 (Dec. 1, 2017), pp. 1499–1511. DOI: 10.1016/j.rser.2017.05.141.

[56] Mohammad Reza Maghami et al. "Power loss due to soiling on solar panel: A review". In: *Renewable and Sustainable Energy Reviews* 59 (June 1, 2016), pp. 1307–1316. DOI: 10.1016/j.rser.2016.01.044.

[57] DNV. *Photovoltaic module degradation DNV.* URL: https://www.dnv.com/Publications/photovoltaic-module-degradation-165278 (visited on 05/18/2021).

[58] Ali Aria Yadmelat. *Solenergibloggen - Forvaltning, Drift og Vedlikehold på solenergianlegg.* Nov. 12, 2019. URL: https://blogg.fusen.no/fdv-forvaltning-drift-vedlikehold-solceller-og-solenergianlegg (visited on 05/10/2021).

[59] Gunnar Ketzler, Wolfgang Römer, and Achim A. Beylich. “The Climate of Norway”. In: World Geomorphological Landscapes (2021). Ed. by Achim A. Beylich, pp. 7–29. DOI: 10.1007/978-3-030-52563-7_2.

[60] Gemini. *Solinnstråling*. URL: https://gemini.no/2018/03/hvor-godt-virker-egentlig-solceller-i-nordisk-klima/solinnstraling/ (visited on 05/12/2021).

[61] Meteoroligisk Institutt. *Norsk Klimaservicesenter*. URL: https://seklima.met.no/observations/ (visited on 05/12/2021).

[62] Energifakta Norge. *The electricity grid*. Apr. 9, 2019. URL: https://energifaktanorge.no/en/norsk-energiforsyning/kraftnett/ (visited on 02/04/2021).

[63] Ministry of Petroleum and Energy. *Power supply and the electricity grid*. Government.no. Publisher: regjeringen.no. July 26, 2016. URL: https://www.regjeringen.no/en/topics/energy/the-electricity-grid/power-supply-and-the-electricity-grid/id2353792/ (visited on 02/04/2021).

[64] Ministry of Petroleum and Energy. *Power Market*. Publisher: regjeringen.no. July 26, 2016. URL: https://www.regjeringen.no/en/topics/energy/the-electricity-grid/the-power-market-and-prices/id2076000/ (visited on 02/04/2021).

[65] Energifakta Norge. *The power market*. Sept. 24, 2019. URL: https://energifaktanorge.no/en/norsk-energiforsyning/kraftmarkedet/ (visited on 02/04/2021).

[66] Nord Pool. *System price and Area price calculations*. URL: https://www.nordpoolgroup.com/trading/Day-ahead-trading/Price-calculation/ (visited on 02/17/2021).

[67] NTE. *Hva påvirker strømprisen?* nte.no. May 12, 2020. URL: https://nte.no/blogg/innlegg/hva-pavirker-stromprisen (visited on 02/09/2021).

[68] NVE. *Norway and the European power market - NVE*. Dec. 22, 2020. URL: https://www.nve.no/norwegian-energy-regulatory-authority/wholesale-market/norway-and-the-european-power-market/ (visited on 02/17/2021).

[69] Nord Pool. *Bidding Zones*. URL: https://www.nordpoolgroup.com/the-power-market/Bidding-areas/ (visited on 02/18/2021).

[70] Nord Pool. *Market data*. URL: https://www.nordpoolgroup.com/Market-data1/Dayahead/Area-Prices/NO/Hourly/ (visited on 05/12/2021).

[71] NVE. *Nettleie - NVE*. Oct. 31, 2019. URL: https://www.nve.no/reguleringsmyndigheten/stromkunde/nettleie/ (visited on 02/02/2021).

[72] EnergiNorge. *Hva er egentlig nettleie og hva påvirker den?* Apr. 2020. URL: https://www.energinorge.no/contentassets/ecb78680d7484879b1385d1f61aa766f/hva-er-egentlig-nettleie-og-hva-pavirker-den.pdf (visited on 04/21/2021).

[73] Agder Energi. *Nettleiepriser 2020 Bedrift*. URL: https://indd.adobe.com/view/b499ac18-ee14-4c07-879e-c087c81a8391 (visited on 05/15/2021).

[74] Elvia. *Nettleiepriser og effekttariff bedrift*. URL: https://www.elvia.no/nettleie/alt-om-nettleie/nettleiepriser-og-effekttariff-for-bedrifter-i-oslo-og-viken (visited on 05/15/2021).

[75] BKK Nett. *Nettleie for bedriftskunder*. URL: https://nett.bkk.no/produktdetaljer?productId=9af3a3e7-9813-489f-9eb4-4fbcb29dd768 (visited on 05/15/2021).

[76] Tensio. *Nettleie, priser og avtaler*. Tensio Trøndelag Sør. URL: https://ts.tensio.no/kunde/nettleie-priser-og-avtaler (visited on 05/15/2021).

[77] Arva. *Nettleiestruktur*. URL: http://www.tromskraftnett.no/naring/nett/prisinformasjon (visited on 05/15/2021).

[78] NVE. *Om forskjeller i nettleie - NVE*. Mar. 31, 2020. URL: https://www.nve.no/reguleringsmyndigheten/nettjenester/nettleie/nettleie-for-forbruk/om-forskjeller-i-nettleie/ (visited on 05/05/2021).
[79] Skatteetaten. *Avgift på elektrisk kraft*. 2021. URL: https://www.skatteetaten.no/bedrift-og-organisasjon/avgifter/saravgifter/om/elektrisk-kraft/ (visited on 04/21/2021).
[80] NVE. *Anleggsbidrag - NVE*. URL: https://www.nve.no/reguleringsmyndigheten/nettjenester/nettilknytning/anleggsbidrag/ (visited on 04/28/2021).
[81] NVE. *Plusskunder - NVE*. URL: https://www.nve.no/reguleringsmyndigheten/nettjenester/nettleie/tariffer-for-produksjon/plusskunder/ (visited on 04/28/2021).
[82] Statistics Norway. *SSB - Elprice*. Feb. 15, 2021. URL: https://www.ssb.no/en/energi-og-industri/artikler-og-publikasjoner/very-low-electricity-price-in-2020 (visited on 02/16/2021).
[83] Kjetil Lund and Anne Vera Skrivarhaug. *Langsiktig Kraftmarkedsanalyse 2020 – 2040*. Oct. 2020. URL: http://publikasjoner.nve.no/rapport/2020/rapport2020_37.pdf (visited on 05/11/2021).
[84] Energi Norge. *Hvorfor betaler vi nettleie og hvorfor øker den?* Mar. 2018. URL: https://www.energinorge.no/contentassets/ecb78680d7484879b1385d1f61aa766f/nettleien---mars-2018.pdf (visited on 05/11/2021).
[85] *Om oss*. Trondheim Havn. URL: https://trondheimhavn.no/om-oss/ (visited on 05/04/2021).
[86] PVsyst. *PVsyst V7 Grid Connected Tutorial*. URL: https://www.pvsyst.com/wp-content/uploads/2020/10/PVsyst_Tutorials_V7_Grid_Connected.pdf (visited on 04/15/2021).
[87] Meteotest AG et al. "Meteonorm Handbook Part 1: Software". In: (Sept. 2020).
[88] Committee appointed by Royal Decree. *Cost-Benefit Analysis*. Oct. 3, 2012. URL: https://www.regjeringen.no/contentassets/5fce956d51364811b8547eebdbcde52c/en-gb/pdfs/nou201220120016000en_pdfs.pdf (visited on 04/09/2021).
[89] *Pearson Product-Moment Correlation*. URL: https://statistics.laerd.com/statistical-guides/pearson-correlation-coefficient-statistical-guide.php (visited on 05/11/2021).
[90] *Correlation Coefficient: Simple Definition, Formula, Easy Steps*. URL: https://www.statisticshowto.com/probability-and-statistics/correlation-coefficient-formula/ (visited on 05/11/2021).

A Load vs Production Graphs

Load vs Production Graphs With Curtailing Production

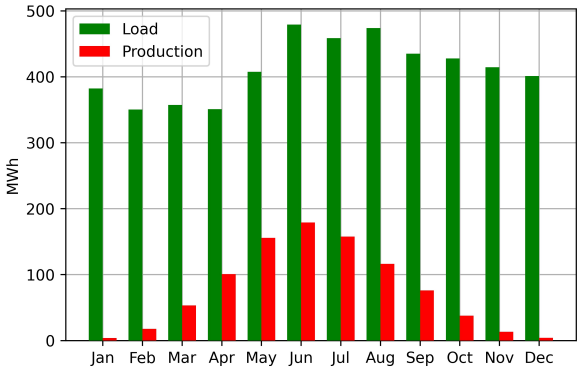

Figure A.1: *Load vs production for Kristiansand.*

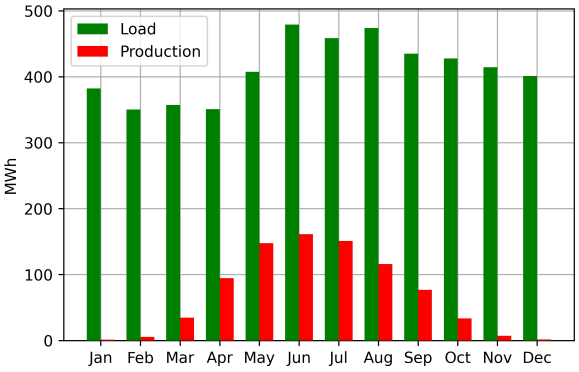

Figure A.2: *Load vs production for Oslo.*

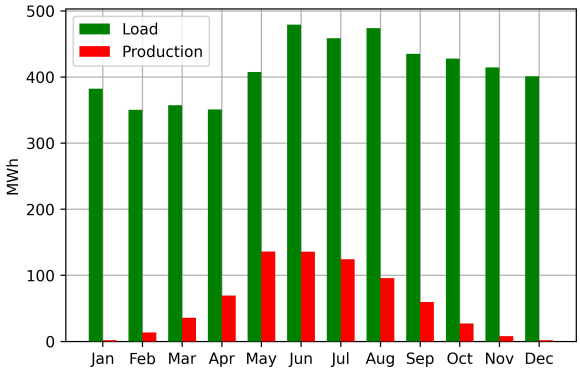

Figure A.3: *Load vs production for Bergen.*

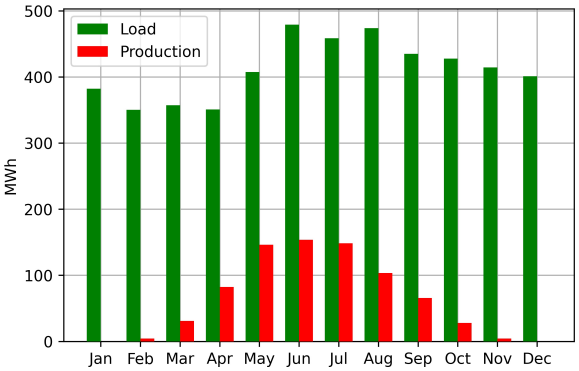

Figure A.4: *Load vs production for Trondheim.*

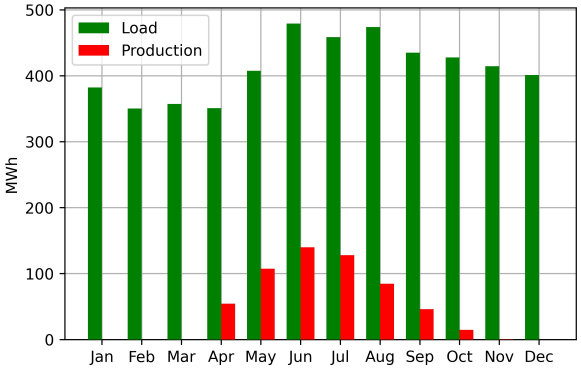

Figure A.5: *Load vs production for Tromsø.*

Load vs Production Graphs Without Curtailing Production

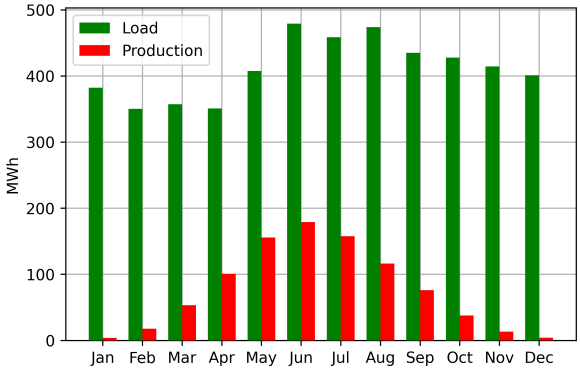

Figure A.6: *Load vs production w.c. Kristiansand*

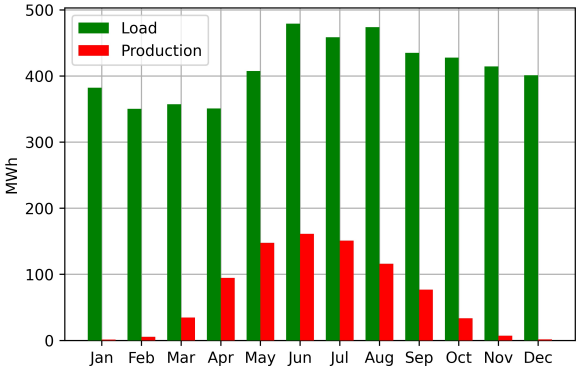

Figure A.7: *Load vs production w.c. Oslo.*

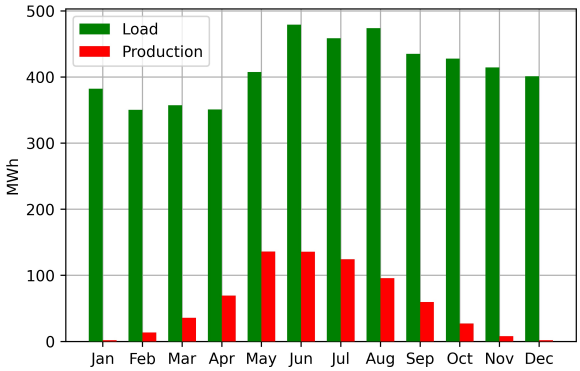

Figure A.8: *Load vs production w.c. Bergen.*

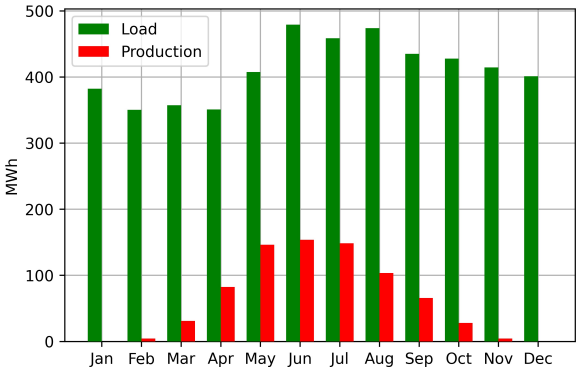

Figure A.9: *Load vs production w.c. Trondheim.*

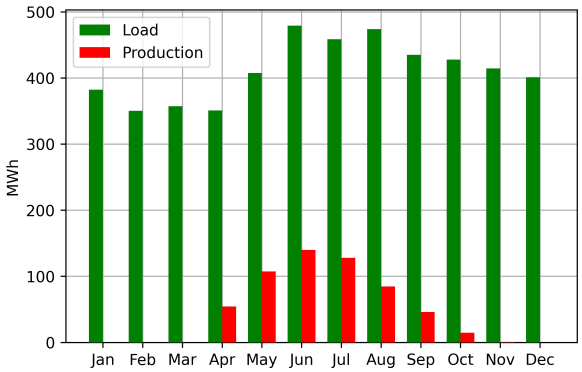

Figure A.10: *Load vs production for Tromsø w.c.*

B Average Hourly-based Production by Month

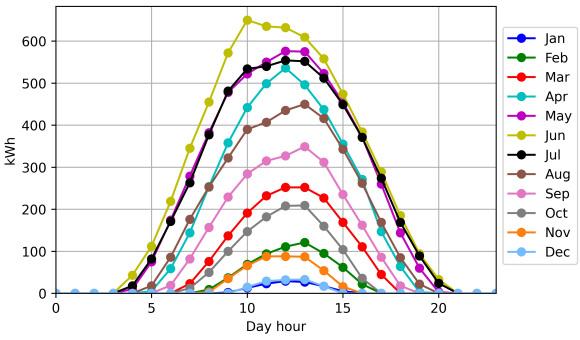

Figure B.1: *Average hourly-based production by month for Kristiansand.*

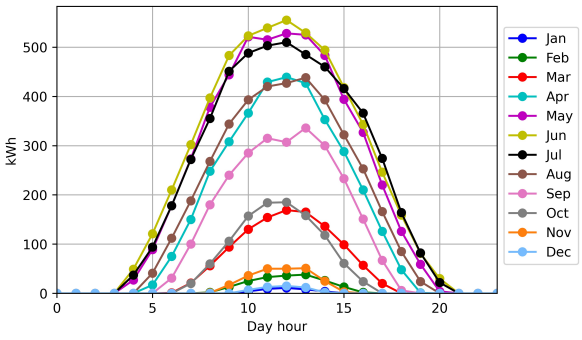

Figure B.2: *Average hourly-based production by month for Oslo.*

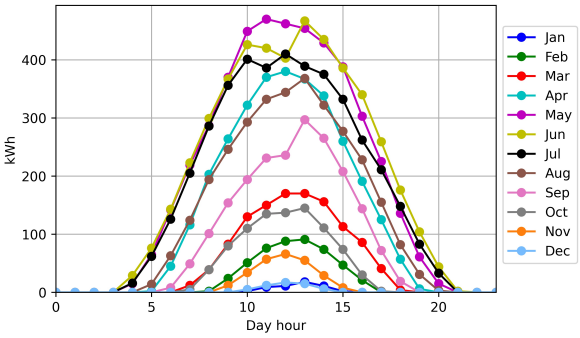

Figure B.3: *Average hourly-based production by month for Bergen.*

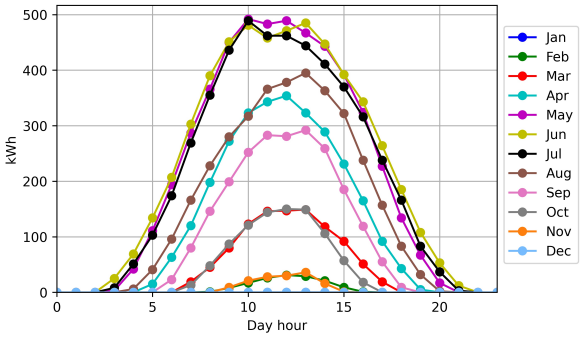

Figure B.4: *Average hourly-based production by month for Trondheim.*

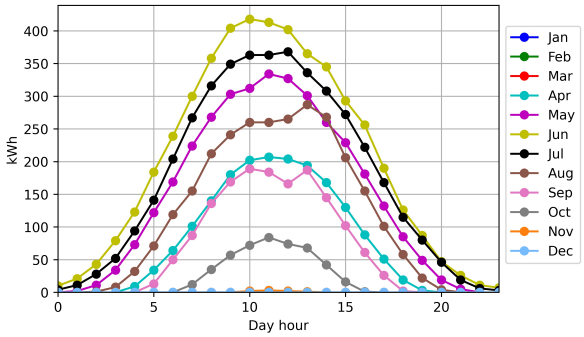

Figure B.5: *Average hourly-based production by month for Tromsø.*

Figures below display average hourly-based production by month without curtailing.

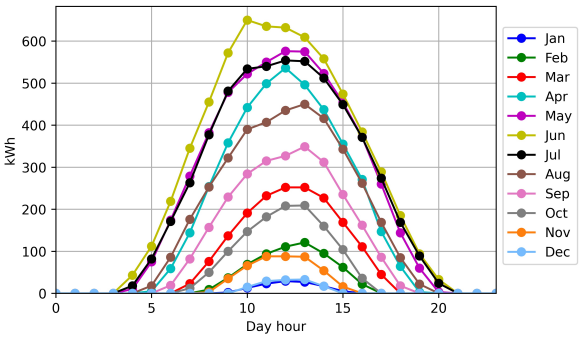

Figure B.6: *Average hourly-based production by month for Kristiansand w.c.*

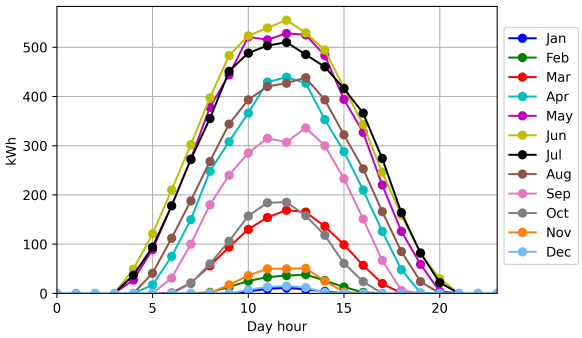

Figure B.7: *Average hourly-based production by month for Oslo w.c.*

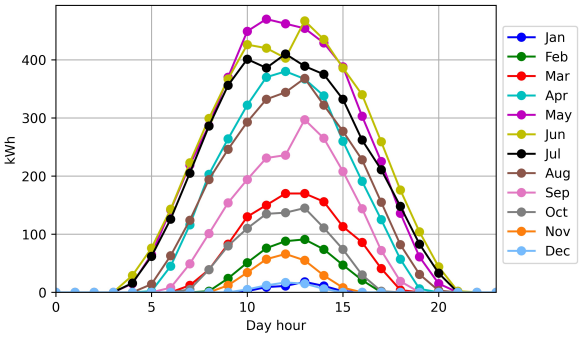

Figure B.8: *Average hourly-based production by month for Bergen w.c.*

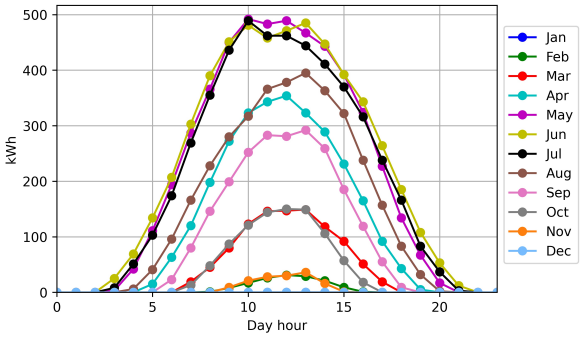

Figure B.9: *Average hourly-based production by month for Trondheim w.c.*

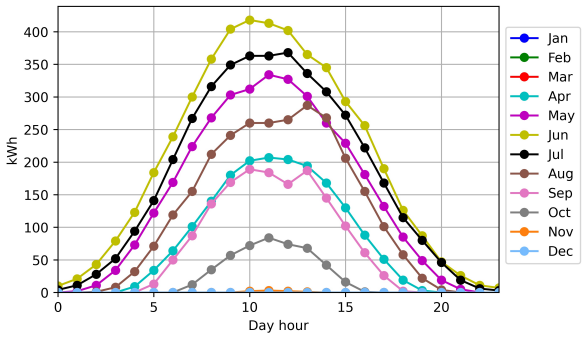

Figure B.10: *Average hourly-based production by month for Tromsø w.c.*

C Real Data From ASKO Midt-Norge

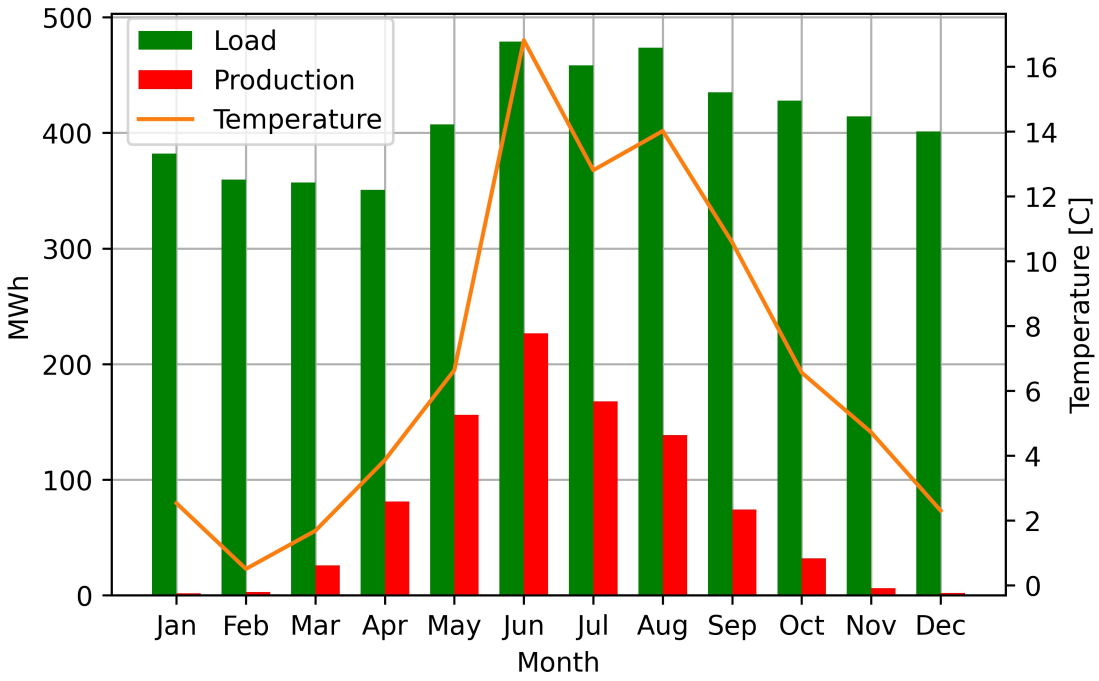

Figure C.1: *Real production, load and temperature from 2020 ASKO Midt-Norge.*

Table C.1: *Correlation between the load profile, PV solar energy production and outside temperature from 2020 ASKO Midt-Norge.*

	Load	**Production**	**Temperature**
Load	1.0000	0.4419	0.3328
Production	0.4419	1.0000	0.5014
Temperature	0.3328	0.5014	1.0000

D Cost of Energy by Segment Without PV System

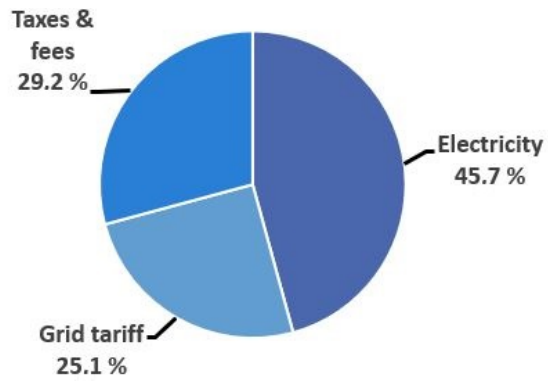

Figure D.1: *The percentage costs for Kristiansand by segment. The total cost is 44.13 MNOK. Values retrieved from table 10.5.*

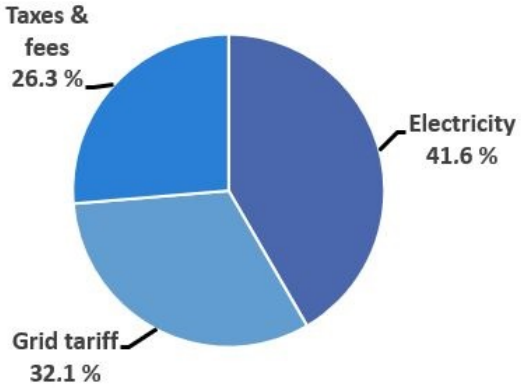

Figure D.2: *The percentage costs for Oslo by segment. The total cost is 48.94 MNOK. Values retrieved from table 10.5.*

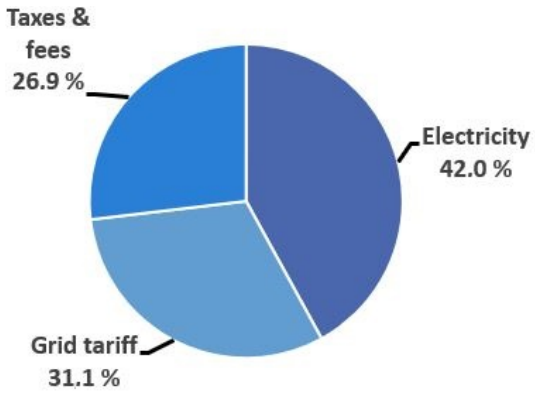

Figure D.3: *The percentage costs for Berge by segment. The total cost is 47.93 MNOK. Values retrieved from table 10.5.*

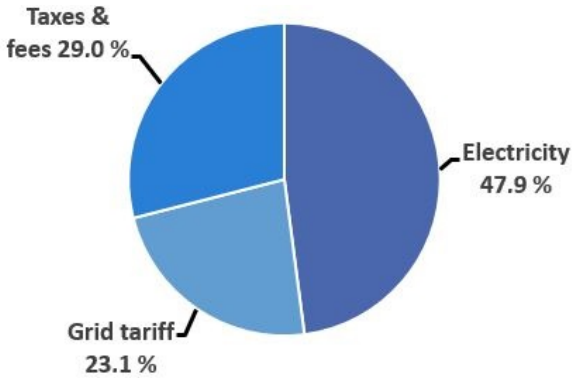

Figure D.4: *The percentage costs for Trondheim by segment. The total cost is 44.44 MNOK. Values retrieved from table 10.5.*

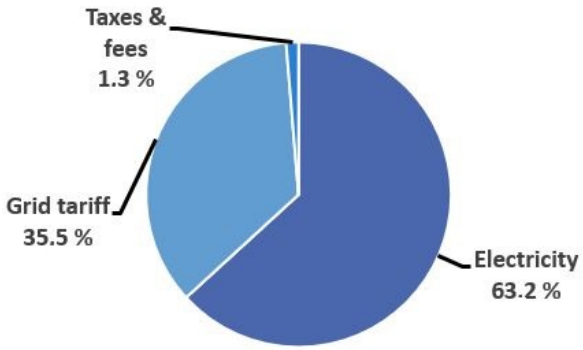

Figure D.5: *The percentage costs for Tromsø by segment. The total cost is 32.23 MNOK. Values retrieved from table 10.5.*

E PVsyst Report

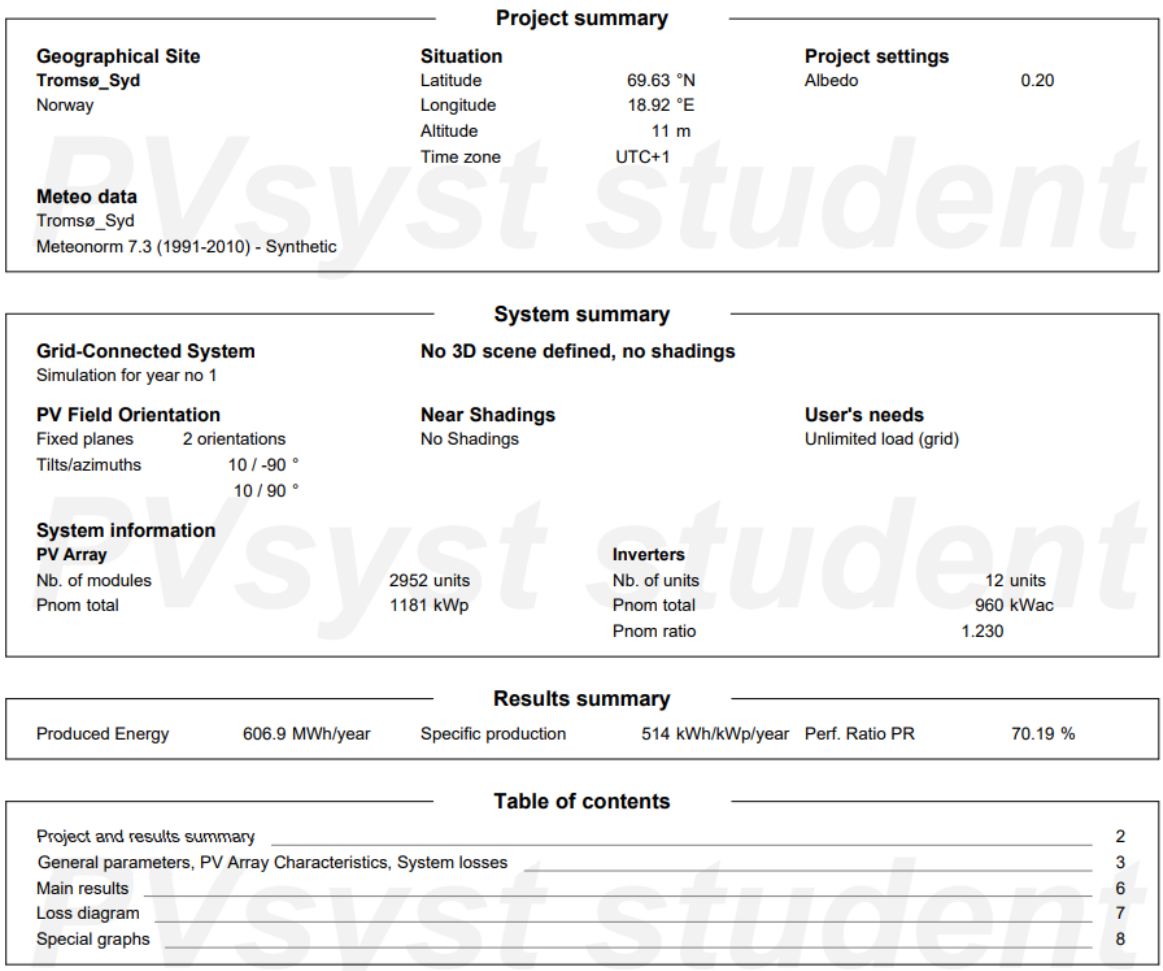

Project summary

Geographical Site
Tromsø_Syd
Norway

Situation
Latitude 69.63 °N
Longitude 18.92 °E
Altitude 11 m
Time zone UTC+1

Project settings
Albedo 0.20

Meteo data
Tromsø_Syd
Meteonorm 7.3 (1991-2010) - Synthetic

System summary

Grid-Connected System
Simulation for year no 1

No 3D scene defined, no shadings

PV Field Orientation
Fixed planes 2 orientations
Tilts/azimuths 10 / -90 °
10 / 90 °

Near Shadings
No Shadings

User's needs
Unlimited load (grid)

System information

PV Array
Nb. of modules 2952 units
Pnom total 1181 kWp

Inverters
Nb. of units 12 units
Pnom total 960 kWac
Pnom ratio 1.230

Results summary

Produced Energy 606.9 MWh/year | Specific production 514 kWh/kWp/year | Perf. Ratio PR 70.19 %

Table of contents

Figure E.1: *Page 2 PVsyst report.*

General parameters

Grid-Connected System — **No 3D scene defined, no shadings**

PV Field Orientation

Orientation		Sheds configuration	Models used	
Fixed planes	2 orientations	No 3D scene defined	Transposition	Perez
Tilts/azimuths	10 / -90 ° 10 / 90 °		Diffuse	Perez, Meteonorm
			Circumsolar	separate

Horizon	Near Shadings	User's needs
Free Horizon	No Shadings	Unlimited load (grid)

PV Array Characteristics

PV module

Manufacturer	Generic
Model	TSM-DE15M-(II)-400
(Original PVsyst database)	
Unit Nom. Power	400 Wp
Number of PV modules	2952 units
Nominal (STC)	1181 kWp
Modules	164 Strings x 18 In series
At operating cond. (50°C)	
Pmpp	1074 kWp
U mpp	661 V
I mpp	1625 A

Inverter

Manufacturer	Generic
Model	SG80KTL
(Original PVsyst database)	
Unit Nom. Power	80.0 kWac
Number of inverters	12 units
Total power	960 kWac
Operating voltage	570-950 V
Pnom ratio (DC:AC)	1.23

Total PV power

Nominal (STC)	1181 kWp
Total	2952 modules
Module area	5999 m²
Cell area	5144 m²

Total inverter power

Total power	960 kWac
Nb. of inverters	12 units
Pnom ratio	1.23

Array losses

Array Soiling Losses

Average loss Fraction 43.8 %

Jan.	Feb.	Mar.	Apr.	May	June	July	Aug.	Sep.	Oct.	Nov.	Dec.
100.0%	100.0%	100.0%	50.0%	25.0%	0.0%	0.0%	0.0%	0.0%	0.0%	50.0%	100.0%

Thermal Loss factor

Module temperature according to irradiance

Uc (const)	20.0 W/m²K
Uv (wind)	0.0 W/m²K/m/s

DC wiring losses

Global array res.	6.7 mΩ
Loss Fraction	1.5 % at STC

Module Quality Loss

Loss Fraction -0.8 %

Module mismatch losses

Loss Fraction 2.0 % at MPP

Strings Mismatch loss

Loss Fraction 0.1 %

Module average degradation

Year no	1
Loss factor	0.2 %/year

Mismatch due to degradation

Imp RMS dispersion	0.4 %/year
Vmp RMS dispersion	0.4 %/year

Figure E.2: *Page 3 PVsyst report.*

Array losses

IAM loss factor

Incidence effect (IAM): Fresnel AR coating, n(glass)=1.526, n(AR)=1.290

0°	30°	50°	60°	70°	75°	80°	85°	90°
1.000	0.999	0.987	0.962	0.892	0.816	0.681	0.440	0.000

Figure E.3: *Page 4 PVsyst report.*

System losses

Unavailability of the system

Time fraction	1.0 % 3.7 days, 3 periods

Figure E.4: *Page 5 PVsyst report.*

Main results

System Production

Produced Energy	606.9 MWh/year	Specific production	514 kWh/kWp/year
		Performance Ratio PR	70.19 %

Normalized productions (per installed kWp)

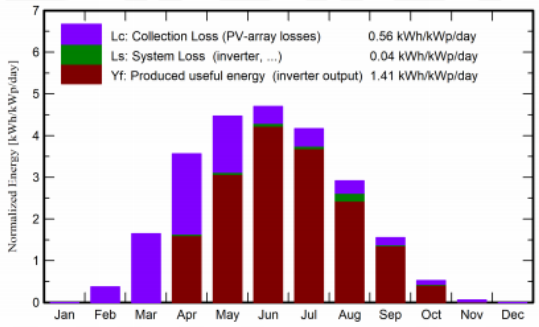

Performance Ratio PR

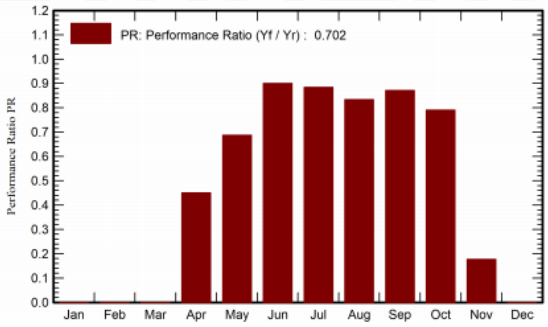

Balances and main results

	GlobHor kWh/m²	DiffHor kWh/m²	T_Amb °C	GlobInc kWh/m²	GlobEff kWh/m²	EArray MWh	E_Grid MWh	PR ratio
January	0.0	0.00	-2.83	0.0	0.0	0.0	0.0	1.000
February	10.4	6.07	-3.37	10.4	0.0	0.0	0.0	1.000
March	50.7	21.11	-2.08	51.1	0.0	0.0	0.0	1.000
April	106.8	39.42	1.34	106.9	49.7	58.2	56.9	0.451
May	139.4	73.73	5.87	138.5	98.7	114.4	112.4	0.687
June	142.4	82.23	9.40	141.0	134.1	152.3	149.9	0.900
July	130.5	73.80	13.52	129.2	122.9	137.3	135.0	0.885
August	91.1	51.27	12.21	90.4	85.5	95.9	89.0	0.834
September	46.8	27.18	7.39	46.7	43.0	49.1	48.1	0.872
October	16.3	10.99	3.32	16.3	14.1	15.9	15.2	0.790
November	1.8	1.39	0.09	1.7	0.7	0.6	0.4	0.177
December	0.0	0.00	-1.81	0.0	0.0	0.0	0.0	1.000
Year	736.2	387.20	3.63	732.2	548.8	623.6	606.9	0.702

Legends

GlobHor	Global horizontal irradiation	EArray	Effective energy at the output of the array
DiffHor	Horizontal diffuse irradiation	E_Grid	Energy injected into grid
T_Amb	Ambient Temperature	PR	Performance Ratio
GlobInc	Global incident in coll. plane		
GlobEff	Effective Global, corr. for IAM and shadings		

Figure E.5: *Page 6 PVsyst report.*

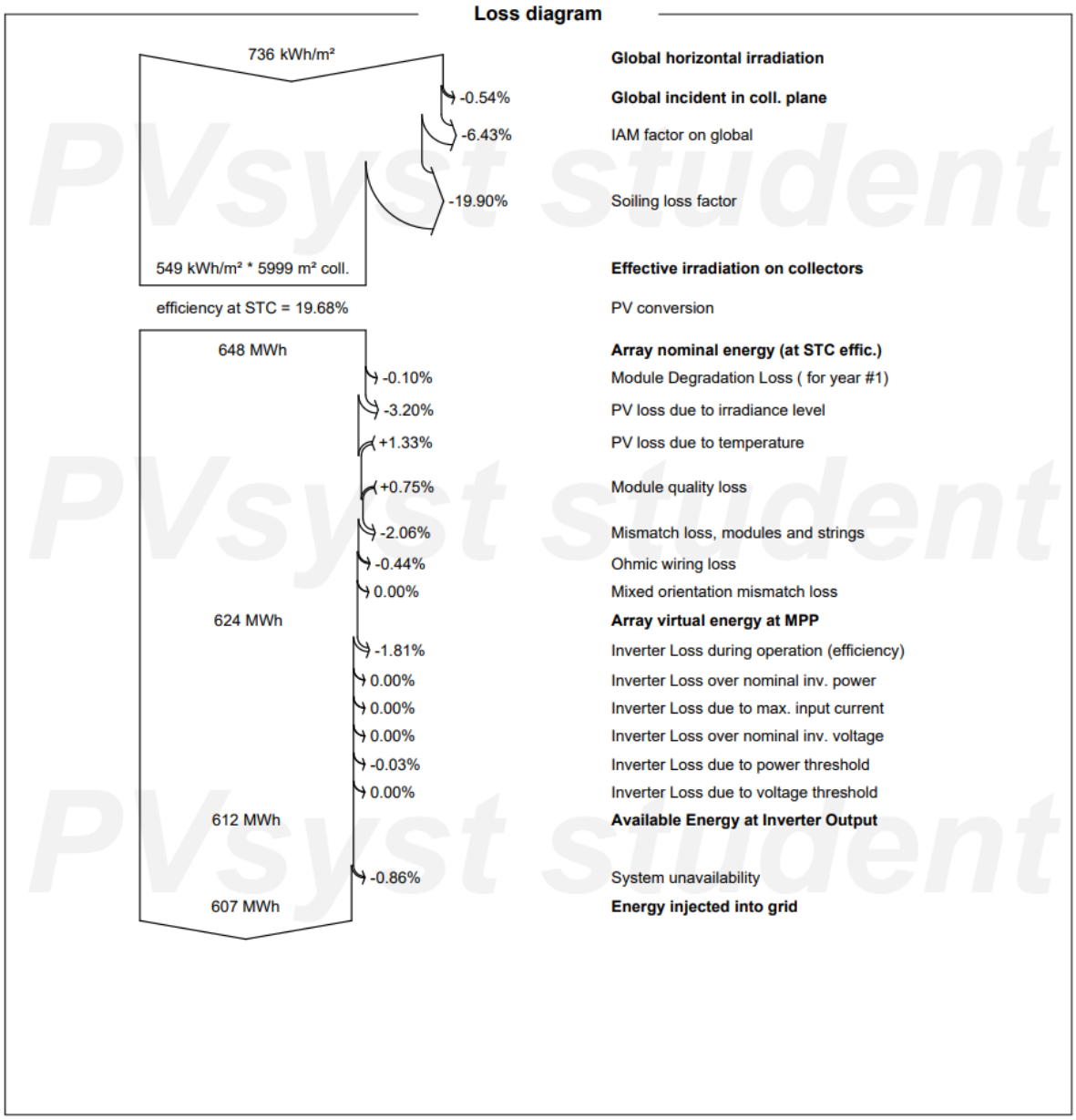

Figure E.6: *Page 7 PVsyst report.*

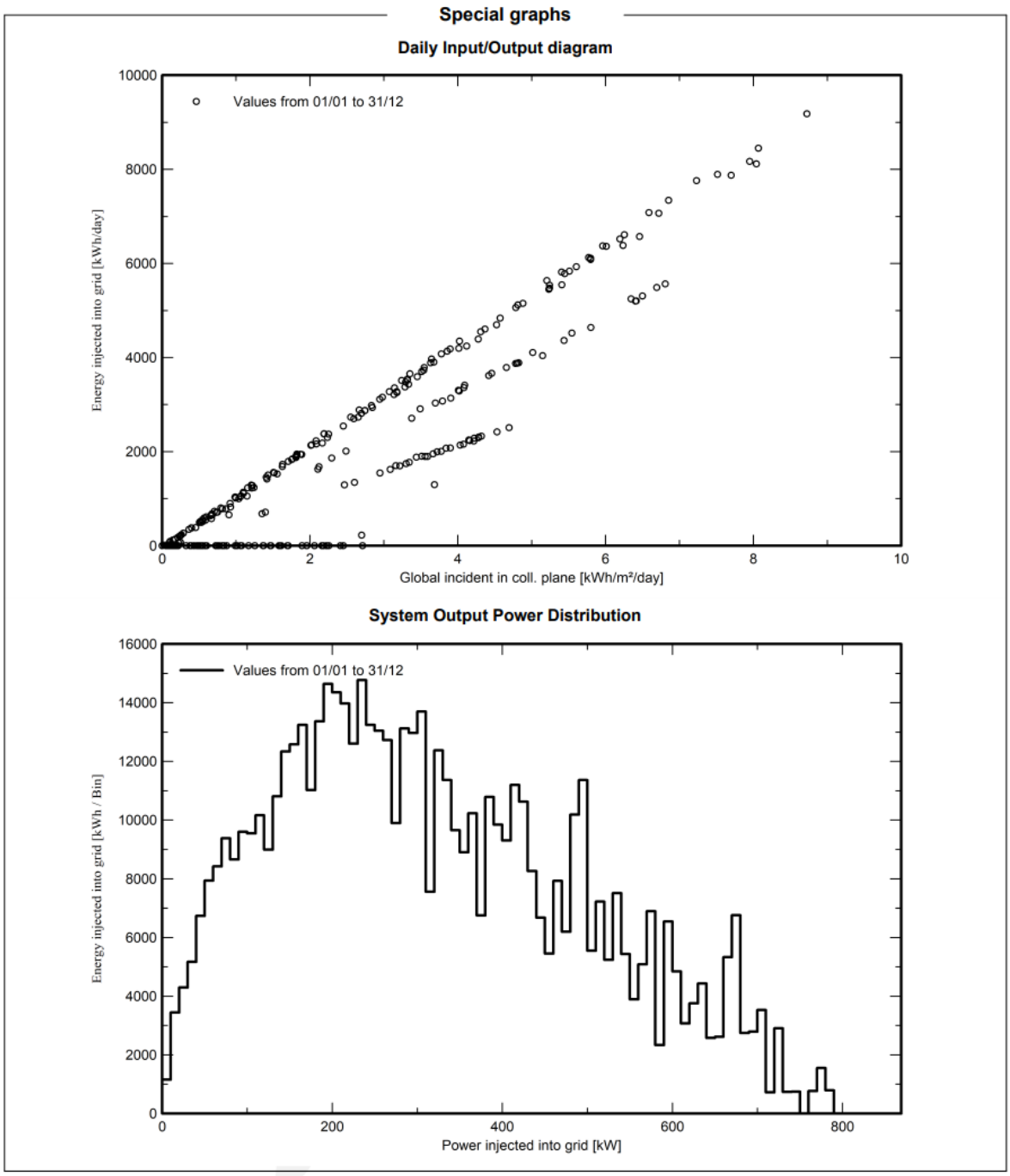

Figure E.7: *Page 8 PVsyst report.*

PV systems on refigerated warehouses

NTNU
Kunnskap for en bedre verden

TrønderEnergi